

**Ligand Directed Pd-Catalyzed C–H Activation:  
Mechanistic Insights and Synthetic Applications**

**by**

**Kara J. Stowers**

**A dissertation submitted in partial fulfillment  
of the requirements for the degree of  
Doctor of Philosophy  
(Chemistry)  
in The University of Michigan  
2012**

**Doctoral Committee:**

**Professor Melanie S. Sanford, Chair  
Professor Levi T. Thompson Jr.  
Associate Professor John P. Wolfe  
Assistant Professor Anne J. McNeil**

© Kara J. Stowers

---

2012

To my Parents, Melanie and Matt  
(Because, without the four of you, I couldn't have made it this far.)

## Acknowledgements

The old adage “it takes a village...” rings true. The completion of this endeavor would not have been possible were it not for the citizens of my village – and I have a great one.

I would first like to thank my advisor Dr. Melanie Sanford. From her I have learned to present, to speak more scientifically, to organize data, to critically think about experiments and data, and how to be a good scientist and citizen of the scientific community. Your consistent encouragement and insistence that I learn as much as I can, stay excited about chemistry, and always do better than my best has been critical to my development. It is from my respect of your expectations, that I have met that challenge to become the scientist I am today. I am profoundly grateful.

I would like to thank my thesis committee members. I completed a research rotation where I was able to work under the direction of John Wolfe. Thank you for your guidance and expectations during those very early days; they shaped a career. I also served on a student committee organizing a symposium for the department while Anne McNeil served as a faculty representative. I enjoyed the guidance and advice Anne supplied, and have continued to enjoy that association over the last few years; including her interest in my research and future plans. Thank you. Finally, I want to thank Levi Thompson for providing helpful suggestions during my candidacy and data meeting, and for being a friendly face during those times.

I have been lucky to work with talented and enthusiastic scientists over the years from the Sanford laboratory. These are the people I would see daily for many many hours and they have also shaped my graduate career. Notably, and from the bottom of my heart, I thank Dr. Lopa Desai and Dr. Dipannita Kalyani who were crucial mentors to the very novice chemist that I was. Thank you for setting the pace and the level of intelligence that I would be responsible for answering to. It's been much appreciated, MORE than you can possibly know. Collaborating with Lopa was a highlight of my graduate career. I also would like to thank labmates Nick Deprez, Kami Hull, Tom Lyons, Nick Ball, Joy Racowski, and Brannon Gary for helpful discussions and being friendly supportive labmates. For putting up with me, working together with me, encouraging me to keep going, for being there as the climate of the lab fluctuated, for snacks and ice cream trips, I would be amiss to not thank Asako Kubota for ALL she has done. Thank you so very much! I would also like to acknowledge Anna Wagner and Yingda Ye for being excellent labmates and scientists as well.

I would also like to acknowledge the ongoing support from friends, roommates and previous mentors. Without the encouragement and mentoring from Dr. Matt Sigman, I wouldn't have come to graduate school. I have appreciated the support and helpful conversations and advice that have continued over the years.

Finally, I would like to thank my parents, Scott and Rebecca Stowers. Their encouragement and love have helped me to be confident and excited about doing difficult things. I appreciate the support that they have rendered although they have been many miles away. Thank you so much! I wouldn't be who I am without you.

# Table of Contents

Dedication.....	ii
Acknowledgements .....	iii
List of Figures .....	vii
List of Tables .....	x
List of Schemes .....	xii
Abstract .....	xiv
Chapter 1: Introduction .....	1
Chapter 2: Competing Directing Groups.....	8
<b>2.1 Introduction</b> .....	8
<b>2.2 Results</b> .....	9
<b>2.3 Discussion</b> .....	20
<b>2.4 Application</b> .....	24
<b>2.5 Conclusions</b> .....	24
<b>2.6 Experimental</b> .....	25
<b>2.7 Characterization</b> .....	26
<b>2.8 References</b> .....	29
Chapter 3: Mechanism of C–H Chlorination .....	33
<b>3.1 Introduction</b> .....	33
<b>3.2 Results</b> .....	34
<b>3.3 Discussion</b> .....	46
<b>3.4 Application</b> .....	50
<b>3.5 Conclusions</b> .....	50
<b>3.6 Experimental</b> .....	51
<b>3.7 Characterization</b> .....	53

<b>3.8 References</b> .....	59
Chapter 4: Olefination of $sp^3$ C-H bonds.....	62
<b>4.1 Introduction</b> .....	62
<b>4.2 Results</b> .....	63
<b>4.3 Discussion</b> .....	73
<b>4.4 Application</b> .....	74
<b>4.5 Conclusions</b> .....	76
<b>4.6 Experimental</b> .....	76
<b>4.7 Characterization</b> .....	77
<b>4.8 References</b> .....	102
Chapter 5: Acetoxylation using Oxygen.....	105
<b>5.1 Introduction</b> .....	105
<b>5.2 Results</b> .....	109
<b>5.3 Discussion</b> .....	114
<b>5.4 Application</b> .....	116
<b>5.5 Conclusions</b> .....	118
<b>5.6 Experimental</b> .....	118
<b>5.7 Characterization</b> .....	119
<b>5.8 References</b> .....	122
Chapter 6: Conclusions and Outlook.....	125

## List of Figures

<b>Figure 1.1.</b> Palladium Insertion into Carbon-Heteroatom Bonds.....	1
<b>Figure 1.2.</b> Examples of Commonly Used Ligands for Metal Coordination .....	3
<b>Figure 1.3.</b> Mechanism for C–H Functionalization .....	3
<b>Figure 1.4.</b> Acetoxylation with Nitrates and O <sub>2</sub> as the Terminal Oxidant.....	6
<b>Figure 2.1.</b> Examples of Biologically Active Molecules Containing Multiple Directing Groups.....	8
<b>Figure 2.2.</b> Hammett Plot for Competition Experiments in AcOH/Ac <sub>2</sub> O .....	12
<b>Figure 2.3.</b> Hammett Plot for Competition Experiments in AcOH/Ac <sub>2</sub> O Corrected for Concentration of Benzylpyridine .....	14
<b>Figure 2.4.</b> Hammett Plot for Competition Experiments in Benzene .....	15
<b>Figure 2.5.</b> Hammett Plot for Individual Initial Rates in AcOH/Ac <sub>2</sub> O .....	16
<b>Figure 2.6.</b> Hammett Plot for Individual Initial Rates in AcOH/Ac <sub>2</sub> O Corrected for Concentration of Benzylpyridine .....	17
<b>Figure 2.7.</b> Hammett Plot for Individual Initial Rates in Benzene .....	17
<b>Figure 2.8.</b> Kinetic Isotope Effect Experiment.....	18
<b>Figure 2.9.</b> Hammett Plot of Stoichiometric Cyclopalladation .....	19
<b>Figure 2.10.</b> Initial Rates Showed Zero Order as a Function of [PhI(OAc) <sub>2</sub> ]. ....	20
<b>Figure 2.11.</b> Proposed Catalytic Cycle for Pd-Catalyzed C–H Bond Acetoxylation .....	20
<b>Figure 2.12.</b> Equilibrium for Substrate Binding and Curtin Hammett Illustration	23
<b>Figure 3.1.</b> Unselective Chlorination of 2-Benzylpyridine.....	35
<b>Figure 3.2.</b> Order in Oxidant for NCS.....	39
<b>Figure 3.3.</b> Order in Oxidant for PhI(OAc) <sub>2</sub> .....	39
<b>Figure 3.4.</b> Plot of Initial Rate ( $\Delta[2]/\Delta t$ ) versus [Pd] for Chlorination fit to $f(x) = a[\text{PdCl}_2]^n$ ( $a = 3.0 \pm 0.2 \times 10^{-4}$ , $n = 1.06 \pm 0.08$ ) .....	40
<b>Figure 3.5.</b> Plot of Initial Rate ( $\Delta[3]/\Delta t$ ) versus [Pd] for Acetoxylation fit to $f(x) = a[\text{Pd}(\text{OAc})_2]^n$ ( $a = 2.0 \pm 0.5 \times 10^{-4}$ , $n = 1.51 \pm 0.22$ ) .....	41



<b>Figure 3.6.</b> Order in Substrate [1] for C–H Chlorination .....	42
<b>Figure 3.7.</b> Plot of Initial Rate ( $\Delta[3]/\Delta t$ ) versus [1] for Acetoxylation fit to $f(x) = a[1]^n$ ( $a = 0.0713 \pm 0.009$ , $n = -1.11 \pm 0.05$ ) .....	43
<b>Figure 3.8.</b> Hammett Plot for C–H Chlorination ( $-\rho$ ) and C–H Acetoxylation ( $+\rho$ ). .....	44
<b>Figure 3.9.</b> Hammett Plot for Chlorination at 0.048 M.....	45
<b>Figure 3.10.</b> Hammett Plot for Chlorination with Pd(OAc) <sub>2</sub> .....	45
<b>Figure 3.11.</b> Competing Ligands for Chlorination Hammett Plot in CH <sub>3</sub> CN.....	46
<b>Figure 3.12.</b> Competing Ligands for Acetoxylation Hammett Plot in CH <sub>3</sub> CN ....	46
<b>Figure 3.13.</b> Formation of Monomeric Complex Pd(X) <sub>2</sub> (L) <sub>2</sub> .....	48
<b>Figure 4.1.</b> Alkene Scope for C–H Bond Alkenylation.....	70
<b>Figure 4.2.</b> Other Methyl Oxime Ether Substrates. ....	71
<b>Figure 4.3.</b> Substrates with Pyridine Directing Groups for sp <sup>2</sup> C–H Activation...	72
<b>Figure 4.4.</b> Possible Mechanism for Product Inhibition .....	73
<b>Figure 4.5.</b> Examples of Naturally Occurring 6,5-Nitrogen Heterocycles .....	74
<b>Figure 4.6.</b> Functionalization of C–H Alkenylated Product <b>14</b> . <sup>a</sup> .....	76
<b>Figure 5.1.</b> Potential Catalytic Cycle for Oxygenation Using O <sub>2</sub> .....	105
<b>Figure 5.2.</b> Pd-Catalyzed Quinoline-Directed Aerobic Oxygenation of Benzylic C–H Bonds .....	107
<b>Figure 5.3.</b> Redox Catalyst Cycle to harness oxidation potential of dioxygen..	107
<b>Figure 5.4.</b> Organocatalytic Aerobic Oxidation of Alcohols .....	108
<b>Figure 5.5.</b> Redox Couples for Oxidation of Methane .....	109
<b>Figure 5.6.</b> Acetoxylation with Nitrates and Oxygen as the Terminal Oxidant .	109
<b>Figure 5.7.</b> Potential Redox Cycle for Nitrate Assisted Acetoxylation .....	115
<b>Figure 5.8</b> Oxidation of a Pd(II) Complex <b>E</b> to form Pd(IV) Nitrosyl Complex <b>F</b>	115
<b>Figure 5.9</b> Nitration of <b>BHT</b> with NO <sub>2</sub> to form <b>4-NO<sub>2</sub>-BHT</b> .....	116
<b>Figure 6.1.</b> Interplay Between Mechanism and New Methodology .....	125

<b>Figure 6.2.</b> Complex Molecule with Multiple Directing Groups and Functionalization Sites.....	125
<b>Figure 6.3.</b> Proposed Mechanistic Studies for Aliphatic Acetoxylation.....	127
<b>Figure 6.4.</b> Naturally Occuring 6,5-N-fused Bicyclic Compounds .....	127
<b>Figure 6.5.</b> Proposed Investigation of the Mechanism of Nitrates as an Oxidant .....	128

## List of Tables

<b>Table 2.1.</b> Acetoxylation of Substituted Benzyl Pyridine Derivatives.....	10
<b>Table 2.2</b> Observed Ratios of Benzylpyridines in Competition.....	12
<b>Table 2.3.</b> Correction for Unprotonated Benzylpyridine Concentration .....	14
<b>Table 2.4.</b> Individual Initial Rates Studies .....	15
<b>Table 2.5.</b> Correction for Observed Individual Initial Rates .....	16
<b>Table 2.6.</b> Rates of Stoichiometric Cyclopalladation .....	19
<b>Table 3.1.</b> Optimization of Chlorination Reaction Conditions .....	36
<b>Table 3.2.</b> Optimization of Chlorination Catalyst .....	37
<b>Table 3.3.</b> Optimization of Acetoxylation Reaction Conditions .....	37
<b>Table 3.4.</b> Intermolecular Kinetic Isotope Effect Data .....	38
<b>Table 3.5.</b> Initial Rate as a Function of [NCS] for Chlorination .....	38
<b>Table 3.6.</b> Initial Rate as a Function of [PhI(OAc) <sub>2</sub> ] for Acetoxylation .....	39
<b>Table 3.7.</b> Initial Rate as a Function of [Pd] for Chlorination .....	40
<b>Table 3.8.</b> Initial Rate as a Function of [Pd] for Acetoxylation .....	41
<b>Table 3.9.</b> Initial Rate as a Function of [1] for Chlorination.....	42
<b>Table 3.10.</b> Initial Rate as a Function of [1] for Acetoxylation .....	42
<b>Table 3.11.</b> Initial Rates for Substrates <b>1a-1e</b> for C–H Chlorination and C–H Acetoxylation .....	44
<b>Table 4.1.</b> Optimization of catalyst, polyoxometalate, additives and O <sub>2</sub> .....	65
<b>Table 4.2.</b> Optimization of Catalyst .....	66
<b>Table 4.3.</b> Pd-Catalyzed Olefination and Cyclization Between Various Pyridines and Ethylacrylate.....	68

<b>Table 4.4.</b> Pd-Catalyzed Olefination and Cyclization Between Pyridines and Ethylacrylate.....	69
<b>Table 5.1.</b> Optimization of nitrate salt as a co-catalyst for palladium catalyzed oxygenation.....	111
<b>Table 5.2.</b> Substrate Scope for Oxygenation.....	112
<b>Table 5.3.</b> Substrate Scope for Acetoxylation of Sterically Hindered Oxime Ethers.....	114
<b>Table 6.1.</b> Selectivity Preferences for Various C–H Functionalization Reactions .....	126

## List of Schemes

<b>Scheme 1.1.</b> Direct Palladium-Catalyzed C–H Bond Functionalization .....	2
<b>Scheme 1.2.</b> Ligand Directed Cyclometallation via C–H Activation .....	2
<b>Scheme 1.3.</b> Competition Between Two Different Directing Groups (L and L')....	4
<b>Scheme 1.4.</b> Mechanistic Comparison Between Chlorination and Acetoxylation.	4
<b>Scheme 1.5.</b> Olefination of $sp^3$ C–H Bonds via C–H Activation .....	5
<b>Scheme 2.1.</b> Competition Between Two Different Directing Groups (L and L')....	9
<b>Scheme 2.2.</b> Competition Between Benzylpyridines <b>2a</b> and <b>6a</b> .....	11
<b>Scheme 3.1.</b> Representative Example of Different Substrate Scope for Acetoxylation versus Chlorination.....	33
<b>Scheme 3.2.</b> General Mechanism for C–H Functionalization.....	34
<b>Scheme 3.3.</b> Rate Limiting Oxidation for Chlorination with Cooperative $^-OAc$ Catalysis .....	47
<b>Scheme 3.4.</b> Two Possible Mechanisms for the Turnover Limiting Step of C–H Chlorination ( <b>1</b> = 2- <i>ortho</i> -tolylpyridine).....	49
<b>Scheme 3.5.</b> Possible Competing Mechanisms for the Turnover Limiting Step of C–H Acetoxylation ( <b>1</b> = 2- <i>ortho</i> -tolylpyridine) .....	50
<b>Scheme 4.1</b> Precedent for Pd-Catalyzed $sp^3$ C–H Olefination.....	63
<b>Scheme 4.2</b> Hypothesized Equilibrium between Olefin Product ( <b>A</b> ) and Cyclized Product ( <b>B</b> ) .....	64
<b>Scheme 4.3</b> Ishii Conditions for Oxidative Heck Reactions with Acrylates .....	64
<b>Scheme 4.4</b> Homo-coupled byproduct of the Olefin Starting Material.....	66
<b>Scheme 4.5.</b> Observance of Selective Mono-Functionalization .....	66
<b>Scheme 4.6.</b> Observance of Mixtures of Acetoxyated Products.....	67
<b>Scheme 4.7</b> Olefination of 8-Methylquinoline to form olefinated product <b>18</b> .....	70
<b>Scheme 4.8</b> Olefination of 2,2-Dimethylcyclopentyl O-Methyloxime Ether .....	71
<b>Scheme 4.9</b> Olefination of N,N-dimethylbenzylamine .....	72
<b>Scheme 4.10</b> Selectivity for $sp^3$ and $sp^2$ C–H Olefination .....	73

<b>Scheme 4.11.</b> Reduction Reactions of <b>2</b> .....	75
<b>Scheme 4.12</b> Deprotonation to Obtain the Alkene Product.....	75
<b>Scheme 5.1.</b> Pd-Catalyzed Benzoic Acid-Directed Aerobic C–H Oxygenation of Arenes .....	106
<b>Scheme 5.2.</b> Acetoxylation of Chlorobenzene .....	108
<b>Scheme 5.3.</b> Acetoxylation with Nitrates and Oxygen as the Terminal Oxidant .....	110
<b>Scheme 5.4.</b> Decomposition of Acetoxyated Product .....	113
<b>Scheme 5.5.</b> C–H Oxygenation to form <b>7</b> and <b>8</b> .....	113
<b>Scheme 5.6</b> Acetoxylation of 8-methylquinoline with Nitrate and Air .....	114
<b>Scheme 5.7.</b> Addition of BHT to the optimized reaction condtions.....	116
<b>Scheme 5.8.</b> Stoichiometric Reductive Elimination of Cl vs OAc Ligands.....	117
<b>Scheme 5.9.</b> Incorporation of chloride using nitrate as a redox co-catalyst. ....	117

## Abstract

Carbon–hydrogen bond activation/functionalization methods provide an attractive strategy for late-stage derivatization of complex molecules. In particular ligand-directed C–H activation allows for the selective functionalization of the C–H bond proximal to the ligand. However, complex mixtures of products could potentially result from multiple C–H transformations especially in pharmaceutically relevant molecules containing multiple coordinating ligands. In order to address this challenge, and allow for controlled and predictable selectivities, a systematic investigation of the factors that determine the relative directing group abilities of different ligands in Pd-catalyzed C–H bond acetoxylation of 2-benzylpyridine derivatives was undertaken. Analysis of the data indicated a direct and quantitative correlation between the basicity of a ligand and its relative reactivity.

Furthermore, understanding the mechanism of these transformations is necessary for optimization and development of novel C–H functionalization reactions. In this regard, a detailed investigation of the mechanism of the Pd-catalyzed C–H acetoxylation and chlorination of 2-*ortho*-tolylpyridine derivatives was conducted. C–H activation was found to be rate-determining for both transformations; however, the electronic requirements for C–H activation in PdCl<sub>2</sub>-catalyzed chlorination differ significantly from those for Pd(OAc)<sub>2</sub>-catalyzed acetoxylation. A comparison of the implicated transition states is used to rationalize how the difference in ligand environment affects the electronic requirements of the rate-determining step.

The understanding gained from these mechanistic investigations was used to develop a new Pd/polyoxometalate-catalyzed method for coupling of alkanes and alkenes. Interception of the palladacycle formed upon C–H activation of 2-alkylpyridine derivatives with electron deficient olefins provides a

new synthetic tool for quickly installing complex functionality and building new motifs from two less reactive and readily available starting materials. This approach provides access to bicyclic structures that are found in biologically relevant molecules. These products can also be manipulated to “unmask” the alkene, thereby rendering it available for subsequent transformations.

Most current methods for C–H acetoxylation are limited to oxidants that are expensive and that generate toxic byproducts. This work also describes the development of a new Pd-catalyzed reaction for directed C–H acetoxylation that uses nitrate as a redox co-catalyst in conjunction with O<sub>2</sub> as the terminal oxidant and acetic acid as the acetate source. This provides an extremely inexpensive and non-waste-generative alternative to commonly used oxidants. The substrate scope of this reaction is described in detail.

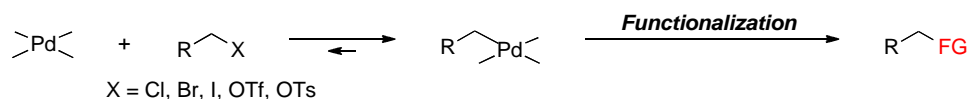


## Chapter 1: Introduction

Over the last decade, there has been an exponential growth of methodology that enables facile functionalization of small molecules, specifically using palladium as a catalyst.<sup>1</sup> Making the case for palladium's utility as a catalyst is easier than before with the Nobel Prize being awarded to palladium-catalyzed cross-coupling reactions in 2010. Palladium has proven to be extremely versatile as a catalyst in a wide variety of reactions, is tolerant of ligands, oxidants and other functional groups and compared to many of the second row transition metals, is reasonably affordable.<sup>2</sup> Although palladium-catalyzed cross-coupling reactions have drastically changed the way chemists synthesize organic molecules and has greatly improved and shortened total syntheses, there are still some classes of transformations that are inherently inaccessible and there are also some disadvantages in terms of atom and step economy.

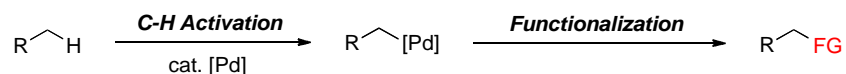
Most palladium-catalyzed cross-coupling reactions require prefunctionalized carbon bonds to serve the purpose of introducing the palladium into the starting material for future functionalization steps.<sup>3</sup> These pre-functional groups are often halogens or oxygen moieties. Due to the thermodynamic preference for palladium insertion (oxidative addition) into the carbon-heteroatom bond, it is more difficult to use palladium to install these same functionalities into new molecules, as well as even to tolerate existing oxygen or halogen moieties under conditions for palladium-catalyzed reactions due to this insertion preference (Figure 1.1).

**Figure 1.1.** Palladium Insertion into Carbon-Heteroatom Bonds



Although efforts to meet these needs are ongoing, it is this inherent limitation in installing heteroatom functionality that leaves a gap in the utility of traditional palladium-catalyzed cross-coupling methodology. Also, the atoms and steps needed to install prefunctionality into molecules prior to applying the reaction conditions adds time and cost that would be advantageous to remove. This void in existing methodology is the space into which C–H activation has taken root and flourished (Scheme 1.1).<sup>4,5,6</sup>

**Scheme 1.1.** Direct Palladium-Catalyzed C–H Bond Functionalization



The foundation for C–H activation began as early studies demonstrated the power of transition metals (Pd, Pt, Ir, Ru, and Rh) for overcoming the “inertness” of C–H bonds via direct insertion.<sup>7</sup> The other challenge for direct C–H functionalization is selectivity as there are often many different C–H bonds in a single molecule. A number of strategies are often employed to get around this obstacle, the one most relevant to this work being the use of chelating ligands (Figure 1.2). Due to the reversible metal chelation or binding of these ligands, the substrates undergo cyclometallation selectively at the C–H bond closest in proximity to the bound metal (Scheme 1.2). The new C–M bond allows for highly site selective transformations of bonds into new C–X bonds (X = O, Cl, Br, I, F, C or N) with the appropriately chosen reagent.<sup>1,3,7</sup> Importantly, most natural products, pharmaceuticals, and agrochemicals contain functional groups or ligands that are suitable directing groups for this type of reaction.

**Scheme 1.2.** Ligand Directed Cyclometallation via C–H Activation

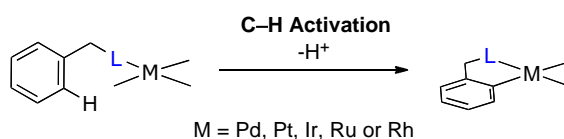
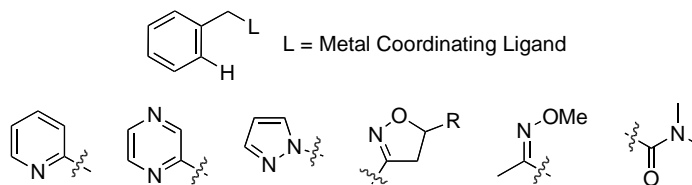
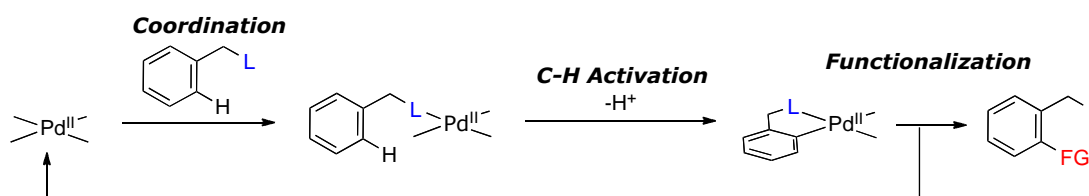


**Figure 1.2.** Examples of Commonly Used Ligands for Metal Coordination



Palladium-catalyzed C–H bond functionalization has emerged as a powerful method for the direct conversion of arenes and alkanes into new products. Palladium is often the metal of choice due to the diversity of functional groups it can tolerate, with the exception of most halogens (ie: ketones, amines, alcohols, heterocycles, aldehydes), as well as install into a molecule. Furthermore, it can insert into both  $sp^3$  and  $sp^2$  C–H bonds.<sup>7</sup> Finally, the complementary reactivity of C–H activation/functionalization methodology to the traditional cross-coupling methodology is attributed in part to the higher oxidation states of palladium often required for functionalization in these reactions (Figure 1.3).<sup>8</sup> Due to the direct insertion and new heteroatom bonds that can be formed from activation of C–H bonds, these transformations could be valuable for late stage derivatization and analog generation in important classes of molecules. My work describes efforts to better define and understand the mechanism of these reactions, as well as an application of the insights gained to design new methodology.

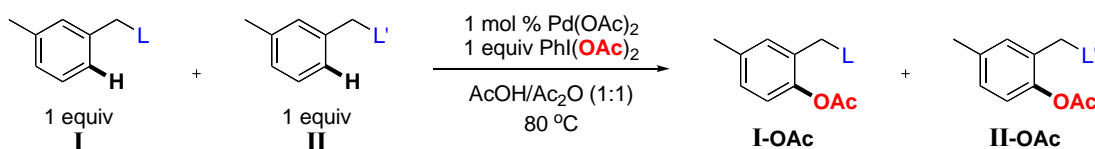
**Figure 1.3.** Mechanism for C–H Functionalization



In Chapter 2, a detailed investigation of factors controlling the dominance of a directing group in Pd-catalyzed ligand-directed arene acetoxylation is described (Scheme 1.3).<sup>9</sup> Mechanistic studies, involving reaction kinetics, Hammett

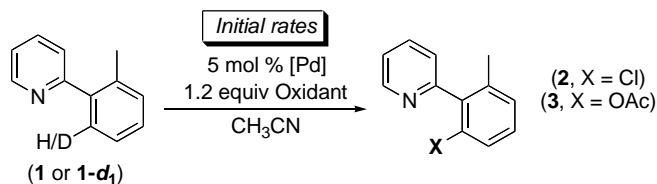
analysis, kinetic isotope effect experiments, and the order in oxidant, have been conducted. Initial rates studies of substrates bearing electronically different directing groups showed that these transformations are accelerated by the use of electron deficient groups. However, in contrast, under conditions where two directing groups are in competition with one another in the same reaction flask, substrates with electron rich directing groups react preferentially. These experiments provide insight into predicting selectivity for complex molecules. These results are discussed in the context of the proposed mechanism for Pd-catalyzed arene acetoxylation.

**Scheme 1.3.** Competition Between Two Different Directing Groups (L and L')



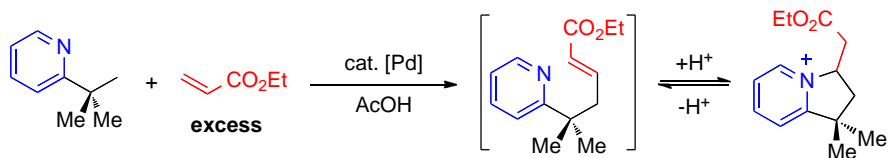
Following the study for acetoxylation, Chapter 3 describes detailed investigations of the mechanism of the Pd-catalyzed C–H chlorination and acetoxylation of 2-*ortho*-tolylpyridine derivatives (Scheme 1.4).<sup>10</sup> A comparison under the conditions examined demonstrates that both reactions proceed via turnover limiting cyclopalladation. However, substrate and catalyst order as well as Hammett data indicate that the intimate mechanism of cyclopalladation differs significantly between PdCl<sub>2</sub>-catalyzed chlorination and Pd(OAc)<sub>2</sub>-catalyzed acetoxylation.

**Scheme 1.4.** Mechanistic Comparison Between Chlorination and Acetoxylation



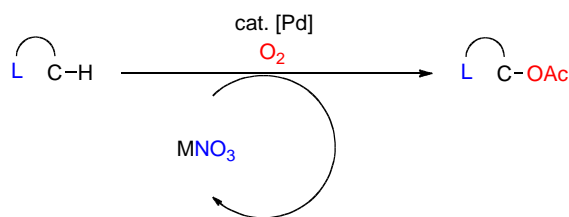
The next part, Chapter 4, describes a new method for the Pd/polyoxometalate-catalyzed aerobic olefination of unactivated  $sp^3$  C–H bonds (Scheme 1.5).<sup>11</sup> Nitrogen heterocycles serve as directing groups, and air is used as the terminal oxidant. The products undergo reversible intramolecular Michael addition, which protects the mono-alkenylated product from over-functionalization. Hydrogenation of the Michael adducts provides access to bicyclic nitrogen-containing scaffolds that are prevalent in alkaloid natural products. In addition, these cationic Michael adducts undergo facile elimination to release  $\alpha,\beta$ -unsaturated olefins, which can be elaborated in numerous C–C and C–heteroatom bond-forming reactions.

**Scheme 1.5.** Olefination of  $sp^3$  C–H Bonds via C–H Activation



Finally, Chapter 5 describes the development of a new method for Pd-catalyzed C–H oxygenation that uses  $O_2$  as the terminal oxidant in the presence of nitrate salts and AcOH (Figure 1.4).<sup>12</sup> The nitrate acts as a redox co-catalyst in conjunction with  $O_2$  and AcOH acts as the acetate source to install C–OAc bonds with very little waste generation. The nitrate salts can be used substoichiometrically and are inexpensive compared with traditional oxidants used in these transformations (e.g.  $PhI(OAc)_2$  \$425.00/mol versus  $NaNO_3$  \$1.00/mol). Both oxime ether and pyridine directing groups are well tolerated. Furthermore, the addition of sodium chloride as a nucleophile under otherwise analogous reaction conditions led to chlorination (which outcompetes acetoxylation). This reaction is the first demonstrated example of chlorination of unactivated  $sp^3$  C–H bonds to date.

**Figure 1.4.** Acetoxylation with Nitrates and O<sub>2</sub> as the Terminal Oxidant



Finally, Chapter 6 concludes the work as a whole and discusses the outlook for C-H functionalization in terms of the methodology explored and future directions for the field.

## Reference

<sup>1</sup> Hartwig, J. F. In *Organotransition Metal Chemistry*; University Science Books.: Mill Valley, California, 2010.

<sup>2</sup> (a) Nicolaou, K. C.; Bulger, P. G.; Sarlah, D. *Angew. Chem. Int. Ed.* **2005**, *44*, 4442-4489. (b) Hegedus, L. S. In *Transition Metals in the Synthesis of Complex Organic Molecules*; University Science Books: Sausalito, California, 1999.

<sup>3</sup> Crabtree, R. H. In *The Organometallic Chemistry of the Transition Metals*; John Wiley & Sons, Inc.: Hoboken, New Jersey, 2005.

<sup>4</sup> (a) Kalyani, D.; Deprez, N. R.; Desai, L. V.; Sanford, M. S. *J. Am. Chem. Soc.* **2005**, *127*, 7330. (b) Kalyani, D.; Sanford, M. S. *Org. Lett.* **2005**, *7*, 4149; (c) Dick, A. R.; Hull, K. L.; Sanford, M. S. *J. Am. Chem. Soc.* **2004**, *126*, 2300; (d) Kalyani, D.; Dick, A. R.; Anani, W. Q.; Sanford, M. S. *Org. Lett.* **2006**, *8*, 2523; (e) Desai, L. V.; Malik, H. A.; Sanford, M. S. *Org. Lett.* **2006**, *8*, 1141; (f) Desai, L. V.; Hull, K. L.; Sanford, M. S. *J. Am. Chem. Soc.* **2004**, *126*, 2300; (g) Hull, K. L.; Anani, W. Q.; Sanford, M. S. *J. Am. Chem. Soc.* **2006**, *128*, 7134. (h) Neufeldt, S. R.; Sanford, M. S. *Org. Lett.* **2010**, *12*, 532-535. (i) Satterfield, A. D.; Kubota, A.; Sanford, M. S. *Org. Lett.* **2011**, *13*, 1076-1079. (j) Kubota, A.; Sanford, M. S. *Synthesis* **2011**, 2579-2589.

<sup>5</sup> (a) Yu, J.; Giri, R.; Chen, X. *Org. Biomol. Chem.* **2006**, *4*, 4041 and references therein; (b) Thu, H. -Y.; Yu, W. -Y.; Che, C. -M. *J. Am. Chem. Soc.* **2006**, *128*, 9048. (c) "Directed Metallation", *Topics in Organometallic Chemistry*, Springer, **2007**, 24 and references therein.

<sup>6</sup> (a) Lyons, T. W.; Sanford, M. S. *Chem. Rev.* **2010**, *110*, 1147-1169 and references therein. (b) Chan, C.-W.; Zhou, Z.; Yu, W.-Y. *Adv. Synth. Catal.* **2011**, 10220-10228. (c) Piechowska, J.; Gryko, D. T. *J. Org. Chem.* **2011**, *76*, 10220-10228. (d) Wasa, M.; Engle, K. M.; Lin, D. W.; Yoo, E. J.;

---

Yu, J.-Q. *J. Am. Chem. Soc.* **2011**, *133*, 19598-19601. (e) Huang, C.; Ghatadze, N.; Chattopadhyay, B.; Gevorgyan, V. *J. Am. Chem. Soc.* **2011**, *133*, 17630-17633. (f) Wei, Y.; Yoshikai, N. *Org. Lett.* **2011**, *13*, 5504-5507.

<sup>7</sup> Shilov, A. E.; Shul'pin, G. B. *Chem. Rev.* **1997**, *97*, 2879-2932.

<sup>8</sup> (a) Sehnal, P.; Taylor, R. J. K.; Fairlamb, I. J. S. *Chem. Rev.* **2010**, *110*, 824-889. (b) Muniz, K. *Angew. Chem. Int. Ed.* **2009**, *48*, 9412-9423.

<sup>9</sup> Chapter 2 Reprinted with permission from Desai, L. V.; Stowers, K. J.; Sanford, M. S. *J. Am. Chem. Soc.* **2008**, *130*, 13285-13293. Copyright 2008. American Chemical Society

<sup>10</sup> Chapter 3 Reprinted with permission from Stowers, K. J.; Sanford, M. S. *Org. Lett.* **2009**, *11*, 4584-4587. Copyright 2009. American Chemical Society

<sup>11</sup> Chapter 4 Reprinted with permission from Stowers, K. J.; Fortner, K. F.; Sanford, M. S. *J. Am. Chem. Soc.* **2011**, *133*, 6541-6544. Copyright 2011. American Chemical Society

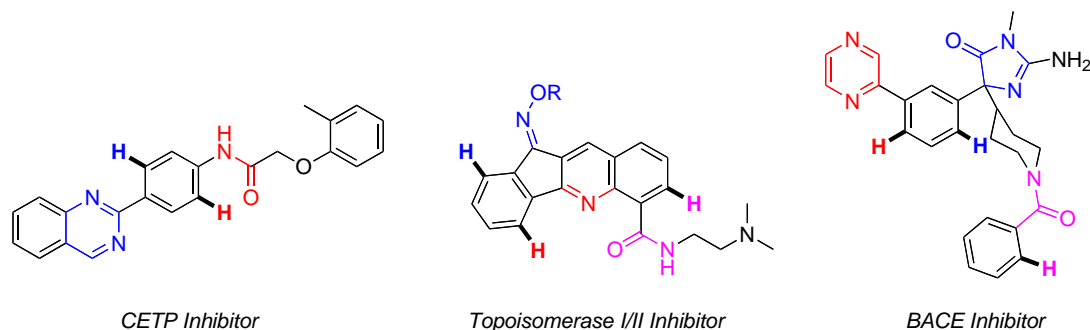
<sup>12</sup> Stowers, K. J.; Sanford, M. S. *manuscript in preparation.* **2012.**

## Chapter 2: Competing Directing Groups

### 2.1 Introduction

The vast majority of current Pd-catalyzed directed C–H functionalization reactions involve organic compounds containing a single directing group.<sup>1,2,3</sup> However, there exist many molecules of interest that have not just one, but multiple functional groups that could bind to the Pd center and direct C–H bond functionalization (for three representative examples, see Figure 2.1).<sup>4</sup> The development of selective, efficient, and high yielding functionalization reactions in this context will require a clear understanding of the factors governing site selectivity and reactivity in the presence of multiple directing groups. Herein is presented a detailed investigation of Pd-catalyzed directed arene acetoxylation as a function of directing group electronics. Also included are experiments probing the mechanism of the reaction. The implications of these results for both the mechanism and the potential synthetic applications of this chemistry are discussed in detail.

**Figure 2.1.** Examples of Biologically Active Molecules Containing Multiple Directing Groups

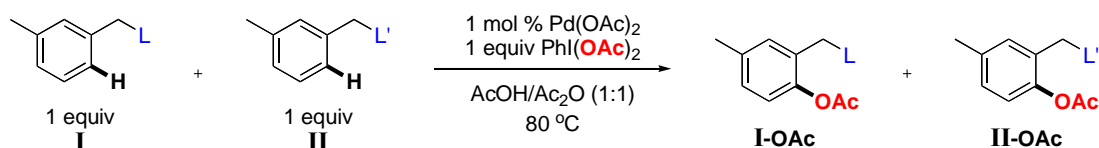




## 2.2 Results

Our first goal was to systematically study how the electronic nature of a directing group affects the distribution of products in Pd-catalyzed C–H bond functionalization with  $\text{PhI}(\text{OAc})_2$ . As shown in Scheme 2.1, we designed a series of experiments to compete two directing groups against one another in the same reaction flask (mimicking situations where two potential ligands are present within the same molecule). In these systems, 1 equivalent of substrate **I** and 1 equivalent of substrate **II** were subjected to a Pd-catalyzed reaction with 1 equivalent of  $\text{PhI}(\text{OAc})_2$ . The ratio of acetoxy products (**I-OAc**/**II-OAc**) was then determined, and this value represents the relative reaction rates of the two directing groups ( $k_A/k_B$ ) under a given set of conditions.

**Scheme 2.1.** Competition Between Two Different Directing Groups (L and L')

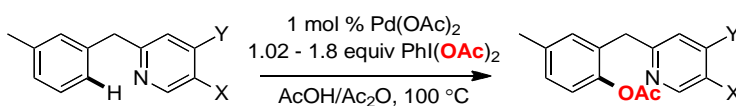


Our initial studies focused on substituted benzylpyridine derivatives as substrates for these transformations. These substrates were selected with several criteria in mind. First, pyridine derivatives are well-known to serve as highly effective directing groups for C–H bond acetoxylation.<sup>1,2c,e,l,l,b,d,3b,d,j,m,o,t</sup> Second, substitution at the *meta*- and *para*-positions of the pyridine ring allows for electronic modification of the directing group. Third, these substrates contain a methyl substituent at the *meta* position of the arene ring, which limits competing di-*ortho*-functionalization that could complicate product ratio analysis.<sup>5</sup> Finally, these substrates contain a methylene spacer between the directing group and the aromatic ring, which is expected to limit electronic communication between the pyridine substituent and the C–H bond being functionalized.<sup>6</sup> This substrate design should allow interpretation of product ratios solely in terms of electronic perturbation of the directing group.

Notably, these experiments were conducted in collaboration with Dr. Lopa Desai, a former graduate student in the Sanford group.

As summarized in Table 2.1, all of the substituted pyridine derivatives **1a-7a** are effective directing groups for Pd-catalyzed C–H bond acetoxylation. Under optimal conditions (1 mol % of Pd(OAc)<sub>2</sub>, 1.02 equiv of PhI(OAc)<sub>2</sub> in AcOH/Ac<sub>2</sub>O at 100 °C), the mono-acetoxylation products **1b-7b** were obtained in 70-93% isolated yield. Importantly, these transformations proceeded with extremely high (>100 : 1) selectivity for *ortho*-functionalization of the aromatic ring; furthermore, the less sterically congested *ortho*-site (*para* to the methyl substituent) underwent acetoxylation with >25 : 1 selectivity in all cases.<sup>5</sup>

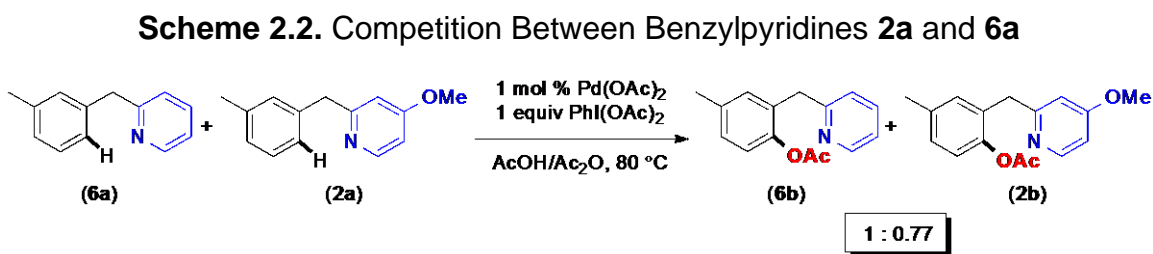
**Table 2.1.** Acetoxylation of Substituted Benzyl Pyridine Derivatives



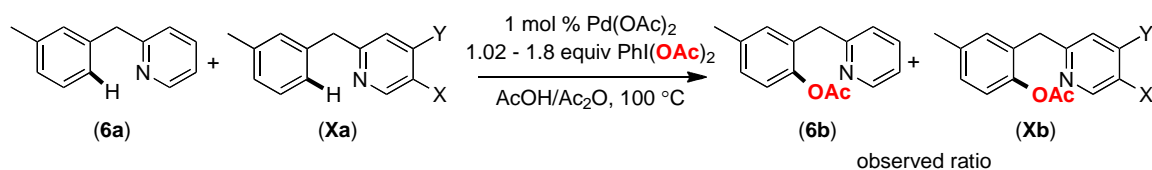
Entry	Substrate	X	Y	Product (Yield)
1	<b>1a</b>	H	CH <sub>3</sub>	<b>1b</b> (70%)
2	<b>2a</b>	H	OCH <sub>3</sub>	<b>2b</b> (75%)
3	<b>3a</b>	H	CF <sub>3</sub>	<b>3b</b> (91%)
4	<b>4a</b>	H	Cl	<b>4b</b> (74%)
5	<b>5a</b>	CH <sub>3</sub>	H	<b>5b</b> (74%)
6	<b>6a</b>	H	H	<b>6b</b> (75%)
7	<b>7a</b>	F	H	<b>7b</b> (93%)

We next carried out competition studies between the electronically varied benzylpyridine derivatives in AcOH/Ac<sub>2</sub>O. This acidic solvent was chosen as a starting point due to its widespread use as the solvent of choice for many C–H functionalization reactions.<sup>1,2c,3a</sup> In these experiments, a 1 : 1 molar ratio of unsubstituted 2-benzylpyridine **6a** and each substituted substrate (**1a-5a** and **7a**) was subjected to 1 equivalent of PhI(OAc)<sub>2</sub> and 1 mol % of Pd(OAc)<sub>2</sub>. Upon completion of the reaction, the yields and ratios of acetoxylation products were determined by gas chromatography. These reactions were repeated in duplicate.

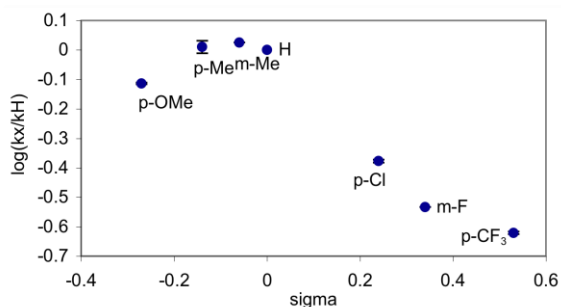
In a representative experiment, the reaction of an equimolar quantity of **6a** and the electron rich substrate **2a** afforded the acetoxyated products **6b** and **2b** in a ratio of 1 : 0.77 ( $k_{6a}/k_{2a} = 1/0.77$ ) (Scheme 2.2).



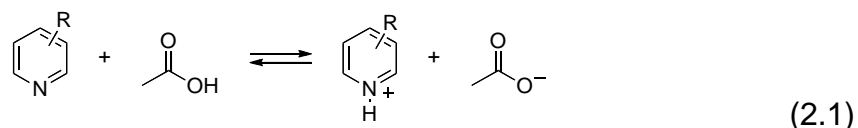
The data from these experiments was used to construct a Hammett plot (Table 2.2, Figure 2.2), which showed a non-linear convex relationship between  $\sigma$  and  $\log(k_X/k_H)$ . Literature reports have demonstrated that such convex plots can be indicative of a change in rate determining step with electronic variation of the substituents.<sup>7</sup> However, in this case, we reasoned that the non-linearity might instead be due to varying degrees of pyridine protonation in the acidic reaction medium (AcOH/Ac<sub>2</sub>O). The  $K_a$  for this acid/base reaction is expected to vary substantially with substitution on the pyridine, thereby changing the concentration of accessible ligand to different extents. As such, we hypothesized that correcting for the concentration of the unprotonated benzyloxybenzylpyridines in AcOH/Ac<sub>2</sub>O might provide a linear Hammett plot for these reactions.

**Table 2.2** Observed Ratios of Benzylpyridines in Competition

Substrate (Xa)	Observed Ratio $k_{Xa}/k_{6a}$
<b>1a</b>	1.07
<b>2a</b>	0.77
<b>3a</b>	0.24
<b>4a</b>	0.42
<b>5a</b>	1.06
<b>7a</b>	0.29

**Figure 2.2.** Hammett Plot for Competition Experiments in AcOH/Ac<sub>2</sub>O

The concentration of each unprotonated benzylpyridine was estimated using the approximation that  $K_a$  is equal to that for the analogous pyridine derivative.<sup>8</sup> The concentrations of **1a-7a** could then be determined using standard acid/base equilibrium to calculate the effective concentration of the substrate (eq 2.1).



The equilibrium expression (eq. 2.1) can be defined as the concentrations of the products divided by the concentrations of the reactants (eq. 2.2). The equilibrium expression can also be defined as the ratio of the rates of acid dissociation (eq. 2.3).

$$K_{\text{eq}} = \frac{[\text{pyr H}^+][\text{AcO}^-]}{[\text{pyridine}][\text{AcOH}]} \quad (2.2)$$

$$K_{\text{eq}} = \frac{K_{\text{a pyridine}}}{K_{\text{a AcOH}}} \quad (2.3)$$

The concentrations of the protonated pyridine and deprotonated acetic acid are both unknown but will be equal to one another, and the initial concentrations of the pyridine and acetic acid can be obtained from the reaction conditions. Furthermore, the  $K_{\text{a}}$  of acetic acid is known and the  $K_{\text{a}}$  of the benzylpyridine can be estimated from published values. The previous equilibrium expressions can be used to solve for the unknown concentration of protonated pyridine  $x$  (eq 2.4).

$$\frac{K_{\text{a pyridine}}}{K_{\text{a AcOH}}} = \frac{x^2}{([\text{pyridine}]_{\text{initial}} - x)([\text{AcOH}]_{\text{initial}} - x)} \quad (2.4)$$

The concentration of the free pyridine can then be obtained from experimental conditions (eq 2.5).

$$\text{conc. of free pyridine} = ([\text{pyridine}]_{\text{initial}} - x) \quad (2.5)$$

The factor  $F$  can simply be defined as the ratio of the concentrations of the unprotonated pyridine substrates obtained from eq 2.5 resulting in equation 2.6.

$$F = \frac{[\text{Xa}]_{\text{corrected}}}{[\text{6a}]_{\text{corrected}}} \quad (2.6)$$

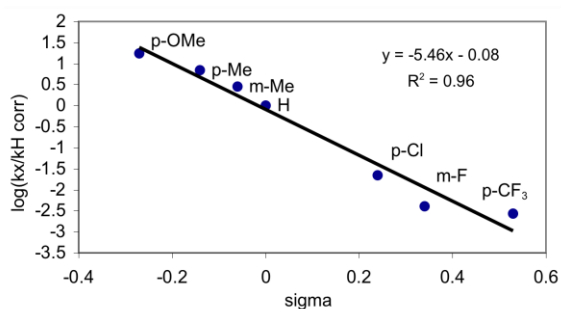
The observed ratio for competing ligands in AcOH can then be adjusted by a factor  $F$  (eq 2.7).

$$\text{ratio}_{\text{corrected}} = F * \text{ratio}_{\text{observed}} \quad (2.7)$$

The experimental ratios of the acetoxylated products ( $k_{\text{X}}/k_{\text{H}}$ ) were then corrected based on the calculated  $F$  factor for each benzylpyridine substrate as summarized in Table 2.3. Gratifyingly, the Hammett plot of this corrected data was linear ( $R^2 = 0.96$ ), and provided a  $\rho$  value of  $-5.46$  for this transformation (Figure 2.3).

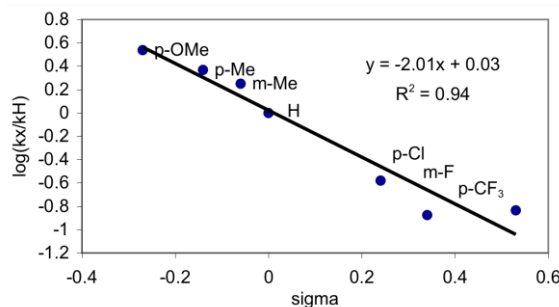
**Table 2.3.** Correction for Unprotonated Benzylpyridine Concentration

Substrate (Xa)	pKa	eff. [pyridine]	Obs. Ratio	Corrected Ratio
1a	6.02	$1.0 \times 10^{-4}$	1.07	7.0
2a	6.55	$3.0 \times 10^{-5}$	0.77	5.0
3a	2.74	$5.3 \times 10^{-2}$	0.24	$3.0 \times 10^{-3}$
4a	3.84	$1.1 \times 10^{-2}$	0.42	$2.2 \times 10^{-2}$
5a	5.63	$3.0 \times 10^{-4}$	1.06	2.8
7a	2.97	$4.3 \times 10^{-2}$	0.29	$4.0 \times 10^{-3}$

**Figure 2.3.** Hammett Plot for Competition Experiments in AcOH/Ac<sub>2</sub>O Corrected for Concentration of Benzylpyridine

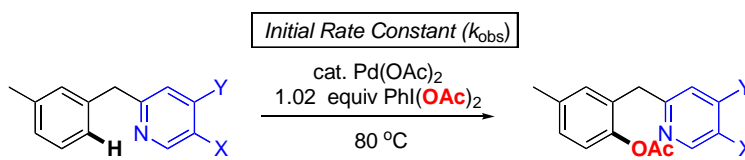
To further gain insights into whether this equilibrium protonation was the source of the non-linearity in AcOH/Ac<sub>2</sub>O, we conducted analogous competition studies in the non-acidic solvent benzene. Under the optimal conditions (5 mol % of Pd(OAc)<sub>2</sub>, 1.02 equiv of PhI(OAc)<sub>2</sub>, 80 °C), these experiments provided a linear Hammett plot ( $R^2 = 0.94$ ) with a  $\rho$  value of  $-2.01$  (Figure 2.4). While the slopes of the Hammett plots in AcOH/Ac<sub>2</sub>O and benzene differ substantially, the negative  $\rho$  values demonstrate that substrates bearing more electron rich directing groups react fastest in both solvents under competition conditions. Notably, the Hammett data looked very similar ( $\rho = -5.20$ ,  $R^2 = 0.94$  in AcOH/Ac<sub>2</sub>O and  $\rho = -1.58$ ,  $R^2 = 0.80$  in benzene) when these competition experiments were analyzed at low conversion (5-15% combined yield of the two products) as opposed to at the completion of the reaction.

**Figure 2.4.** Hammett Plot for Competition Experiments in Benzene



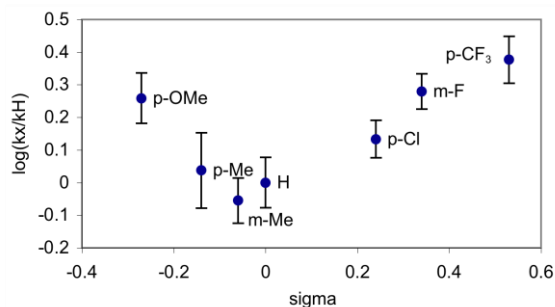
We next sought to determine if the reaction rates of **1a-7a** in isolation showed a similar trend to the competition studies discussed above. As such, we measured the initial rate of Pd-catalyzed C–H activation/acetoxylation in AcOH/Ac<sub>2</sub>O for each benzylpyridine derivative on its own (Table 2.4). A Hammett plot was then constructed from the ratio of the initial rates. This plot showed a non-linear concave relationship between  $\sigma$  and  $\log(k_x/k_H)$  (Figure 2.5). Such concave Hammett plots can be indicative of a change in mechanism as a function of substituent electronics.<sup>7</sup> However, based on the results from the competition experiments above, we hypothesized that the non-linearity was more likely due to competitive protonation of the pyridine.

**Table 2.4.** Individual Initial Rates Studies



Substrate (Xa)	Initial Rates (M/s)
<b>1a</b>	229 x 10 <sup>3</sup>
<b>2a</b>	382 x 10 <sup>3</sup>
<b>3a</b>	525 x 10 <sup>3</sup>
<b>4a</b>	298 x 10 <sup>3</sup>
<b>5a</b>	188 x 10 <sup>3</sup>
<b>7a</b>	391 x 10 <sup>3</sup>

**Figure 2.5.** Hammett Plot for Individual Initial Rates in AcOH/Ac<sub>2</sub>O



Again, correction of the benzyipyridine concentrations based on pyridine  $K_a$  values was examined.<sup>8</sup> Using equations 2.2 through 2.5, the free pyridine concentrations were calculated. Based on the corrected values of the concentration, the adjusted initial rates ( $k'_{\text{obs}}$ ) for the reaction were determined (eq 2.8).

$$k'_{\text{obs}} = k_{\text{obs}} * \frac{[\text{pyridine}_{\text{free}}]}{[\text{pyridine}]} \quad (2.8)$$

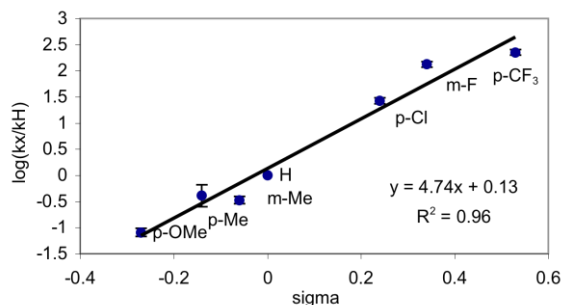
Plotting the adjusted product ratios did indeed result in a linear Hammett plot ( $R^2 = 0.96$ ), this time with a rho value of +4.74 (Table 2.5, Figure 2.6).

**Table 2.5.** Correction for Observed Individual Initial Rates

Substrate	pK <sub>a</sub>	Obs. Initial rate (M/s)	Adj. Initial rate (M/s)
1a	6.02	2.3 x 10 <sup>5</sup>	4.0 x 10 <sup>2</sup>
2a	6.55	3.8 x 10 <sup>5</sup>	1.0 x 10 <sup>2</sup>
3a	2.74	5.3 x 10 <sup>5</sup>	2.3 x 10 <sup>5</sup>
4a	3.84	3.0 x 10 <sup>5</sup>	2.8 x 10 <sup>4</sup>
5a	5.63	1.9 x 10 <sup>5</sup>	1.1 x 10 <sup>3</sup>
7a	2.97	3.9 x 10 <sup>5</sup>	1.4

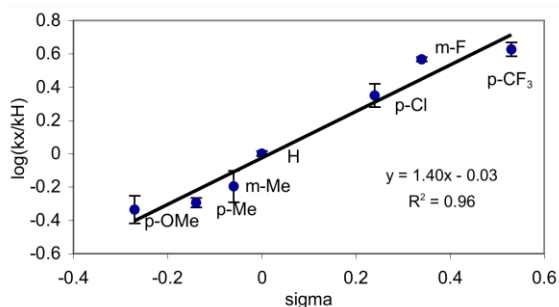


**Figure 2.6.** Hammett Plot for Individual Initial Rates in AcOH/Ac<sub>2</sub>O Corrected for Concentration of Benzylpyridine



Analogous rate studies were also performed in benzene. As shown in Figure 2.7, these provided a linear Hammett plot ( $R^2 = 0.96$ ) with a  $\rho$  value of +1.40. The positive  $\rho$  value obtained in both solvents shows that electron-withdrawing substituents on the pyridine accelerate the rate of acetoxylation. Importantly, this is opposite to the results of the competition experiments. As discussed below, these results suggest that two different steps in the catalytic cycle bearing opposite electronic requirements control the relative rates of functionalization in the presence and absence of other directing groups.

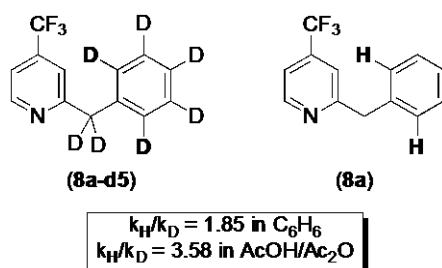
**Figure 2.7.** Hammett Plot for Individual Initial Rates in Benzene



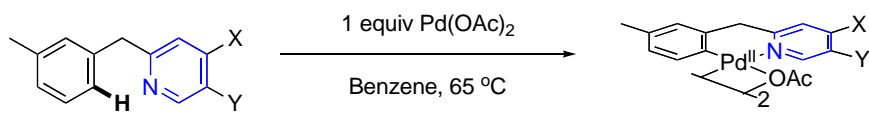
In addition to probing the electronic effect of different directing groups, we also set out to gather insight about the rate-determining step. Dr. Lopa Desai conducted a kinetic isotope experiment using substrate **8a** and substrate **8a-d-5**. By comparing the initial rates of the two substrates, we determined there was a

$k_H/k_D$  value of 1.85 in  $C_6H_6$  and 3.58 in  $AcOH/Ac_2O$  as summarized in Figure 2.8. This value is consistent with a primary kinetic isotope effect (KIE) where C–H(D) bond breaking occurs at some point between the catalyst resting state and the rate-determining step of the reaction. Importantly, similar KIE values (ranging from 1.8 to 4.4) have been observed in related Pd-catalyzed C–H functionalization reactions that proceed by rate-limiting C–H activation.<sup>2h,3e,g,i,m,n,u</sup>

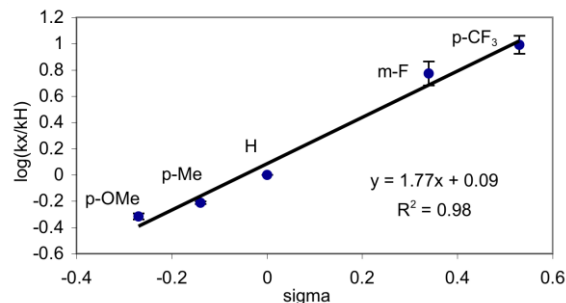
**Figure 2.8.** Kinetic Isotope Effect Experiment



Additional support for C–H activation as the rate-limiting step of the reaction came from stoichiometric studies of the reactions of **1a-7a** with  $Pd(OAc)_2$  (Figure 2.9). The rates of cyclopalladation were monitored in benzene using UV-vis spectroscopy. As shown in Figure 2.9, a Hammett plot was constructed and showed a  $\rho$  value of +1.77 for stoichiometric C–H activation. This value is similar in both sign and magnitude to that obtained in the catalytic individual rate studies ( $\rho = 1.40$  in benzene), providing further evidence to support turnover-limiting cyclopalladation.

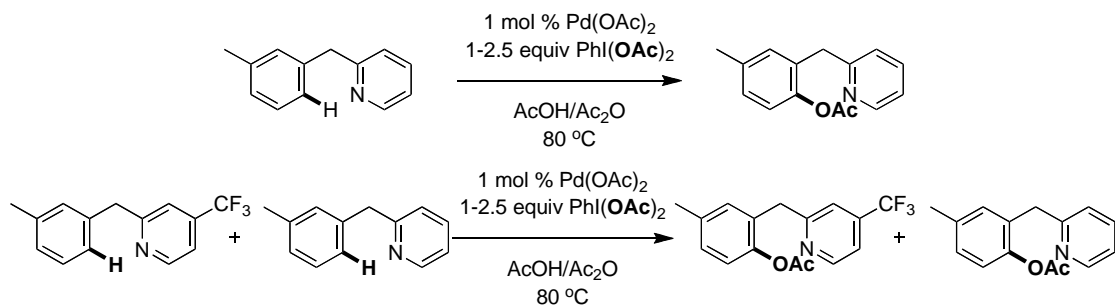
**Table 2.6.** Rates of Stoichiometric Cyclopalladation

Substrate	Initial rate ( $\times 10^3$ ) (M/s)	$\lambda$ (nm)
<b>1a</b>	0.22	320
<b>2a</b>	0.18	325
<b>3a</b>	3.75	350
<b>6a</b>	0.38	310
<b>7a</b>	2.20	330

**Figure 2.9.** Hammett Plot of Stoichiometric Cyclopalladation

We also investigated the order in oxidant for the reaction. Under our optimal conditions for acetoxylation with substrate **6a** the reaction was found to be zero order in  $\text{PhI}(\text{OAc})_2$ . To ensure that the oxidant was not involved in the rate-determining step under conditions where directing groups were in competition, Dr. Lopa Desai tested the order of oxidant in the presence of another substrate (**3a**) for completeness. Under all conditions the oxidant was not involved in the rate determining step and had an order of zero.

**Figure 2.10.** Initial Rates Showed Zero Order as a Function of  $[\text{PhI}(\text{OAc})_2]$ .

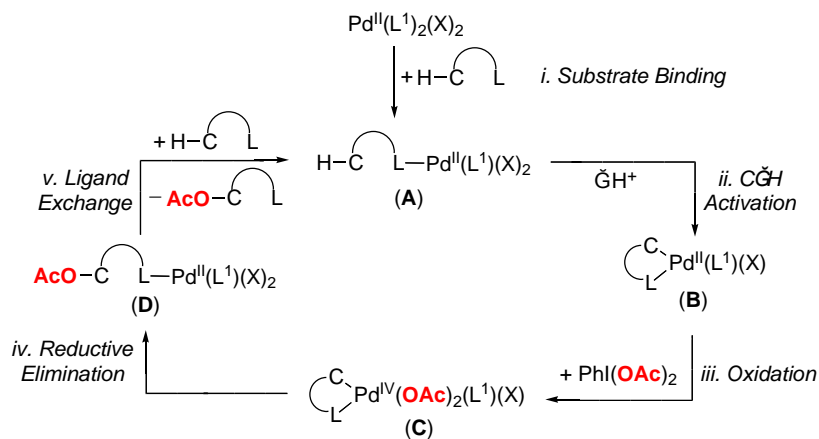


Each of these pieces of mechanistic data can be taken together to better understand the governing principles for directing groups.

### 2.3 Discussion

With all these results in hand, we sought to determine which mechanistic steps dictate the relative and absolute reactivity of a directing group in Pd-catalyzed C–H bond acetoxylation. As summarized in Figure 2.11, the proposed catalytic cycle for these transformations is believed to involve five steps: (i) ligand coordination to the Pd catalyst to generate complex **A**, (ii) cyclometalation to form palladacycle **B**, (iii) oxidation of **B** by  $\text{PhI}(\text{OAc})_2$  to afford a  $\text{Pd}^{\text{IV}}$  intermediate **C**, (iv) C–O bond forming reductive elimination to generate  $\text{Pd}^{\text{II}}$  complex **D**, and (v) ligand exchange to release the product and coordinate a new substrate to the metal center.

**Figure 2.11.** Proposed Catalytic Cycle for Pd-Catalyzed C–H Bond Acetoxylation



Literature precedent can be used to predict how electronic modification of the directing group (L) will affect each step of the catalytic cycle, and thereby gain insights into the selectivity-determining step(s) of these transformations. Modification of L is expected to have a large influence on the thermodynamics (and therefore  $K_{eq}$ ) associated with steps *i* and *v*. Prior work has shown that, with all else being equal, more electron donating ligands form stronger bonds to Pd<sup>II</sup> than their electron deficient analogues.<sup>9,10</sup>

The cyclopalladation reaction (step *ii*) is believed to proceed by an electrophilic mechanism<sup>11</sup> and/or by rate-limiting formation of an agostic intermediate followed by deprotonation.<sup>12,13</sup> Both mechanisms involve the Pd acting as an electrophile; as such, the rate of this step is expected to be accelerated by electron withdrawing ancillary ligands (L).<sup>11,14</sup> The rate of C–O bond-forming reductive elimination from Pd<sup>IV</sup> is also expected to be increased by the presence of electron withdrawing ancillary ligands (L).<sup>15</sup> On the other hand, literature precedent has shown that the oxidation of Pd<sup>II</sup> complexes (step *iii* of the catalytic cycle) is accelerated with more electron donating ligands, which render the metal center more nucleophilic.<sup>16</sup> We can interpret our experimental data on the basis of this analysis in order to gain insights into the selectivity-determining step(s) under individual kinetics and competition conditions.

*Individual Rate Studies.* The individual rate studies with substituted benzylpyridines (Scheme 2.3, Figures 2.6 and 2.7) afforded Hammett plots with  $\rho$  of +1.40 in benzene and +4.74 in AcOH, indicating that the reaction is accelerated with less-basic benzylpyridines. On the basis of the analysis above, these values suggest that either cyclopalladation (step *ii*) or C–O bond-forming reductive elimination (step *iv*) is rate determining.<sup>17</sup> We propose that cyclopalladation is rate-limiting in these systems when considering the complete picture. First, literature precedent suggests that reductive elimination will be fast under our reaction conditions (80 °C), since Pd<sup>IV</sup> complexes of general structure **C** are typically unstable at room temperature.<sup>17,18</sup> Second, the observed KIE

indicates that C–H bond breaking occurs between the catalyst resting state and the rate determining step. Also, the reaction is zero order in oxidant, so the rate-determining step is likely to precede oxidation. In addition, the stoichiometric cyclopalladation electronics are wholly consistent with the electronic effects seen for the catalytic reaction kinetic experiments.

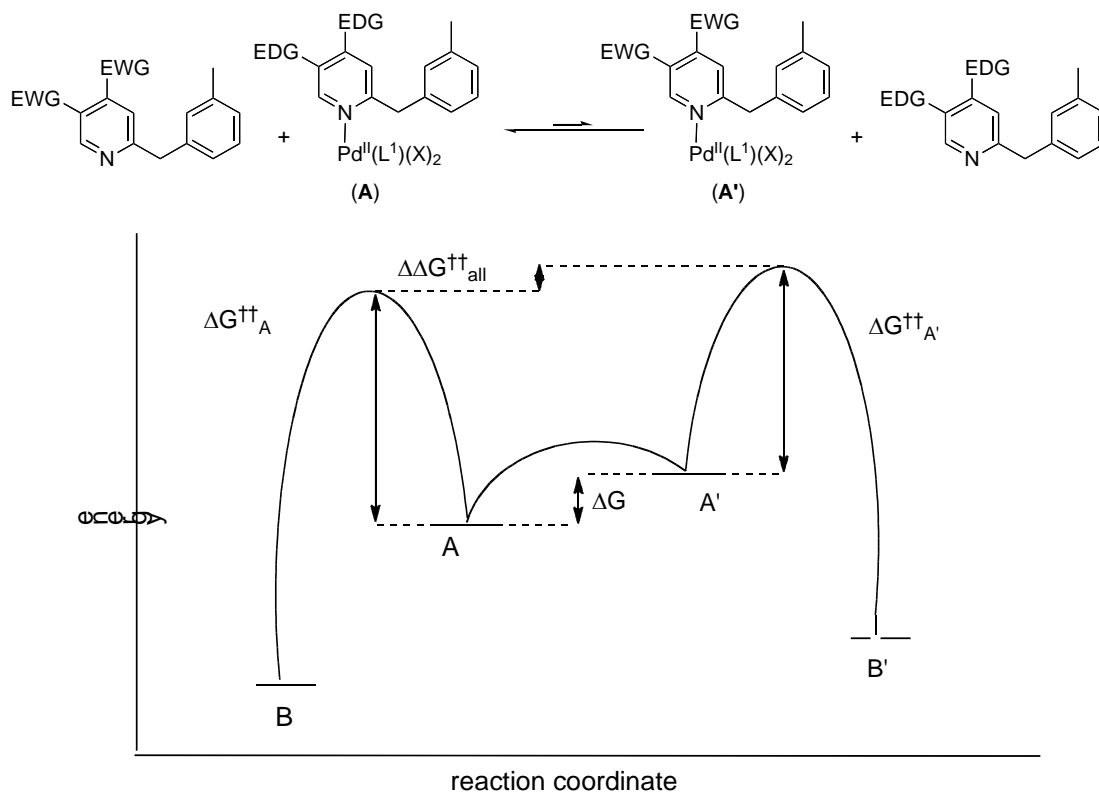
We note that the catalytic experiments described above provided significantly different  $\rho$  values in AcOH/Ac<sub>2</sub>O (+4.74) versus C<sub>6</sub>H<sub>6</sub> (+1.4). Importantly, solvent has also been shown to have a significant effect on the rates of stoichiometric cyclopalladation reactions.<sup>19,20</sup> As such, we propose that the difference in magnitude between the two solvents may be the result of a change in the nature/position of the transition state for C–H activation as a function of reaction medium.

*Competition Experiments.* When multiple potential coordinating functional groups are present in solution, substrates containing more basic directing groups react preferentially. This insight can be concluded from observation of the large negative  $\rho$  value from Hammett plots with substituted benzylpyridine derivatives (Figures 2.3 and 2.4). Furthermore, work completed by Dr. Lopa Desai demonstrated that the most basic directing group (pyridine in substrate **6a**) outcompetes all other tested directing groups (amides, oxime ethers, isoxazolines).<sup>21</sup> In addition, it was demonstrated that heterocyclic ligands with  $pK_a$  values greater than zero (pyridine, pyrimidine, pyrazine, pyrazole) outcompete all substrates with  $pK_a$  values less than zero (oxime ethers, amides and isoxazolines). The above results suggest that either ligand binding/exchange (steps *i* and *v*) or oxidation (step *iii*) controls the relative reactivity of the two substrates under these conditions. Oxidation can be ruled out based on observing the order in oxidant to be zero.

We propose that selectivity under these competition conditions is controlled by the ligand coordination step. More specifically, we propose there are two possible coordination complexes that can form (**A** and **A'** in Figure 2.12) and are expected

to be in rapid equilibrium under the reaction conditions. The coordinated complex (**A** or **A'**) can then undergo cyclopalladation to form the cyclopalladated complexes (**B** or **B'**) from which the acetoxyated products are derived. This type of regime follows selectivity as governed by the Curtin Hammett principle. According to the Curtin Hammett principle, the product distribution from these transformations will be determined by ( $\Delta\Delta G^{\ddagger}_{\text{all}} = \Delta G + \Delta G^{\ddagger}_{\text{AA}'}$ ). The  $\Delta\Delta G^{\ddagger}_{\text{all}}$  term represents the sum of the difference in activation energy added to the difference in thermodynamic energy. This principle is illustrated schematically in Figure 2.12.

**Figure 2.12.** Equilibrium for Substrate Binding and Curtin Hammett Illustration



The  $\Delta G^{\ddagger}_{\text{AA}'}$  term represents the difference in activation energy for the two C–H activation reactions ( $\Delta G^{\ddagger}_{\text{AA}'} = \Delta G^{\ddagger}_{\text{A}} - \Delta G^{\ddagger}_{\text{A}'}$ ). The  $\Delta G$  term represents the difference in energy between the two coordination complexes **A** and **A'** ( $\Delta G =$

$G^{\circ}_{A'} - G^{\circ}_A$ ). (This value can be either positive or negative in sign.) If the sum of these two terms ( $\Delta G + \Delta G^{\ddagger}_{AA}$ ) is positive in sign then formation of **B** is favored, while if the sum is negative in sign then the formation of **B'** is favored. As such, the proposed effects of the equilibrium for ligand exchange in the competition experiments are consistent with the Curtin-Hammett principle as long as the difference in the energy ( $\Delta G$ ) between the two Pd<sup>II</sup> pyridine coordination complexes is greater than the difference in the activation energies ( $\Delta G^{\ddagger}_{AA'}$ ) for the C–H activation step (the putative slow step of these transformations).

## 2.4 Application

The observed effects in the competition studies have important implications for future applications of this chemistry. In non-acidic solvents like benzene, the basicity of a directing group appears to serve as a reasonable predictor of its relative reactivity. However, an acidic solvent can be used to attenuate inherent reactivity differences by effectively “protecting” a potential ligand in its protonated form. We anticipate that this and related strategies can be pursued to obtain, alter, or improve the selectivity of directed C-H functionalization in the context of complex molecules. Future studies will continue to explore how these effects (and the effects of other solvents and additives) translate into predicting and controlling the dominant directing group in more complex systems.

## 2.5 Conclusions

In summary, we have conducted detailed studies to elucidate the electronic requirements of a directing group in Pd-catalyzed directed arene acetoxylation reactions. Under conditions where there is an individual directing group, the reaction is fastest with those substrates that contain electron-withdrawing substituents on the directing group and a significant kinetic isotope effect is observed, indicating that cyclopalladation is turnover limiting. However, under competition conditions, substrates with electron rich directing groups react preferentially, suggesting that their relative reactivities are dictated by  $K_{eq}$  for substrate coordination under these conditions. We anticipate that the mechanistic



insights gleaned from this and related work will ultimately prove valuable in future applications of this chemistry.

## 2.6 Experimental

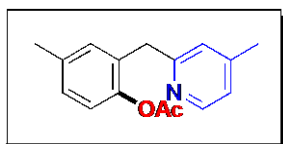
*General Procedure for Directed C–H Bond Acetoxylation.* In a 20 mL vial,  $\text{PhI}(\text{OAc})_2$  (0.49-0.86 mmol, 1.02-1.80 equiv) and  $\text{Pd}(\text{OAc})_2$  (1.08 mg, 0.0048 mmol, 0.01 equiv) were combined in a mixture of AcOH (2.0 mL) and  $\text{Ac}_2\text{O}$  (2.0 mL). Substrate (0.48 mmol, 1.0 equiv) was added, the vial was sealed with a Teflon-lined cap, and the resulting solution was heated at 100 °C for 3-24 h. The reaction was cooled to room temperature, and the solvent was removed under vacuum. The resulting brown oil was purified by chromatography on silica gel. Each substrate was optimized for reaction time and equivalent of the oxidant as described in the characterization section.

*General Procedure for Kinetics Experiments.* Kinetics experiments were run in two dram vials sealed with Teflon-lined caps. Each data point represents a reaction in an individual vial, with each vial containing an identical concentration of oxidant, catalyst, and substrate. The vials were charged with  $\text{PhI}(\text{OAc})_2$  (0.0158 g, 0.049 mmol, 1.02 equiv, added as a solid), substrate (0.048 mmol, 1.0 equiv, added as a 0.96 M stock solution in AcOH), and  $\text{Pd}(\text{OAc})_2$  (0.11 mg, 0.00048 mmol, 0.01 equiv, added as a 0.0096 M stock solution in AcOH), and the resulting mixtures were diluted to a total volume of 400  $\mu\text{L}$  of a 1 : 1 mixture of AcOH and  $\text{Ac}_2\text{O}$ . The vials were then heated at 80 °C for various amounts of time. Reactions were quenched by cooling the vial at 0 °C for 5 min, followed by the addition of a 2% solution of pyridine in  $\text{CH}_2\text{Cl}_2$  (2 mL). An internal standard (pyrene) was then added, and the reactions were analyzed by gas chromatography. Each reaction was monitored by gas chromatography to ~10% (8.6-11.0%) conversion, and rate constants were calculated for each reaction using the initial rates method. Each kinetics experiment was run in triplicate, and the data shown in the Hammett plots represent an average of these three runs.

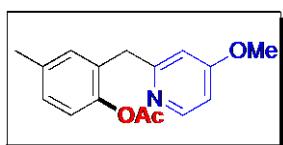
*General Procedure for Competition Experiments.* A two dram vial was sequentially charged with  $\text{PhI}(\text{OAc})_2$  (0.0158 g, 0.049 mmol, 1.02 equiv, added

as a solid), substrate A (0.048 mmol, 1.0 equiv, added as a 0.96 M stock solution in AcOH), substrate B (0.048 mmol, 1.0 equiv, added as a 0.96 M stock solution in AcOH), and Pd(OAc)<sub>2</sub> (0.11 mg, 0.00048 mmol, 0.01 equiv, added as a 0.0096 M stock solution in AcOH), and the resulting mixtures were diluted to a total volume of 400 μL of a 1 : 1 mixture of AcOH and Ac<sub>2</sub>O. The reaction was heated at 80 °C for 12 h, and then cooled to room temperature. A GC standard (pyrene) was added, and the reaction was analyzed by gas chromatography.

## 2.7 Characterization

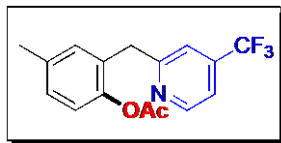


The reaction was run for 4 h with 1.1 equiv of PhI(OAc)<sub>2</sub>. The product 1b was obtained as a yellow oil (91.9 mg, 75% yield, R<sub>f</sub> = 0.27 in 64% hexanes/36% ethyl acetate). <sup>1</sup>H NMR (CDCl<sub>3</sub>): δ 8.36 (d, *J* = 5.2 Hz, 1H), 7.07-7.04 (multiple peaks, 2H), 6.94-6.90 (multiple peaks, 2H), 6.84 (s, 1H), 4.00 (s, 2H), 2.29 (s, 3H), 2.24 (s, 3H), 2.16 (s, 3H). <sup>13</sup>C{<sup>1</sup>H} NMR (CDCl<sub>3</sub>): δ 169.40, 159.59, 148.81, 147.47, 146.76, 135.75, 131.71, 130.98, 128.31, 123.65, 122.29, 122.21, 39.10, 20.89, 20.80, 20.70. IR (thin film): 1760 cm<sup>-1</sup>. HRMS electrospray (*m/z*): [M+Na<sup>+</sup>] Calcd for C<sub>16</sub>H<sub>17</sub>NO<sub>2</sub>, 278.1157; Found, 278.1147.

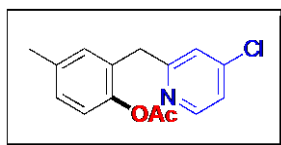


The reaction was run for 4 h with 1.02 equiv of PhI(OAc)<sub>2</sub>. The product 2b was obtained as a yellow oil (91.2 mg, 70% yield, R<sub>f</sub> = 0.27 in 45% hexanes/55% ethyl acetate). <sup>1</sup>H NMR (500 MHz, CDCl<sub>3</sub>): δ 8.36 (d, *J* = 5.6 Hz, 1H), 7.09-7.07 (multiple peaks, 2H), 6.95 (d, *J* = 8.0 Hz, 1H), 6.66 (dd, *J* = 6.0, 2.4 Hz, 1H), 6.55 (d, *J* = 2.4 Hz, 1H), 4.01 (s, 2H), 3.77 (s, 3H), 2.32 (s, 3H) 2.20 (s, 3H). <sup>13</sup>C{<sup>1</sup>H} NMR (500 MHz CDCl<sub>3</sub>): δ 169.36, 166.05, 161.53, 150.25, 146.78, 135.74, 131.65, 130.72, 128.35, 122.21, 108.74, 107.56, 54.86, 39.19, 20.76, 20.70. IR

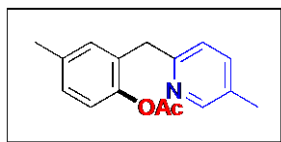
(thin film): 1759  $\text{cm}^{-1}$ . HRMS electrospray ( $m/z$ ):  $[\text{M}+\text{Na}^+]$  Calcd for  $\text{C}_{16}\text{H}_{17}\text{NO}_3$ , 294.1106; Found, 294.1108.



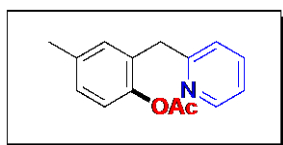
The reaction was run for 4.5 h with 1.02 equiv of  $\text{PhI}(\text{OAc})_2$ . The product 3b was obtained as a colorless oil (135.1 mg, 91% yield,  $R_f = 0.27$  in 79% hexanes/21% ethyl acetate).  $^1\text{H}$  NMR (500 MHz,  $\text{CDCl}_3$ ):  $\delta$  8.71 (d,  $J = 5.5$  Hz, 1H), 7.34 (d,  $J = 5.0$  Hz, 1H), 7.29 (s, 1H), 7.11-7.09 (multiple peaks, 2H), 6.96 (d,  $J = 8.5$  Hz, 1H), 4.12 (s, 2H), 2.33 (s, 3H), 2.19 (s, 3H).  $^{13}\text{C}\{^1\text{H}\}$  NMR ( $\text{CDCl}_3$ ):  $\delta$  169.26, 161.59, 150.22, 146.82, 138.66 (q,  $^2J_{\text{C-F}} = 33.7$  Hz), 136.06, 131.71, 129.95, 128.88, 122.76 (q,  $^1J_{\text{C-F}} = 271.7$  Hz), 122.43, 118.47 (q,  $^3J_{\text{C-F}} = 3.7$  Hz), 116.96 (q,  $^3J_{\text{C-F}} = 3.7$  Hz), 39.47, 20.82, 20.71.  $^{19}\text{F}\{^1\text{H}\}$  NMR ( $\text{CDCl}_3$ ):  $\delta$  -64.85. IR (thin film): 1753  $\text{cm}^{-1}$ . HRMS electrospray ( $m/z$ ):  $[\text{M}+\text{Na}^+]$  Calcd for  $\text{C}_{16}\text{H}_{14}\text{F}_3\text{NO}_2$ , 332.0874; Found, 332.0868.



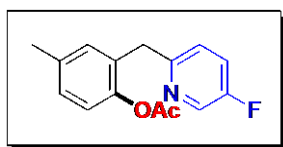
The reaction was run for 6 h with 1.02 equiv of  $\text{PhI}(\text{OAc})_2$ . The product 4b was obtained as a yellow oil (97.9 mg, 74% yield,  $R_f = 0.27$  in 80% hexanes/20% ethyl acetate).  $^1\text{H}$  NMR ( $\text{CDCl}_3$ ):  $\delta$  8.42 (d,  $J = 5.2$  Hz, 1H), 7.13 (dd,  $J = 5.6$  Hz, 2.0 Hz, 1H), 7.09-7.07 (multiple peaks, 2H), 7.06 (d,  $J = 2.0$  Hz, 1H), 6.95 (d,  $J = 8.8$  Hz, 1H), 4.03 (s, 2H), 2.32 (s, 3H), 2.20 (s, 3H).  $^{13}\text{C}\{^1\text{H}\}$  NMR ( $\text{CDCl}_3$ ):  $\delta$  169.32, 161.62, 149.98, 146.76, 144.35, 136.97, 131.68, 130.06, 128.74, 123.16, 122.36, 121.75, 39.09, 20.80, 20.74. IR (thin film): 1760  $\text{cm}^{-1}$ . HRMS electrospray ( $m/z$ ):  $[\text{M}+\text{Na}^+]$  Calcd for  $\text{C}_{15}\text{H}_{14}\text{ClNO}_2$ , 298.0611; Found, 298.0600.



The reaction was run for 4 h with 1.1 equiv of  $\text{PhI}(\text{OAc})_2$ . The product 5b was obtained as a yellow oil (90.7 mg, 74% yield,  $R_f = 0.27$  in 64% hexanes/36% ethyl acetate).  $^1\text{H}$  NMR ( $\text{CDCl}_3$ ):  $\delta$  8.36 (t,  $J = 0.8$  Hz, 1H), 7.37 (dd,  $J = 8.0$  Hz, 2.4 Hz, 1H), 7.08-7.05 (multiple peaks, 2H), 6.94 (d,  $J = 2.0$  Hz, 1H), 6.92 (d,  $J = 1.6$  Hz, 1H), 4.01 (s, 2H), 2.30 (s, 3H), 2.28 (s, 3H) 2.18 (s, 3H).  $^{13}\text{C}\{^1\text{H}\}$  NMR ( $\text{CDCl}_3$ ):  $\delta$  169.43, 156.89, 149.43, 146.75, 137.02, 135.76, 131.66, 131.14, 130.46, 128.27, 122.29, 122.19, 38.75, 20.80, 20.76, 17.96 IR (thin film): 1760  $\text{cm}^{-1}$ . HRMS electrospray (m/z):  $[\text{M}+\text{Na}^+]$  Calcd for  $\text{C}_{16}\text{H}_{17}\text{NO}_2$ , 278.1157; Found, 278.1150.



The reaction was run for 6 h with 1.02 equiv of  $\text{PhI}(\text{OAc})_2$ . The product 6b was obtained as a yellow oil (86.9 mg, 75% yield,  $R_f = 0.27$  in 70% hexanes/30% ethyl acetate).  $^1\text{H}$  NMR ( $\text{CDCl}_3$ ):  $\delta$  8.52 (dd,  $J = 4.8, 1.6$  Hz, 1H), 7.54 (dt,  $J = 7.6, 1.6$  Hz, 1H), 7.11-7.02 (multiple peaks, 4H), 6.94 (d,  $J = 8.0$  Hz, 1H), 4.06 (s, 2H), 2.30 (s, 3H), 2.16 (s, 3H).  $^{13}\text{C}\{^1\text{H}\}$  NMR ( $\text{CDCl}_3$ ):  $\delta$  169.37, 159.88, 149.03, 146.79, 136.44, 135.78, 131.72, 130.83, 128.38, 122.85, 122.24, 121.24, 39.21, 20.78, 20.69. IR (thin film): 1759  $\text{cm}^{-1}$ . HRMS electrospray (m/z):  $[\text{M}+\text{H}]^+$  calcd for  $\text{C}_{15}\text{H}_{15}\text{NO}_2$ , 242.1181; found, 242.1177.



The reaction was run for 10 h with 1.02 equiv of  $\text{PhI}(\text{OAc})_2$ . The product 7b was obtained as a colorless oil (115.7 mg, 93% yield,  $R_f = 0.27$  in 80% hexanes/20% ethyl acetate).  $^1\text{H}$  NMR (500 MHz,  $\text{CDCl}_3$ ):  $\delta$  8.38 (d,  $J = 3.0$  Hz, 1H), 7.29 (td,  $J = 8.5, 3.0$  Hz, 1H), 7.09-7.07 (multiple peaks, 2H), 7.04 (dd,  $J = 8.8, 4.5$  Hz, 1H), 6.94 (d,  $J = 8.0$  Hz, 1H), 4.03 (s, 2H), 2.31 (s, 3H), 2.20 (s, 3H).  $^{13}\text{C}\{^1\text{H}\}$  NMR ( $\text{CDCl}_3$ ):  $\delta$  169.47, 158.15 (d,  $^1J_{\text{C-F}} = 252.7$  Hz), 155.94 (d,  $^3J_{\text{C-F}} = 4.2$  Hz), 146.81, 137.10 (d,  $^2J_{\text{C-F}} = 23.4$  Hz), 135.99, 131.65, 130.80, 128.61, 123.65 (d,  $^4J_{\text{C-F}} = 4.4$  Hz), 123.31 (d,  $^2J_{\text{C-F}} = 18.3$  Hz), 122.38, 38.49, 20.86,

20.80.  $^{19}\text{F}\{^1\text{H}\}$  NMR ( $\text{CDCl}_3$ ):  $\delta$   $\square$ -130.93. IR (thin film): 1760  $\text{cm}^{-1}$ . HRMS electrospray (m/z):  $[\text{M}+\text{Na}^+]$  Calcd for  $\text{C}_{15}\text{H}_{14}\text{FNO}_2$ , 282.0906; Found, 282.0905.

## 2.8 References

<sup>1</sup> (a) Kubota, A.; Sanford, M. S. *Synthesis* **2011**, 2579-2589. (b) Neufeldt, S. R.; Sanford, M. S. *Org. Lett.* **2010**, 12, 532-535. (c) Hull, K. L.; Sanford, M. S. *J. Am. Chem. Soc.* **2007**, 129, 11904. (d) Hull, K. L.; Lanni, E. L.; Sanford, M. S. *J. Am. Chem. Soc.* **2006**, 128, 14047. (e) Hull, K. L.; Anani, W. Q.; Sanford, M. S. *J. Am. Chem. Soc.* **2006**, 128, 7134. (f) Kalyani, D.; Dick, A. R.; Anani, W. Q.; Sanford, M. S. *Tetrahedron* **2006**, 62, 11483. (g) Kalyani, D.; Dick, A. R.; Anani, W. Q.; Sanford, M. S. *Org. Lett.* **2006**, 8, 2523. (h) Desai, L. V.; Malik, H. A.; Sanford, M. S. *Org. Lett.* **2006**, 8, 1141. (i) Kalyani, D.; Sanford, M. S. *Org. Lett.* **2005**, 7, 4149. (j) Kalyani, D.; Deprez, N. R.; Desai, L. V.; Sanford, M. S. *J. Am. Chem. Soc.* **2005**, 127, 7330. (k) Desai, L. V.; Hull, K. L.; Sanford, M. S. *J. Am. Chem. Soc.* **2004**, 126, 2300. (l) Dick, A. R.; Hull, K. L.; Sanford, M. S. *J. Am. Chem. Soc.* **2004**, 126, 2300.

<sup>2</sup> For selected examples of palladium-catalyzed directed C–H activation/C–heteroatom bond forming reactions, see: (a) Huang, C.; Ghatadze, N.; Chattopadhyay, B.; Gevorgyan, V. *J. Am. Chem. Soc.* **2011**, 133, 17630-17633. (b) Wei, Y.; Yoshikai, N. *Org. Lett.* **2011**, 13, 5504-5507. (c) Lyons, T. W.; Sanford, M. S.; *Chem. Rev.* **2010**, 110, 1147-1169. (d) Inamoto, K.; Saito, T.; Katsuno, M.; Sakamoto, T.; Hiroya, K. *Org. Lett.* **2007**, 9, 2931. (e) Thu, H. Y.; Yu, W. Y.; Che, C. M. *J. Am. Chem. Soc.* **2006**, 128, 9048. (f) Wan, X.; Ma, Z.; Li, B.; Zhang, K.; Cao, S.; Zhang, S.; Shi, Z. *J. Am. Chem. Soc.* **2006**, 128, 7416. (g) Reddy, B. V. S.; Reddy, L. R.; Corey, E. J. *Org. Lett.* **2006**, 8, 3391. (h) Wang, D.; Hao, X.; Wu, D.; Yu, J. Q. *Org. Lett.* **2006**, 8, 3387. (i) Yu, J. Q.; Giri, R.; Chen, X. *Org. Biomol. Chem.* **2006**, 4, 4041 and references therein. (j) Tsang, W. C. P.; Zheng, N.; Buchwald, S. L. *J. Am. Chem. Soc.* **2005**, 127, 14560. (k) Giri, R.; Liang, J.; Lei, J. G.; Li, J. J.; Wang, D. H.; Chen, X.; Naggar, I. C.; Guo, C.; Foxman, B. M.; Yu, J. Q. *Angew. Chem., Int. Ed.* **2005**, 44, 7420. (l) Giri, R.; Chen, X.; Yu, J. Q. *Angew. Chem., Int. Ed.* **2005**, 44, 2112. (m) Dangel, B. D.; Johnson, J. A.; Sames, D. *J. Am. Chem. Soc.* **2001**, 123, 8149.

<sup>3</sup> For selected examples of palladium-catalyzed directed C–H activation/C–C bond forming reactions, see: (a) Chen, X.; Engle, K. M.; Wang, D.-H.; Yu, J.-Q. *Angew. Chem., Int. Ed.* **2009**, 48, 5094-5115. (b) Yu, W.-Y.; Sit, W. N.; Lai, K.-M.; Zhou, Z.; Chan, A. S. C. *J. Am. Chem. Soc.* **2008**, 130, 3304. (c) Beccalli, E. M.; Broggini, G.; Martinelli, M.; Sottocornola, S. *Chem. Rev.* **2007**, 107, 5318. (d) Alberico, D.; Scott, M. E.; Lautens, M. *Chem. Rev.* **2007**, 107, 174. (e) Cai, G.; Fu, Y.; Li, Y.; Wan, X.; Shi, Z. *J. Am. Chem. Soc.* **2007**, 129, 7666. (f) Giri, R.; Maugel, N. L.; Li, J. J.; Wang, D. H.; Breazzano, S. P.; Saunders, L. B. Yu, J. Q. *J. Am. Chem. Soc.* **2007**, 129, 3510. (g) Xia, J.-B.; You, S.-L. *Organometallics*

**2007**, 26, 4869. (h) Chiong, H. A.; Daugulis, O. *Org. Lett.* **2007**, 9, 1449. (i) Shi, Z. J.; Li, B.; Wan, X.; Cheng, J.; Fang, Z.; Cao, B.; Qin, C.; Wang, Y. *Angew. Chem., Int. Ed.* **2007**, 46, 5554. (j) Chen, X.; Goodhue, C. E.; Yu, J. Q. *J. Am. Chem. Soc.* **2006**, 128, 12634. (k) Chen, X.; Li, J. J.; Hao, X. S.; Goodhue, C. E.; Yu, J. Q. *J. Am. Chem. Soc.* **2006**, 128, 78. (l) Orito, K.; Miyazawa, M.; Nakamura, T.; Horibata, A.; Ushito, H.; Nagasaki, H.; Yuguchi, M.; Yamashita, S.; Yamazaki, T.; Tokuda, M. *J. Org. Chem.* **2006**, 71, 5951. (m) Zaitsev, V. G.; Shabashov, D.; Daugulis, O. *J. Am. Chem. Soc.* **2005**, 127, 13154. (n) Zaitsev, V. G.; Daugulis, O. *J. Am. Chem. Soc.* **2005**, 127, 4156. (o) Shabashov, D.; Daugulis, O. *Org. Lett.* **2005**, 7, 3657. (p) Daugulis, O.; Zaitsev, V. G. *Angew. Chem., Int. Ed.* **2005**, 44, 4046. (q) Orito, K.; Horibata, A.; Nakamura, T.; Ushito, H.; Nagasaki, H.; Yuguchi, M.; Yamashita, S.; Tokuda, M. *J. Am. Chem. Soc.* **2004**, 126, 14342. (r) Wakui, H.; Kawasaki, S.; Satoh, T.; Miura, M.; Nomura, M. *J. Am. Chem. Soc.* **2004**, 126, 8658. (s) Hennessy, E. J.; Buchwald, S. L. *J. Am. Chem. Soc.* **2003**, 125, 12084. (t) Ritleng, V.; Sirlin, C.; Pfeffer, M. *Chem. Rev.* **2002**, 102, 1731. (u) Boele, M. D. K.; van Strijdonck, G. P. F.; de Vries, A. H. M.; Kamer, P. C. J.; de Vries, J. G.; van Leeuwen, P. W. N. M. *J. Am. Chem. Soc.* **2002**, 124, 1586. (v) Dyker, G. *Angew. Chem., Int. Ed. Engl.* **1999**, 38, 1698. (w) Tremont, S. J.; Rahman, H. U. *J. Am. Chem. Soc.* **1984**, 106, 5759.

<sup>4</sup> (a) Ali, A.; Hunt, J. A.; Kallashi, F.; Kowalchick, J. E.; Kim, D.; Smith, C. J.; Sinclair, P. J.; Sweis, R. F.; Taylor, G. E.; Thompson, C. F.; Chen, L.; Quraishi, N. PCT Int. Appl. WO 2007070173, **2007**. (b) Zhou, P.; Bernotas, R. C.; Li, Y.; Nowak, P. W.; Cole, D. C.; Manas, E. S.; Fan, Y.; Yan, Y. PCT Int. Appl. WO 2007078813, **2007**. (c) Chen, J.; Deady, L. W.; Kaye, A. J.; Finlay, G. J.; Baguley, B. C.; Denny, W. A. *Bioorg. Med. Chem.* **2002**, 10, 2381

<sup>5</sup> Kalyani, D.; Sanford, M. S. *Org. Lett.* **2005**, 7, 4149.

<sup>6</sup> Notably a similar strategy has for electronically isolating a n aryl ring from a directing group has been recently reported by Yu and co-workers in mechanistic studies of Pd-catalyzed oxazoline-directed arene oxygenation: Li, J. J.; Giri, R.; Yu, J. Q. *Tetrahedron* **2008**, 64, 6987.

<sup>7</sup> Anslyn, E.K.; Dougherty, D.A. *Modern Physical Organic Chemistry*, University Science Books: Sausalito, **2006**, 448

<sup>8</sup> All  $pK_a$  values used are in solution phase. (a) [research.chem.psu.edu/brpgroup/pKa\\_compilation.pdf](http://research.chem.psu.edu/brpgroup/pKa_compilation.pdf) (b) Borowiak-Resterna, A.; Szymanowski, J.; Voelkel, A. *J. Radioanal. Nucl. Chem. Art.* **1996**, 208, 75-86.

<sup>9</sup> (a) Jeon, S. L.; Loveless, D. M.; Yount, W. C.; Craig, S. L. *Inorg. Chem.* **2006**, 45, 11060. (b) Manen, H-J; Nakashima, K.; Shinkai, S.; Kooijman, H.; Spek, A. L.; Veggel, F. C. J. M.; Reinhoudt, D. N. *Eur. J. Inorg. Chem.* **2000**, 2533.

- 
- <sup>10</sup> Yagyu, T.; Iwatsuki, S.; Aizawa, S.; Funahashi, S. *Bull. Chem. Soc. Jpn.* **1998**, *71*, 1857.
- <sup>11</sup> (b) Ryabov, A. D. *Chem. Rev.* **1990**, *90*, 403 and references therein. (c) Ryabov, A. D.; Sakodinskaya, I. K.; Yatsimirsky, A. K. *J. Chem. Soc., Dalton Trans.* **1985**, 2629.
- <sup>12</sup> Davies, D. L.; Donald, S. M. A.; Macgregor, S. A. *J. Am. Chem. Soc.* **2005**, *127*, 13754.
- <sup>13</sup> (a) Lafrance, M.; Gorelsky, S. I.; Fagnou, K. *J. Am. Chem. Soc.* **2007**, *129*, 14570. (b) Stuart, D. R.; Fagnou, K. *Science* **2007**, *316*, 1172. (c) Lafrance, M.; Fagnou, K. *J. Am. Chem. Soc.* **2006**, *128*, 16496. (d) Lafrance, M.; Rowley, C. N.; Woo, T. K.; Fagnou, K. *J. Am. Chem. Soc.* **2006**, *128*, 8754. (e) Garcia-Cuadrado, D.; Braga, A. A. C.; Maseras, F.; Echavarren, A. M. *J. Am. Chem. Soc.* **2006**, *128*, 1066. (f) Campeau, L. C.; Parisien, Jean, A.; Fagnou, K. *J. Am. Chem. Soc.* **2006**, *128*, 581. (g) Campeau, L. C.; Parisien, M.; Leblanc, M.; Fagnou, K. *J. Am. Chem. Soc.* **2004**, *126*, 9186.
- <sup>14</sup> Gutierrez, M. A.; Newkome, G. R.; Selbin, J. *J. Organomet. Chem.* **1980**, *202*, 341.
- <sup>15</sup> For examples of analogous electronic effects in reductive elimination from Pd<sup>II</sup>, see: (a) Graham, D. C.; Cavell, K. J.; Yates, B. F. *Dalton Trans.* **2006**, 1768. (b) Nolan, S. P. In *Palladium in Organic Synthesis*; Tsuji, J. Topics in Organometallic Chemistry; Springer-Verlag: Berlin, Germany, **2005**, Vol. 14, pp 241-272.
- <sup>16</sup> (a) Valk, J. M.; Boersma, J.; van Koten, G. *Organometallics* **1996**, *15*, 4366. (b) Alsters, P. L.; Teunissen, H. T.; Boersma, J.; Spek, A. L.; van Koten, G. *Organometallics* **1993**, *12*, 4691.
- <sup>17</sup> Stability/reductive elimination from Pd<sup>IV</sup> complexes with one alkyl/aryl ligand and 3 other X-type ligands: Alsters, P. L.; Engel, P. F.; Hogerheide, M. P.; Copijn, M.; Spek, A. L.; van Koten, G. *Organometallics* **1993**, *12*, 1831.
- <sup>18</sup> Some Pd<sup>IV</sup> complexes containing multiple  $\sigma$ -alkyl and/or  $\sigma$ -aryl ligands have been isolated and shown to be stable at room temperature or above. (a) Markies, B. A.; Canty, A. J.; Boersma, J.; van Koten, G. *Organometallics* **1994**, *13*, 2053. (b) Byers, P. K.; Canty, A. J.; Skelton, B. W.; White, A. H. *J. Chem. Soc., Chem. Commun.*, **1986**, 1722. However, the proposed intermediate in the current transformations is a mono-aryl Pd<sup>IV</sup> species (**B**). (c) Dick, A. R.; Kampf, J. W.; Sanford, M. S. *J. Am. Chem. Soc.* **2005**, *127*, 12790.
- <sup>19</sup> (a) Gomez, M.; Granell, J.; Martinez, M. *Eur. J. Inorg. Chem.* **2000**, 217. (b) Ryabov, A. D. *Inorg. Chem.* **1987**, *26*, 1252.

---

<sup>20</sup> A similar  $\rho$  value of -1.7 to -2.1 in DMSO was observed by Craig et al in studying the substituted pyridine coordination to 1,4-phenylene bridged bimetallic palladium complexes containing tridentate ligands

<sup>21</sup> Desai, L. V.; Stowers, K. J.; Sanford, M. S. *J. Am. Chem. Soc.* **2008**, *130*, 13285-13293.



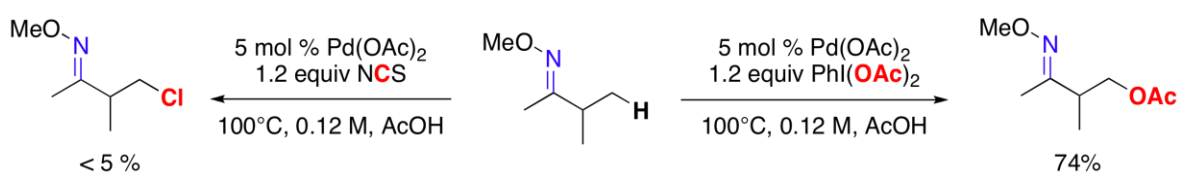
## Chapter 3: Mechanism of C–H Chlorination

### 3.1 Introduction

Palladium-catalyzed ligand-directed C–H bond functionalization has become a valuable synthetic method for the selective oxidation of organic molecules.<sup>1</sup> Over the past 5 years, numerous Pd-catalyzed reactions have been developed for the directed oxygenation,<sup>2</sup> halogenation,<sup>3</sup> amination,<sup>4</sup> sulfonylation,<sup>5</sup> and arylation<sup>1</sup> of both  $sp^2$  and  $sp^3$  C–H bonds. Furthermore, these transformations have been applied to structurally diverse organic scaffolds, including amino acid derivatives<sup>2c</sup> and drug substrates.<sup>6</sup>

While significant progress has been made in the development of new reactions, detailed mechanistic studies in this area have received considerably less attention.<sup>7,8</sup> One major question which has yet to be studied concerns the differences between the substrate scope of chlorination versus the scope of acetoxylation. For example, as summarized in Scheme 3.1, the oxime ether of 3-methyl butanone undergoes Pd-catalyzed C–H acetoxylation with  $\text{PhI}(\text{OAc})_2$  in 74% yield, while under analogous conditions <5% of the chlorinated product was generated using N-chlorosuccinimide (NCS) as oxidant.

**Scheme 3.1.** Representative Example of Different Substrate Scope for Acetoxylation versus Chlorination

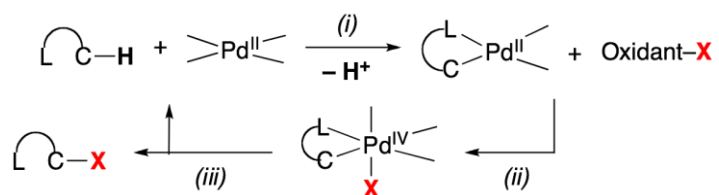


It is notable that both sets of conditions tolerate and functionalize similar  $sp^2$  hybridized C–H bonds, albeit typically with different yields. One way to further understand this divergent reactivity would be to study the mechanism of

chlorination as compared to acetoxylation. An improved mechanistic understanding could facilitate (i) the development of new catalysts with improved catalytic activity and substrate scope as well as (ii) the rational implementation of strategies for controlling the chemo-, diastereo-, enantio- and site-selectivity of C–H functionalization reactions. This chapter describes an investigation of the mechanism of pyridine-directed C–H bond chlorination with *N*-chlorosuccinimide (NCS). We report on the optimization of the precatalyst, elucidation of the turnover limiting step, and mechanistic comparison to related Pd-catalyzed C–H acetoxylation reactions.

Pd-catalyzed C–H functionalization has been proposed to proceed by the general catalytic cycle outlined in Scheme 3.2.<sup>3,8c,9</sup> This cycle begins with ligand directed C–H activation (*i*), which is followed by oxidation of the resulting palladacycle to a monomeric Pd<sup>IV</sup> species (or a related Pd<sup>III</sup>–Pd<sup>III</sup> dimer) (*ii*).<sup>7e,8c,d</sup> Finally, C–X bond-forming reductive elimination (*iii*) regenerates the catalyst and releases the functionalized product. Previous studies have demonstrated that electrophilic chlorinating reagents like *N*-chlorosuccinimide (NCS)<sup>3c</sup> and PhICl<sub>2</sub><sup>8c,10</sup> can promote the stoichiometric two electron oxidation of Pd(II) complexes, demonstrating the viability of step (*ii*) of the proposed catalytic cycle for chlorination reactions. However, detailed investigations to determine the turnover limiting step, the kinetic isotope effect, and the electronic requirements of C–H chlorination had not been explored prior to this work.

**Scheme 3.2.** General Mechanism for C–H Functionalization

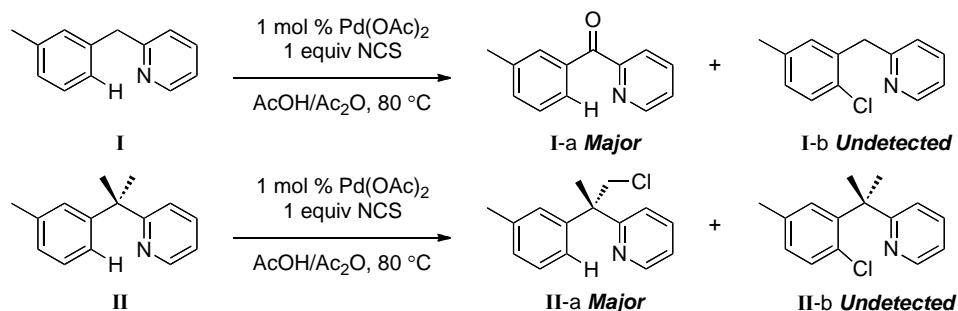


### 3.2 Results

Initial studies focused on the 2-benzylpyridine substrates that were used in previous mechanistic studies of Pd-catalyzed C–H acetoxylation (Chapter 2).

Unfortunately, substrates of this type (**I**) reacted with NCS to form undesired benzylic chlorination side products (**I-a**) as demonstrated in Figure 3.1. Next, a related substrate with the benzylic position blocked was synthesized (**II** in Figure 3.1). However, in this case chlorination of the adjacent  $sp^3$  C–H bond occurred under the reaction conditions to form **II-a**. While it was interesting to see  $sp^3$  C–H chlorination (which has proven challenging in previous studies by our group), the selectivity was insufficient for rigorous rate studies. Thus we next switched to the 2-*ortho*-tolylpyridine-based substrates.

**Figure 3.1.** Unselective Chlorination of 2-Benzylpyridine

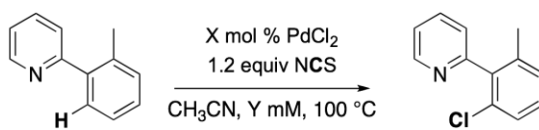


Our mechanistic investigation focused on using 2-*ortho*-tolylpyridine (**1**) with NCS and PhI(OAc)<sub>2</sub> to form chlorinated and acetoxyated products, respectively. This substrate possesses several desirable features. First, it undergoes selective mono-functionalization. Second, it participates cleanly in both C–H chlorination and C–H acetoxylation reactions, thus allowing direct comparison of these two transformations. Finally, the pyridine ring is readily modified, which facilitates analysis of electronic effects in these systems.

Our studies of chlorination began with conditions analogous to those in the literature: 5 mol % of Pd(OAc)<sub>2</sub> and 1.2 equiv of NCS in CH<sub>3</sub>CN with [2-*ortho*-tolylpyridine] = 0.12 M.<sup>3c</sup> Reactions were analyzed by gas chromatography versus an internal standard (pyrene), and all % yield values represent an average of three separate runs. However, at this concentration the reactions did not remain homogeneous, which led to inconsistent kinetics; furthermore, when

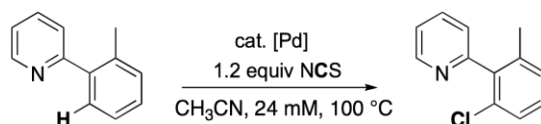
[2-*ortho*-tolylpyridine] was lowered, competing formation of acetoxyated product was observed (presumably derived from the Pd(OAc)<sub>2</sub> catalyst), which complicated kinetic analysis. For chlorination, we found that the optimal concentration that afforded good yield and mass balance in acetonitrile was 24 mM (Table 3.1).

**Table 3.1.** Optimization of Chlorination Reaction Conditions



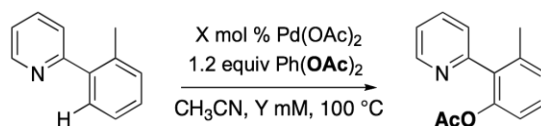
X mol % Pd	Y (mM)	% yield
1.0	120	11
2.5	120	45
5.0	120	23
5.0	80	53
5.0	48	72
<b>5.0</b>	<b>24</b>	<b>93</b>

With Pd(OAc)<sub>2</sub> as the catalyst, formation of the acetoxyated side product occurred. As a result, we examined a number of alternative palladium catalysts containing chloride based ligands and found that using PdCl<sub>2</sub> or PdCl<sub>2</sub>(CH<sub>3</sub>CN)<sub>2</sub> (which is presumably formed in situ) as the catalyst afforded good yields of the desired chlorination reaction (Table 3.2).

**Table 3.2.** Optimization of Chlorination Catalyst

Catalyst	% yield
Pd(OAc) <sub>2</sub>	41
PdCl <sub>2</sub> (PhCN) <sub>2</sub>	11
PdCl <sub>2</sub> (CH <sub>3</sub> CN) <sub>2</sub>	97
PdCl <sub>2</sub>	95

We next set out to optimize the acetoxylation reaction under similar conditions. As summarized in Table 3.3, a series of experiments revealed that the Pd(OAc)<sub>2</sub>-catalyzed *ortho*-acetoxylation of 2-*ortho*-tolylpyridine proceeds in high (77%) yield, using 5 mol % Pd(OAc)<sub>2</sub> at 48 mM in acetonitrile.

**Table 3.3.** Optimization of Acetoxylation Reaction Conditions

X mol % Pd	Y (mM)	% yield
1.0	120	10
2.5	120	19
5.0	120	57
5.0	80	70
<b>5.0</b>	<b>48</b>	<b>77</b>
5.0	24	32

With optimal conditions for the chlorination and acetoxylation of 2-*ortho*-tolylpyridine in hand, we examined the intermolecular kinetic isotope effect (KIE) for the two reactions to determine if breaking of the C-H bond occurs at some point between the catalyst resting state and the rate-determining step of the reaction. The Pd-catalyzed functionalizations of 2-*ortho*-tolylpyridine and deuterated 2-*ortho*-tolylpyridine were monitored by GC, and the initial rates

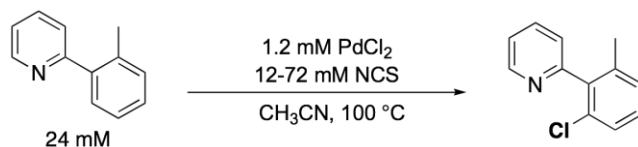
method was used to determine the rate at each [oxidant]. As shown in Table 3.4, a large 1° isotope effect was observed in both systems, with  $k_H/k_D = 4.4 \pm 0.2$  for chlorination and  $k_H/k_D = 4.3 \pm 0.5$  for acetoxylation. These KIE values are similar in magnitude to the values (1.85 in C<sub>6</sub>H<sub>6</sub> and 3.58 in AcOH/Ac<sub>2</sub>O) found in the benzylpyridine acetoxylation studies.

**Table 3.4.** Intermolecular Kinetic Isotope Effect Data

Catalyst	Oxidant	$k_H/k_D$
PdCl <sub>2</sub>	NCS	$4.4 \pm 0.2$
Pd(OAc) <sub>2</sub>	PhI(OAc) <sub>2</sub>	$4.3 \pm 0.5$

We next established the kinetic order in each reaction component, starting with the oxidant. The initial rate was measured for multiple concentrations of oxidant as shown in Tables 3.5 and 3.6. The initial rates were then plotted for both NCS and PhI(OAc)<sub>2</sub> as shown in Figures 3.2 and 3.3. The initial rates were independent of [oxidant] over a wide range of concentrations (0.5-3.0 equiv of oxidant relative to substrate) for both chlorination and acetoxylation.

**Table 3.5.** Initial Rate as a Function of [NCS] for Chlorination



[NCS] mM	Equiv	Initial rate ( x 10 <sup>-4</sup> mM/s)
12	0.5	$3.5 \pm 0.5$
24	1.0	$4.6 \pm 0.2$
28.8	1.2	$3.2 \pm 0.1$
48	1.5	$3.6 \pm 0.2$
72	2.0	$5.6 \pm 0.2$

**Figure 3.2.** Order in Oxidant for NCS

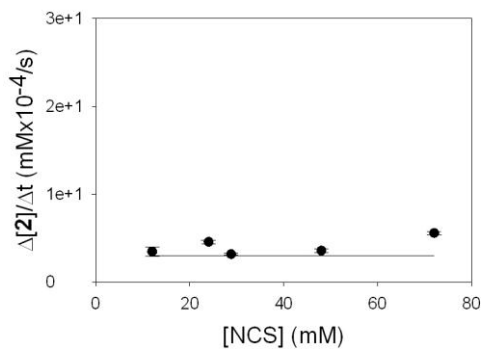
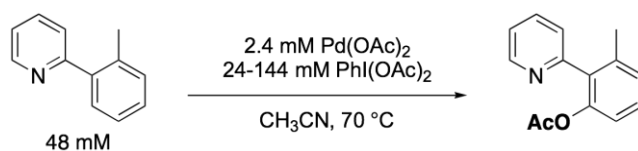
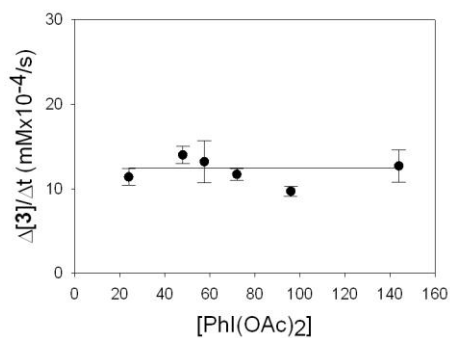


**Table 3.6.** Initial Rate as a Function of [PhI(OAc)<sub>2</sub>] for Acetoxylation



[PhI(OAc) <sub>2</sub> ] mM	Equiv	Initial rate ( x 10 <sup>-4</sup> mM/s)
24	0.5	11.4 ± 1.0
48	1.0	14.0 ± 1.0
57.6	1.2	13.2 ± 2.5
72	1.5	11.7 ± 0.7
96	2.0	9.7 ± 0.6
144	3.0	12.7 ± 1.9

**Figure 3.3.** Order in Oxidant for PhI(OAc)<sub>2</sub>

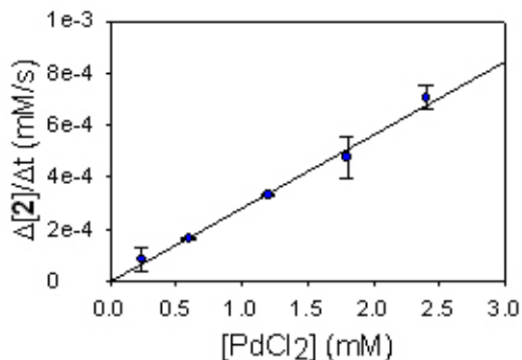


The order in palladium was next determined for each transformation by varying the catalyst loading from 1 to 10 mol % under otherwise identical conditions (Tables 3.7 and 3.8). As shown in Figure 3.4, chlorination showed a first order dependence on [Pd] over this catalytically relevant concentration range.

**Table 3.7.** Initial Rate as a Function of [Pd] for Chlorination

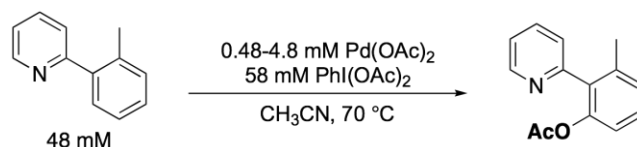
[PdCl <sub>2</sub> ] mM	mol %	Initial rate ( x 10 <sup>-4</sup> mM/s)
0.24	1.0	0.82 ± 0.48
0.6	2.5	1.64 ± 0.02
1.2	5.0	3.28 ± 0.05
1.8	7.5	4.72 ± 0.80
2.4	10.0	7.04 ± 0.46

**Figure 3.4.** Plot of Initial Rate ( $\Delta[2]/\Delta t$ ) versus [Pd] for Chlorination fit to  $f(x) = a[\text{PdCl}_2]^n$  ( $a = 3.0 \pm 0.2 \times 10^{-4}$ ,  $n = 1.06 \pm 0.08$ )

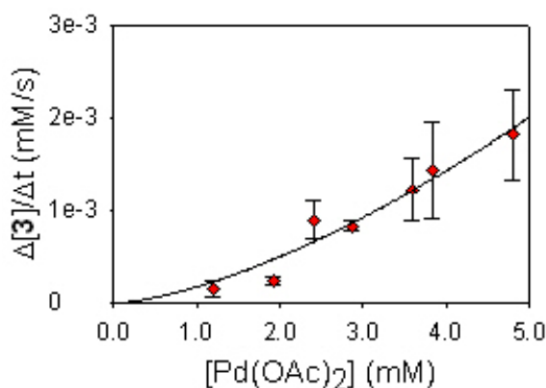


In contrast, for the C–H acetoxylation reaction, a weighted non-linear least squares fit to the equation:  $f(x) = a[\text{Pd}]^n$  provided an order ( $n$ ) of  $1.51 \pm 0.22$  (Figure 3.5).

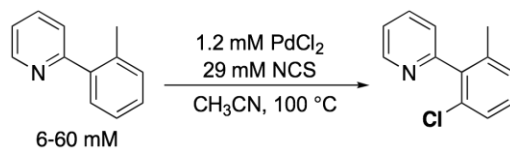


**Table 3.8.** Initial Rate as a Function of [Pd] for Acetoxylation

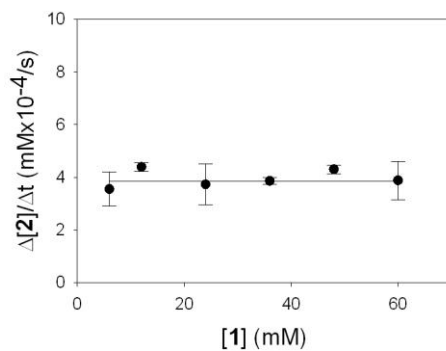
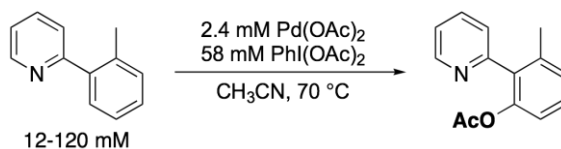
[Pd(OAc) <sub>2</sub> ] mM	mol %	Initial rate ( x 10 <sup>-4</sup> mM/s)
1.2	2.5	1.6 ± 0.8
1.92	4.0	2.5 ± 0.4
2.4	5.0	8.0 ± 1.0
2.88	6.0	8.4 ± 0.6
3.6	7.5	12.3 ± 3.4
3.84	8.0	14.3 ± 5.2
4.8	10.0	18.2 ± 4.9

**Figure 3.5.** Plot of Initial Rate ( $\Delta[3]/\Delta t$ ) versus [Pd] for Acetoxylation fit to  $f(x) = a[\text{Pd}(\text{OAc})_2]^n$  ( $a = 2.0 \pm 0.5 \times 10^{-4}$ ,  $n = 1.51 \pm 0.22$ )

Finally, the order in substrate 2-*ortho*-tolylpyridine was examined, using 0.25 equiv to 2.5 equiv of 2-*ortho*-tolylpyridine relative to oxidant (Tables 3.9-3.10). Again, the chlorination and acetoxylation reactions showed different results (Figure 3.6-3.7). For chlorination, a plot of initial rate versus [2-*ortho*-tolylpyridine] showed that the rate was independent of [2-*ortho*-tolylpyridine]. In contrast, the acetoxylation reactions showed an inverse 1<sup>st</sup> order dependence on [2-*ortho*-tolylpyridine].

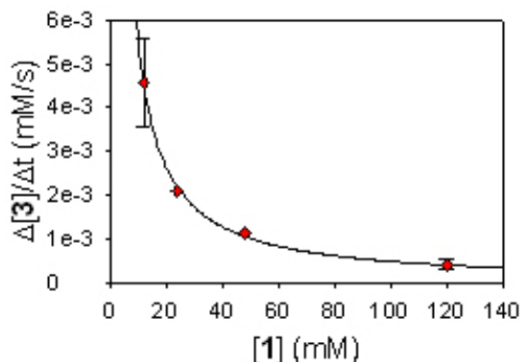
**Table 3.9.** Initial Rate as a Function of [1] for Chlorination

[1] mM	equiv rel to 0.024 mmol	rate ( x 10 <sup>-4</sup> mM/s)
6	0.25	3.55 ± 0.65
12	0.5	4.39 ± 0.17
24	1.0	3.73 ± 0.78
36	1.5	3.86 ± 0.12
48	2.0	4.30 ± 0.17
60	2.5	3.88 ± 0.73

**Figure 3.6.** Order in Substrate [1] for C–H Chlorination**Table 3.10.** Initial Rate as a Function of [1] for Acetoxylation

[1] mM	equiv rel to 0.024 mmol	Initial rate ( x 10 <sup>-4</sup> mM/s)
12	0.25	45.7 ± 10.0
24	0.5	21.0 ± 0.01
48	1.0	9.4 ± 0.1
120	2.5	4.1 ± 1.1

**Figure 3.7.** Plot of Initial Rate ( $\Delta[3]/\Delta t$ ) versus  $[1]$  for Acetoxylation fit to  $f(x) = a[1]^n$  ( $a = 0.0713 \pm 0.009$ ,  $n = -1.11 \pm 0.05$ )

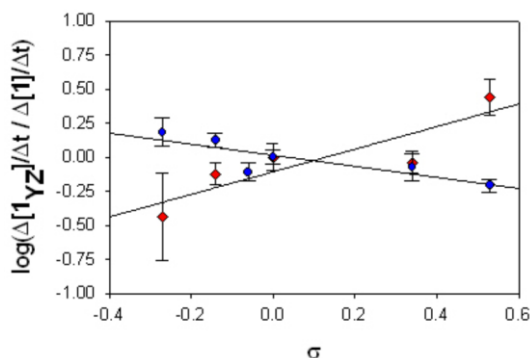


To gain insight into the electronic requirements of these reactions, we next probed the initial rate of C–H functionalization with a series of electronically different 2-*ortho*-tolylpyridines. Hammett plots for both C–H chlorination and C–H acetoxylation showed a modest correlation with the  $\sigma$  values of the Y and Z substituents as shown in Figure 3.8. Very different  $\rho$  values were observed for the two reactions, with  $\rho = -0.43$  for chlorination and  $\rho = +0.89$  for acetoxylation. Interpretation of the Hammett data is somewhat complicated by the conjugated biaryl system in **1**, since substitution of Y and Z can influence the electronics of both the pyridine (which binds to the metal) and the *ortho*-C–H bond (which undergoes activation). We note that the observed  $\rho$  value for C–H acetoxylation (+0.89 in MeCN) is reasonably similar to that found for benzylpyridines where the pyridine and aryl group are electronically isolated (+1.40 in benzene).<sup>7b</sup> Thus, we hypothesize that the effect observed here is predominantly due to pyridine electronics.

**Table 3.11.** Initial Rates for Substrates **1a-1e** for C–H Chlorination and C–H Acetoxylation

Substrate	Initial rate (mM/s x 10 <sup>-4</sup> )	
	NCS	PhI(OAc) <sub>2</sub>
<b>1a</b>	4.91 ± 1.10	4.32 ± 0.31
<b>1b</b>	4.27 ± 0.30	8.83 ± 0.70
<b>1c</b>	2.50 ± 0.30	---
<b>1</b>	3.23 ± 0.30	11.80 ± 0.20
<b>1d</b>	2.70 ± 0.60	10.80 ± 0.70
<b>1e</b>	2.00 ± 0.20	32.60 ± 0.80

**Figure 3.8.** Hammett Plot for C–H Chlorination ( $-\rho$ ) and C–H Acetoxylation ( $+\rho$ ).



We were concerned that the dilution of the chlorination reaction could potentially affect the Hammett plot. Therefore, we repeated the Hammett plot for chlorination at 48 mM. Under these conditions, a similar  $\rho$  value was obtained ( $-0.63$  versus  $-0.41$ , respectively, Figure 3.9). Therefore, this increase in concentration did not appear to alter the  $\rho$  value for the reaction. We also changed the catalyst for C-H chlorination from PdCl<sub>2</sub> to Pd(OAc)<sub>2</sub>. Under these conditions, there was a slight increase in the observed electronic effect with a  $\rho$  value of  $-1.05$  (Figure 3.10).

**Figure 3.9.** Hammett Plot for Chlorination at 0.048 M

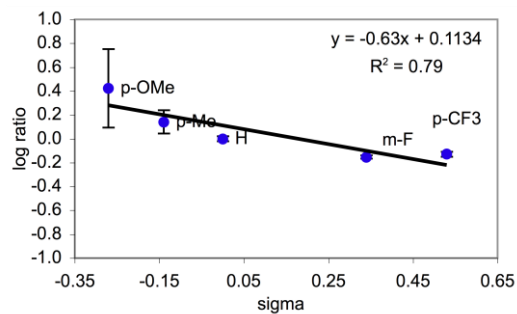
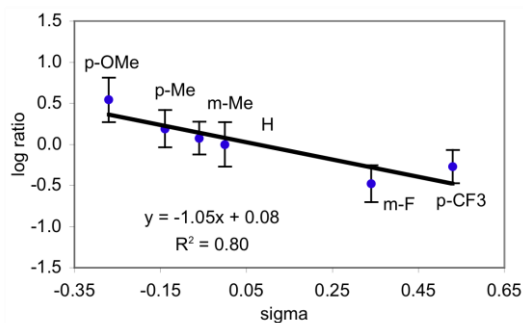


**Figure 3.10.** Hammett Plot for Chlorination with Pd(OAc)<sub>2</sub>



We also looked at these ligands under competition conditions at the same concentrations for both chlorination and acetoxylation. In acetonitrile, the Hammett values were both negative. These plots suggest that for both functionalizations, ligand equilibration has the most influence on the selectivity preference (Figure 3.11 and 3.12) which is consistent with results from similar studies described in Chapter 2.<sup>7b</sup>

**Figure 3.11.** Competing Ligands for Chlorination Hammett Plot in CH<sub>3</sub>CN

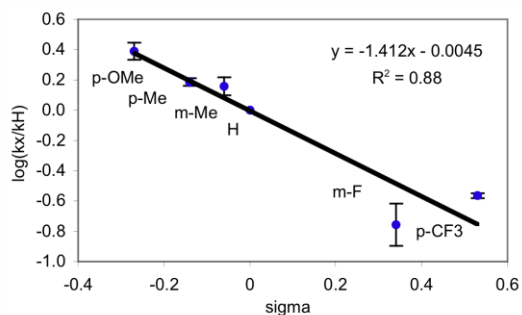
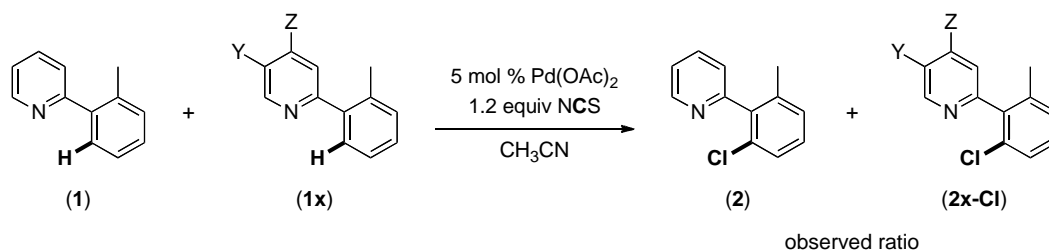
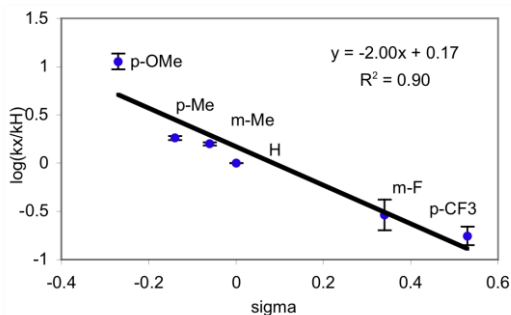
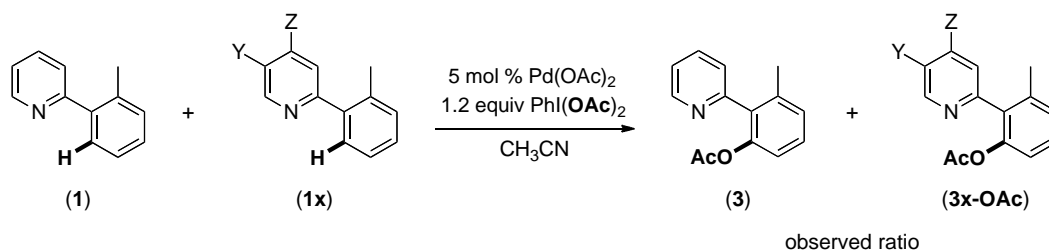


**Figure 3.12.** Competing Ligands for Acetoxylation Hammett Plot in CH<sub>3</sub>CN

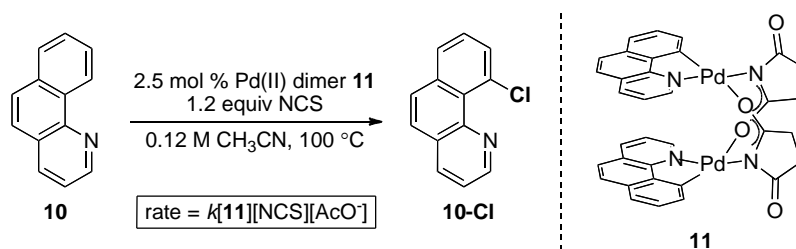


### 3.3 Discussion

The data presented here offers valuable insights into the mechanistic similarities and differences between the Pd-catalyzed chlorination and acetoxylation of substrate **1**. The large 1<sup>o</sup> intermolecular KIE coupled with the

zero order dependence on [oxidant] provide strong evidence that both transformations proceed via turnover limiting cyclopalladation. This zero-order dependence is in interesting contrast to the C–H arylation of 3-methyl-2-phenylpyridine with  $[\text{Ar}_2\text{I}]\text{BF}_4$ , which involves turnover limiting oxidation of a cyclometalated Pd(II) dimer.<sup>7e</sup> However, a report also showed that under almost analogous conditions with the addition of acetic acid, oxidation is turnover limiting (Scheme 3.3).<sup>8c,d</sup> In this report, the conditions are at a much higher concentration of MeCN (0.12 M) and use a palladium dimer as the catalyst. Furthermore, the acetate source is required for the utility of chlorination under the specified conditions. It is thought that the mechanism in this case proceeds through a 2-electron oxidation of the palladium dimer to form a bimetallic intermediate that can then undergo reductive elimination to install the desired halogen. This example shows that in some cases a bimetallic intermediate is possible, however, as the conditions optimized for chlorination excluded acetate entirely, this mechanism can be ruled out as operative.

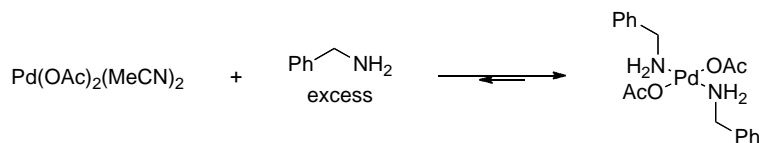
**Scheme 3.3.** Rate Limiting Oxidation for Chlorination with Cooperative  $\text{OAc}^-$  Catalysis



While the rate determining step appears to be the same in both of the current systems in acetonitrile, the different Hammett  $\rho$  values as well as the different kinetic orders  $[\text{Pd}]$  and in **[1]** are consistent with different mechanisms for cyclopalladation in the  $\text{PdCl}_2$  versus  $\text{Pd}(\text{OAc})_2$ -catalyzed reactions. Significant literature precedent has shown that  $\text{PdX}_2$  ( $\text{X} = \text{OAc}$  or  $\text{Cl}$ ) reacts rapidly and quantitatively with excess amine or pyridine derivatives ( $\text{L}$ ) to form monomeric complexes of general structure  $\text{Pd}(\text{X})_2(\text{L})_2$ .<sup>10</sup> For example,  $\text{Pd}(\text{OAc})_2(\text{ba})_2$  ( $\text{ba} =$

benzylamine), has been directly observed in the Pd(OAc)<sub>2</sub>-mediated cyclometalation of ba in MeCN.<sup>11</sup>

**Figure 3.13.** Formation of Monomeric Complex Pd(X)<sub>2</sub>(L)<sub>2</sub>

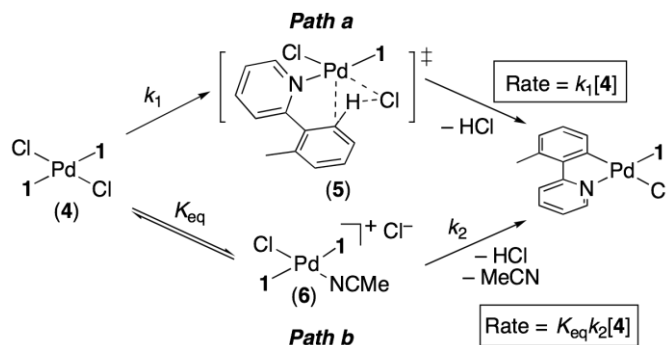


As such, we propose that the catalyst resting state during both C–H functionalizations is most likely Pd(X)<sub>2</sub>(**1**)<sub>2</sub> (X = Cl, **4**; X = OAc, **7**) (Schemes 3.3 and 3.4). A dimeric resting state followed by C–H activation at a dimeric intermediate is also possible based on the kinetic data for C–H chlorination. However, literature reports suggest that dimeric complexes like Pd<sub>2</sub>(X)<sub>4</sub>(L)<sub>2</sub> only predominate in solution under conditions where L : [Pd] < 2 : 1.<sup>12</sup>

In the chlorination reaction in acetonitrile (Scheme 3.4), the observed zero order dependence on [2-*ortho*-tolylpyridine] suggests that cyclometalation at Pd(Cl)<sub>2</sub>(**1**)<sub>2</sub> (**4**) proceeds by either: (a) direct C–H activation via a 5-coordinate transition state such as **5**<sup>13</sup> or (b) pre-equilibrium chloride dissociation followed by C–H activation at cationic complex **6**.<sup>14</sup> Paths *a* and *b* are both consistent with the observed kinetic orders of 1 in [Pd] and 0 in [2-*ortho*-tolylpyridine].<sup>12</sup> Furthermore, both mechanisms have been proposed for related cyclometalation reactions in the literature.<sup>13,14</sup> We tend to favor path *b*, as it offers a better explanation of the Hammett ρ value of –0.43. The latter can be rationalized based on increased lability of Cl<sup>–</sup> (at complex **4**) and MeCN (at complex **6**) with more electron releasing pyridine ligands. This increase in electron density on the metal would lead to an increase in both *K*<sub>eq</sub> and *k*<sub>1</sub>, thereby affording faster reactions with more electron rich pyridines.

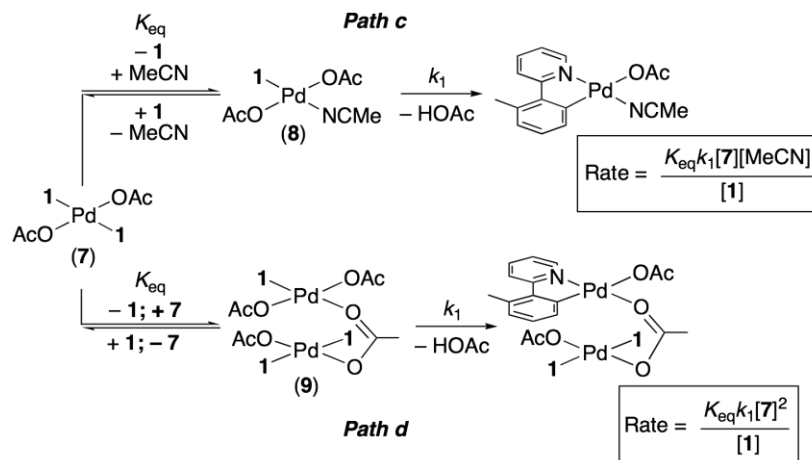


**Scheme 3.4.** Two Possible Mechanisms for the Turnover Limiting Step of C–H Chlorination (**1** = 2-*ortho*-tolylpyridine)



For the acetoxylation reaction, the observed inverse order dependence on [**1**] implicates pre-equilibrium dissociation of **1** from Pd(OAc)<sub>2</sub>(**1**)<sub>2</sub> prior to C–H activation. As shown in Scheme 3.5, this dissociation could generate monomeric species Pd(OAc)<sub>2</sub>(**1**)(MeCN) (**8**) (path *c*) or an acetate-bridged dimer such as Pd<sub>2</sub>(OAc)<sub>4</sub>(**1**)<sub>3</sub> (**9**) (path *d*), and cyclometalation could then occur at either of these intermediates. Path *c* is expected to show a 1<sup>st</sup> order dependence on [Pd], while path *d* should be 2<sup>nd</sup> order in [Pd]. We propose that these competing 1<sup>st</sup> and 2<sup>nd</sup> order mechanisms could be responsible for the observed 1.5 order dependence on [Pd] in this system. An alternative explanation would be that the catalyst resting state is a mixture of monomeric and dimeric Pd species.<sup>8c</sup> However, we believe that this is unlikely in the current system, as literature precedent suggests that the reaction between 10–100 equiv **1** and Pd(OAc)<sub>2</sub> to form Pd(OAc)<sub>2</sub>(**1**)<sub>2</sub> should be fast and nearly quantitative, particularly at 70 °C.<sup>13,14</sup> The Hammett  $\rho$  value of +0.89 is fully consistent with this mechanistic proposal, as electron withdrawing substituents on the pyridine ligand should both increase  $K_{\text{eq}}$  and render complexes **8** and **9** more electrophilic (and thereby more reactive towards C–H activation).<sup>13b,c</sup> Notably, mechanisms similar to both *c*<sup>11</sup> and *d*<sup>12</sup> have been proposed for the stoichiometric cyclometalation of benzylamine at Pd(OAc)<sub>2</sub> in MeCN.

**Scheme 3.5.** Possible Competing Mechanisms for the Turnover Limiting Step of C–H Acetoxylation (**1** = 2-*ortho*-tolylpyridine)



### 3.4 Application

There are several important implications of these studies. First, it is clear that the ligand environment at Pd during C–H activation is significantly different in these two transformations. If this result proves general, it has potential implications for diastereoselective reactivity in the C–H functionalization of chiral substrates upon changing the catalyst/oxidant combination. In addition, the structures of the key intermediates (as well as the possibility of competing mechanisms) should inform the selection of chiral ligands for asymmetric C–H functionalization reactions. Finally, the development of more highly active C–H chlorination and acetoxylation catalysts will require accelerating the cyclometalation step of the catalytic cycle. Because most ancillary ligands decrease the rate of directed C–H activation relative to that with simple Pd salts, determining appropriate ligands is a particularly intriguing challenge that will necessitate innovative solutions informed by fundamental organometallic chemistry.

### 3.5 Conclusions

In summary, this chapter describes the mechanism of Pd-catalyzed directed C–H chlorination and acetoxylation of 2-*ortho*-tolylpyridine. Under the conditions

examined, both reactions proceed via turnover limiting cyclopalladation. However, kinetic order and Hammett data indicate that the intimate mechanism of C–H activation differs significantly between PdCl<sub>2</sub>-catalyzed chlorination and Pd(OAc)<sub>2</sub>-catalyzed acetoxylation. Ongoing work seeks to further explore the proposed mechanisms computationally as well as exploit the current results for the development of new C–H functionalization catalysts.

### 3.6 Experimental

The derivatives of 2-*ortho*-tolylpyridine substrates were prepared via Pd-catalyzed Suzuki coupling between 2-methylphenylboronic acid and the corresponding halopyridine derivative using a modification of a literature procedure.<sup>15</sup> The halopyridines were all commercially available except for 2-chloro-4-methoxypyridine, which was prepared according to a literature method.<sup>16</sup>

*Standard Procedure for Acetoxylation:* In a 20 mL vial, NCS (0.28 mmol, 1.20 equiv) and Pd(OAc)<sub>2</sub> (2.8 mg, 0.012 mmol, 0.05 equiv) were combined in AcOH (10 mL). The substrate (0.24 mmol, 1.0 equiv) was added, the vial was sealed with a Teflon-lined cap, and the resulting solution was heated at 100 °C for 12 h. The reaction was cooled to room temperature, and the solvent was removed under vacuum. The resulting brown oil was purified by chromatography on silica gel.

*Standard Procedure for Chlorination:* In a 20 mL vial, PhI(OAc)<sub>2</sub> (0.28 mmol, 1.2 equiv) and Pd(OAc)<sub>2</sub> (2.8 mg, 0.012 mmol, 0.05 equiv) were combined in AcOH (5 mL). The substrate (0.24 mmol, 1.0 equiv) was added, the vial was sealed with a Teflon-lined cap, and the resulting solution was heated at 100 °C for 12 h. The reaction was cooled to room temperature, and the solvent was removed under vacuum. The resulting brown oil was purified by chromatography on silica gel.

**General Information for rate studies.** The rate studies were measured using the method of initial rates. In each experiment, the reaction was monitored to ~10% (8-12%) conversion. Each experiment was run in triplicate, and all kinetic

orders and Hammett data represent an average of these three runs. Error analysis was conducted by taking the average and standard deviation of the obtained initial rates. Linear regression was performed by using least squares fit equations and calculations.<sup>17</sup> Notably, the acetoxylation and chlorination reactions were examined at different concentrations (0.048 versus 0.024 M, respectively) because the data for each reaction was significantly more reproducible under these conditions. However, we have also examined the chlorination reactions at 0.048 M, and the same Hammett trends are observed.

*Typical Procedure for Chlorination Kinetics:* Kinetics experiments were run in two dram vials sealed with Teflon-lined caps. Each data point represents a reaction in an individual vial, with each vial containing a constant concentration of oxidant, catalyst, and substrate. The vials were each sequentially charged with NCS (3.85 mg, 0.0288 mmol, 1.2 equiv, added as a 0.096 M stock solution in CH<sub>3</sub>CN), substrate (0.024 mmol, 1.0 equiv, added as a 0.48 M stock solution in CH<sub>3</sub>CN), and PdCl<sub>2</sub> (0.21 mg, 0.0012 mmol, 0.05 equiv, added as a 0.024 M stock solution in CH<sub>3</sub>CN), and the resulting mixtures were diluted to a total volume of 1 mL of CH<sub>3</sub>CN. The vials were then heated at 100 °C for various amounts of time. Reactions were quenched by cooling the vial to 0 °C for 5 min, followed by the addition of a 2% solution of pyridine in CH<sub>2</sub>Cl<sub>2</sub> (2 mL). A GC standard (pyrene) was then added, and the reactions were analyzed by gas chromatography.

*Typical Procedure for Acetoxylation Kinetics:* Kinetics experiments were run in two dram vials sealed with Teflon-lined caps. Each data point represents a reaction in an individual vial, with each vial containing an identical concentration of oxidant, catalyst, and substrate. The vials were charged with PhI(OAc)<sub>2</sub> (9.28 mg, 0.0288 mmol, 1.2 equiv, added as a solid), substrate (0.024 mmol, 1.0 equiv, added as a 0.48 M stock solution in CH<sub>3</sub>CN), and Pd(OAc)<sub>2</sub> (0.28 mg, 0.0012 mmol, 0.05 equiv, added as a 0.024 M stock solution in CH<sub>3</sub>CN), and the resulting mixtures were diluted to a total volume of 500 μL CH<sub>3</sub>CN. The vials were then heated at 70 °C for various amounts of time. Reactions were quenched by cooling the vial to 0 °C for 5 min, followed by the addition of a 2%

solution of pyridine in CH<sub>2</sub>Cl<sub>2</sub> (2 mL). A GC standard (pyrene) was then added, and the reactions were analyzed by gas chromatography.

### **Hammett Studies**

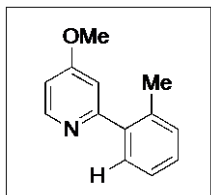
*Chlorination.* The general procedure for chlorination was used, with NCS (3.85 mg, 0.0288 mmol), substrate (0.024 mmol), and PdCl<sub>2</sub> (0.21 mg, 0.0012 mmol) in CH<sub>3</sub>CN. Reactions were conducted at 100 °C, and each reported initial rate represents an average of three unique kinetics experiments.

*Acetoxylation.* The general procedure for acetoxylation was used with PhI(OAc)<sub>2</sub> (9.28 mg, 0.0288 mmol), substrate (0.024 mmol), and Pd(OAc)<sub>2</sub> (0.27 mg, 0.0012 mmol) in CH<sub>3</sub>CN. Reactions were conducted at 70 °C, and each reported initial rate represents an average of three unique kinetics experiments.

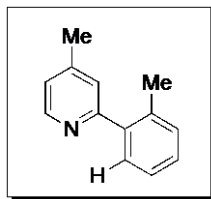
## **3.7 Characterization**

### II. Synthesis and Characterization of 2-*ortho*-Tolylpyridine Substrates

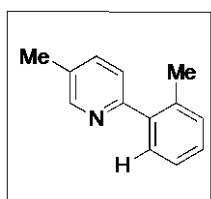
The derivatives of 2-*ortho*-tolylpyridine substrates were prepared via Pd-catalyzed Suzuki coupling between 2-methylphenylboronic acid and the corresponding halopyridine derivative using a modification of a literature procedure.



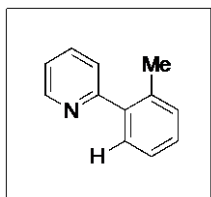
The product was obtained as a colorless solid ( $R_f = 0.3$  in 70% hexanes/30% ethyl acetate). mp = 48.5 °C. <sup>1</sup>H NMR (CDCl<sub>3</sub>): δ 8.46 (d,  $J = 5.6$  Hz, 1H), 7.34 (d,  $J = 6.8$  Hz, 1H), 7.25-7.21 (multiple peaks, 3H), 6.87 (d,  $J = 2.8$  Hz, 1H), 6.74 (dd,  $J = 5.8, 2.8$  Hz, 1H), 3.82 (s, 3H), 2.33 (s, 3H). <sup>13</sup>C{<sup>1</sup>H} NMR (CDCl<sub>3</sub>): δ 165.87, 161.80, 150.51, 140.71, 135.83, 130.78, 129.52, 128.34, 125.89, 110.28, 107.99, 55.22, 20.35. HRMS electrospray (m/z): [M-H]<sup>+</sup> calcd for C<sub>13</sub>H<sub>12</sub>NO, 198.0919; found, 198.0919.



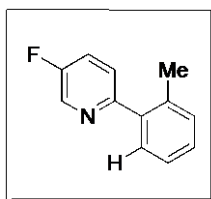
The product was obtained as a colorless liquid ( $R_f = 0.25$  in 80% hexanes/20% ethyl acetate).  $^1\text{H}$  NMR ( $\text{CDCl}_3$ ):  $\delta$  8.52 (d,  $J = 5.6$  Hz, 1H), 7.35 (dt,  $J = 6.0, 1.6$  Hz, 1H), 7.29-7.21 (multiple peaks, 3H), 7.20 (dd,  $J = 1.6, 0.8$  Hz, 1H), 7.04 (dt,  $J = 4.4, 0.8$  Hz, 1H), 2.38 (s, 3H), 2.34 (s, 3H).  $^{13}\text{C}\{^1\text{H}\}$  NMR ( $\text{CDCl}_3$ ):  $\delta$  160.09, 149.08, 147.26, 140.74, 135.89, 130.79, 129.69, 128.25, 125.91, 125.09, 122.76, 21.27, 20.39. HRMS electrospray ( $m/z$ ):  $[\text{M}-\text{H}]^+$  calcd for  $\text{C}_{13}\text{H}_{12}\text{N}$ , 182.0970; found, 182.0967.



The product was obtained as a colorless liquid ( $R_f = 0.25$  in 80% hexanes/20% ethyl acetate).  $^1\text{H}$  NMR ( $\text{CDCl}_3$ ):  $\delta$  8.49 (d,  $J = 1.6$  Hz, 1H), 7.51 (dd,  $J = 7.6, 2.4$  Hz, 1H), 7.34 (m, 1H), 7.25-7.22 (multiple peaks, 4H), 2.35 (s, 3H), 2.32 (s, 3H).  $^{13}\text{C}\{^1\text{H}\}$  NMR ( $\text{CDCl}_3$ ):  $\delta$  157.22, 149.63, 140.45, 136.67, 135.75, 130.99, 130.71, 129.64, 128.06, 125.86, 123.53, 20.35, 18.19. HRMS electrospray ( $m/z$ ):  $[\text{M}-\text{H}]^+$  calcd for  $\text{C}_{13}\text{H}_{12}\text{N}$ , 182.0970; found, 182.0965.

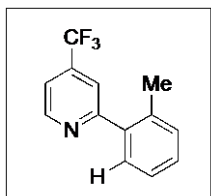


The product (**1**) was obtained as a colorless liquid ( $R_f = 0.25$  in 88% hexanes/12% ethyl acetate). The  $^1\text{H}$  and  $^{13}\text{C}$  NMR spectra of this product matched those reported in the literature.<sup>3</sup>



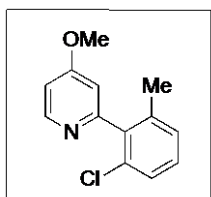
The product was obtained as a colorless liquid ( $R_f = 0.25$  in 80% hexanes/20% ethyl acetate).  $^1\text{H}$  NMR ( $\text{CDCl}_3$ ):  $\delta$  8.51 (d,  $J = 2.8$  Hz, 1H),

7.41 (dt,  $J = 8.8, 3.2$  Hz, 1H), 7.36-7.31 (multiple peaks, 2H), 7.28-7.20 (multiple peaks, 3H), 2.31 (s, 3H).  $^{13}\text{C}\{^1\text{H}\}$  NMR ( $\text{CDCl}_3$ ):  $\delta$  158.54 (d,  $J = 254.3$  Hz), 156.41, 139.62, 137.54 (d,  $J = 23.2$  Hz), 136.00, 131.03, 129.79, 128.62, 126.14, 125.06 (d,  $J = 3.8$  Hz), 123.15 (d,  $J = 3.5$  Hz), 20.49.  $^{19}\text{F}$  NMR ( $\text{CDCl}_3$ ):  $\delta$  -130.11. HRMS electrospray ( $m/z$ ):  $[\text{M}-\text{H}]^+$  calcd for  $\text{C}_{12}\text{H}_9\text{FN}$ , 186.0719; found, 186.0725.

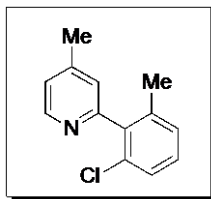


The product was obtained as a colorless liquid ( $R_f = 0.25$  in 80% hexanes/20% ethyl acetate).  $^1\text{H}$  NMR ( $\text{CDCl}_3$ ):  $\delta$  8.87 (d,  $J = 5.2$  Hz, 1H), 7.63 (d,  $J = 0.8$  Hz, 1H), 7.46 (dt,  $J = 5.6, 0.8$  Hz, 1H), 7.40 (d,  $J = 7.6$  Hz, 1H), 7.36-7.28 (multiple peaks, 3H), 2.38 (s, 3H).  $^{13}\text{C}\{^1\text{H}\}$  NMR ( $\text{CDCl}_3$ ):  $\delta$  161.67, 150.38, 139.30, 138.77 (q,  $J = 33.9$  Hz), 136.10, 131.25, 129.85, 129.17, 126.34, 123.13 (q,  $J = 271.6$  Hz), 119.86 (q,  $J = 3.4$  Hz), 117.38 (q,  $J = 3.4$  Hz), 20.44.  $^{19}\text{F}$  NMR ( $\text{CDCl}_3$ ):  $\delta$  -64.81. HRMS electrospray ( $m/z$ ):  $[\text{M}-\text{H}]^+$  calcd for  $\text{C}_{13}\text{H}_9\text{F}_3\text{N}$ , 236.0687; found, 236.0688.

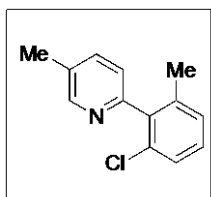
### III. Synthesis and Characterization of Chlorinated Products



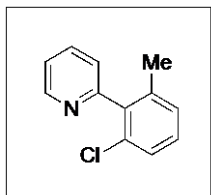
The product was obtained as a yellow oil ( $R_f = 0.3$  in 70% hexanes/30% ethyl acetate).  $^1\text{H}$  NMR ( $\text{CDCl}_3$ ):  $\delta$  8.49 (d,  $J = 5.6$  Hz, 1H), 7.35-7.24 (multiple peaks, 3H), 6.96 (dd,  $J = 5.6, 2.5$  Hz, 1H), 6.90 (d,  $J = 2.0$  Hz, 1H), 3.93 (s, 3H), 2.07 (s, 3H).  $^{13}\text{C}\{^1\text{H}\}$  NMR ( $\text{CDCl}_3$ ):  $\delta$  166.16, 159.11, 150.99, 139.40, 138.70, 133.12, 129.17, 128.71, 127.06, 111.11, 108.84, 55.43, 20.52. HRMS electrospray ( $m/z$ ):  $[\text{M}-\text{H}]^+$  calcd for  $\text{C}_{13}\text{H}_{11}\text{ClNO}$ , 232.0529; found, 232.0525.



The product was obtained as a yellow oil ( $R_f = 0.25$  in 80% hexanes/20% ethyl acetate).  $^1\text{H}$  NMR ( $\text{CDCl}_3$ ):  $\delta$  8.53 (d,  $J = 4.8$  Hz, 1H), 7.35-7.25 (multiple peaks, 3H), 7.23 (ddd,  $J = 5.2, 1.6$  Hz, 0.8 1H), 7.18 (d,  $J = 2.8$  Hz, 1H), 3.93 (s, 3H), 2.07 (s, 3H).  $^{13}\text{C}\{^1\text{H}\}$  NMR ( $\text{CDCl}_3$ ):  $\delta$  157.48, 149.50, 147.73, 139.46, 138.78, 133.24, 129.08, 128.71, 127.05, 125.86, 123.55, 21.35, 20.61. HRMS electrospray (m/z):  $[\text{M}-\text{H}]^+$  calcd for  $\text{C}_{13}\text{H}_{11}\text{ClN}$ , 216.0580; found, 216.0581.

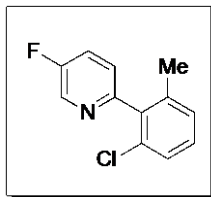


The product was obtained as a yellow oil ( $R_f = 0.2$  in 85% hexanes/15% ethyl acetate).  $^1\text{H}$  NMR ( $\text{CDCl}_3$ ):  $\delta$  8.52 (d,  $J = 1.2$  Hz, 1H), 7.69 (m, 1H), 7.33 (m, 1H), 7.30-7.21 (multiple peaks, 3H), 2.39 (s, 3H), 2.05 (s, 3H).  $^{13}\text{C}\{^1\text{H}\}$  NMR ( $\text{CDCl}_3$ ):  $\delta$  154.82, 150.24, 139.38, 138.94, 137.07, 133.42, 131.97, 129.04, 128.73, 127.06, 124.49, 20.64, 18.53. HRMS electrospray (m/z):  $[\text{M}-\text{H}]^+$  calcd for  $\text{C}_{13}\text{H}_{11}\text{ClN}$ , 216.0580; found, 216.0579.

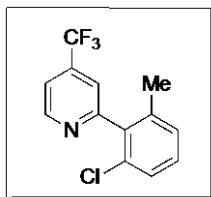


The product (2) was obtained as a yellow oil ( $R_f = 0.20$  in 85% hexanes/15% ethyl acetate).  $^1\text{H}$  NMR ( $\text{CDCl}_3$ ):  $\delta$  8.70 (dd,  $J = 4.8, 0.8$  Hz, 1H), 7.90 (td,  $J = 7.6, 2.0$ , 1H), 7.41-7.26 (multiple peaks, 5H), 2.06 (s, 3H).  $^{13}\text{C}\{^1\text{H}\}$  NMR ( $\text{CDCl}_3$ ):  $\delta$  157.71, 149.80, 139.36, 138.77, 136.55, 133.23, 129.21, 128.77, 127.10, 125.13, 122.54, 20.61. HRMS electrospray (m/z):  $[\text{M}-\text{H}]^+$  calcd for  $\text{C}_{12}\text{H}_9\text{ClN}$ , 202.0423; found, 202.0423.



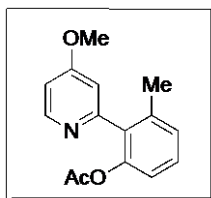


The product was obtained as a yellow oil ( $R_f = 0.20$  in 85% hexanes/15% ethyl acetate).  $^1\text{H NMR}$  ( $\text{CDCl}_3$ ):  $\delta$  8.57 (d,  $J = 2.8$  Hz, 1H), 7.49 (td,  $J = 8.4, 3.2$  Hz, 1H), 7.31-7.28 (multiple peaks, 2H), 7.21 (t,  $J = 8.0$  Hz, 1H), 7.16 (d,  $J = 8.0$  Hz, 1H), 2.07 (s, 3H).  $^{13}\text{C}\{^1\text{H}\}$  NMR ( $\text{CDCl}_3$ ):  $\delta$  158.72 ( $J = 255.1$  Hz), 153.72 ( $J = 4.6$  Hz), 138.95, 138.33 ( $J = 23.3$  Hz), 137.98, 133.38, 129.42, 128.86, 126.92, 126.12 ( $J = 4.2$  Hz), 123.41 ( $J = 18.3$  Hz), 20.63.  $^{19}\text{F NMR}$  ( $\text{CDCl}_3$ ):  $\delta$  -128.46. HRMS electrospray ( $m/z$ ):  $[\text{M}-\text{H}]^+$  calcd for  $\text{C}_{12}\text{H}_8\text{ClFN}$ , 220.0329; found, 220.0328.



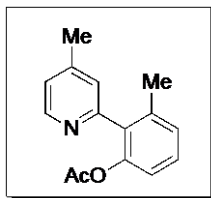
The product was obtained as a yellow oil ( $R_f = 0.20$  in 85% hexanes/15% ethyl acetate).  $^1\text{H NMR}$  ( $\text{CDCl}_3$ ):  $\delta$  9.01 (d,  $J = 5.2$  Hz, 1H), 7.77 (dd,  $J = 4.4, 0.8$  Hz, 1H), 7.74 (d,  $J = 0.8$  Hz, 1H), 7.42-7.35 (multiple peaks, 2H), 7.32 (ddd,  $J = 6.8, 1.6, 0.8$  Hz, 1H), 2.09 (s, 3H).  $^{13}\text{C}\{^1\text{H}\}$  NMR ( $\text{CDCl}_3$ ):  $\delta$  159.13, 150.86, 138.93 (q,  $J = 34.0$  Hz), 138.68, 138.16, 133.09, 129.84, 129.03, 127.33, 123.01 (q,  $J = 271.4$  Hz), 121.04 (q,  $J = 3.5$  Hz), 118.20 (q,  $J = 3.4$  Hz), 20.61.  $^{19}\text{F NMR}$  ( $\text{CDCl}_3$ ):  $\delta$  -64.72. HRMS electrospray ( $m/z$ ):  $[\text{M}-\text{H}]^+$  calcd for  $\text{C}_{13}\text{H}_8\text{ClF}_3\text{N}$ , 270.0297; found, 270.0298.

#### IV. Synthesis and Characterization of Acetoxylated Products

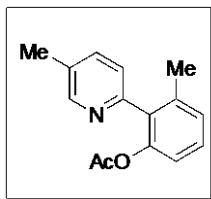


The product was obtained as a yellow oil ( $R_f = 0.25$  in 70% hexanes/30% ethyl acetate).  $^1\text{H NMR}$  ( $\text{CDCl}_3$ ):  $\delta$  8.51 (dd,  $J = 5.2, 1.2$  Hz, 1H), 7.30 (t,  $J = 7.6$  Hz, 1H), 7.17 (d,  $J = 7.6$  Hz, 1H), 6.97 (d,  $J = 8.4$  Hz, 1H), 6.81-6.79 (multiple peaks, 2H), 3.85 (s, 3H), 2.16 (s, 3H), 1.98 (s, 3H).  $^{13}\text{C}\{^1\text{H}\}$  NMR

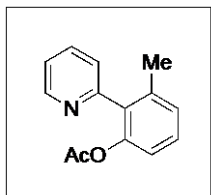
(CDCl<sub>3</sub>):  $\delta$  169.86, 165.94, 157.48, 150.80, 148.50, 138.36, 133.75, 129.05, 128.18, 120.17, 110.70, 108.86, 55.41, 20.85, 20.04. HRMS electrospray (m/z): [M]<sup>+</sup> calcd for C<sub>15</sub>H<sub>15</sub>NO<sub>3</sub>, 257.1052; found, 257.1046. IR (thin film) 1766 cm<sup>-1</sup>.



The product was obtained as a yellow oil ( $R_f$  = 0.3 in 70% hexanes/30% ethyl acetate). <sup>1</sup>H NMR (CDCl<sub>3</sub>):  $\delta$  8.57 (dd,  $J$  = 4.8, 1.2 Hz, 1H), 7.31 (t,  $J$  = 7.6 Hz, 1H), 7.18 (dd,  $J$  = 7.6, 0.8 Hz, 1H), 7.10-7.01 (multiple peaks, 2H), 6.98 (dd,  $J$  = 8.0, 0.8 Hz, 1H), 2.39 (s, 3H), 2.16 (s, 3H), 1.98 (s, 3H). <sup>13</sup>C{<sup>1</sup>H} NMR (CDCl<sub>3</sub>):  $\delta$  169.76, 155.78, 149.44, 148.63, 147.41, 138.40, 133.82, 128.94, 128.17, 125.71, 123.33, 120.17, 21.28, 20.78, 20.13. HRMS electrospray (m/z): [M]<sup>+</sup> calcd for C<sub>15</sub>H<sub>15</sub>NO<sub>2</sub>, 241.1103; found, 241.1096. IR (thin film) 1765 cm<sup>-1</sup>.

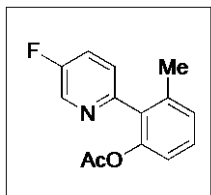


The product was obtained as a yellow solid ( $R_f$  = 0.20 in 80% hexanes/20% ethyl acetate). <sup>1</sup>H NMR (CDCl<sub>3</sub>):  $\delta$  8.54 (dd,  $J$  = 1.6, 0.8 Hz, 1H), 7.54 (m, 1H), 7.29 (t,  $J$  = 8.0 Hz, 1H), 7.16 (t,  $J$  = 6.4 Hz, 2H), 6.97 (d,  $J$  = 8.0 Hz, 1H), 2.39 (s, 3H), 2.15 (s, 3H), 1.96 (s, 3H). <sup>13</sup>C{<sup>1</sup>H} NMR (CDCl<sub>3</sub>):  $\delta$  169.80, 153.10, 150.20, 148.73, 138.61, 136.78, 133.78, 131.73, 128.91, 128.22, 124.34, 120.15, 20.85, 20.17, 18.50. HRMS electrospray (m/z): [M]<sup>+</sup> calcd for C<sub>15</sub>H<sub>15</sub>NO<sub>2</sub>, 241.1103; found, 241.1098. IR (thin film) 1761 cm<sup>-1</sup>.

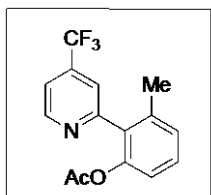


The product (3) was obtained as a yellow oil ( $R_f$  = 0.25 in 80% hexanes/20% ethyl acetate). <sup>1</sup>H NMR (CDCl<sub>3</sub>):  $\delta$  8.72 (dd,  $J$  = 4.0, 1.2 Hz, 1H), 7.74 (tt,  $J$  = 7.6, 1.6 Hz, 1H), 7.33-7.25 (multiple peaks, 3H), 7.18 (d,  $J$  = 8.0 Hz,

1H), 6.98 (d,  $J = 8.0$  Hz, 1H), 2.15 (s, 3H), 1.94 (s, 3H).  $^{13}\text{C}\{^1\text{H}\}$  NMR ( $\text{CDCl}_3$ ):  $\delta$  169.74, 156.10, 149.78, 148.60, 138.39, 136.20, 133.84, 129.06, 128.23, 124.94, 122.29, 120.18, 20.77, 20.12. HRMS electrospray ( $m/z$ ):  $[\text{M}]^+$  calcd for  $\text{C}_{14}\text{H}_{13}\text{NO}_2$ , 227.0946; found, 227.0947. IR (thin film)  $1763\text{ cm}^{-1}$ .



The product was obtained as a yellow oil ( $R_f = 0.2$  in 90% hexanes/10% ethyl acetate).  $^1\text{H}$  NMR ( $\text{CDCl}_3$ ):  $\delta$  8.53 (d,  $J = 2.8$  Hz, 1H), 7.42 (td,  $J = 8.4, 3.2$  Hz, 1H), 7.30-7.22 (multiple peaks, 2H), 7.14 (d,  $J = 8.0$  Hz, 1H), 6.94 (d,  $J = 8.4$  Hz, 1H), 2.11 (s, 3H), 1.94 (s, 3H).  $^{13}\text{C}\{^1\text{H}\}$  NMR ( $\text{CDCl}_3$ ):  $\delta$  169.66, 158.62 (d,  $J = 255.4$  Hz), 152.07 (d,  $J = 4.6$  Hz), 148.66, 138.54, 138.08 (d,  $J = 23.2$  Hz), 132.87, 129.31, 128.31, 125.88 (d,  $J = 4.3$  Hz), 123.10 (d,  $J = 18.3$  Hz), 120.25, 20.81, 20.15.  $^{19}\text{F}$  NMR ( $\text{CDCl}_3$ ):  $\delta$   $-128.74$ . HRMS electrospray ( $m/z$ ):  $[\text{M}]^+$  calcd for  $\text{C}_{14}\text{H}_{12}\text{FNO}_2$ , 245.0852; found, 245.0850. IR (thin film)  $1765\text{ cm}^{-1}$ .



The product was obtained as a yellow oil ( $R_f = 0.2$  in 90% hexanes/10% ethyl acetate).  $^1\text{H}$  NMR ( $\text{CDCl}_3$ ):  $\delta$  8.87 (d,  $J = 5.2$  Hz, 1H), 7.48 (s, 1H), 7.46 (d,  $J = 5.2$  Hz, 1H), 7.32 (t,  $J = 8.0$  Hz, 1H), 7.17 (d,  $J = 8.0$  Hz, 1H), 6.98 (d,  $J = 8.0$  Hz, 1H), 2.15 (s, 3H), 1.93 (s, 3H).  $^{13}\text{C}\{^1\text{H}\}$  NMR ( $\text{CDCl}_3$ ):  $\delta$  169.46, 157.51, 150.77, 148.51, 138.62 (q,  $J = 34.1$  Hz), 138.39, 132.39, 129.74, 128.50, 122.98 (q,  $J = 271.6$  Hz), 120.77 (q,  $J = 3.5$  Hz), 120.77, 117.83 (q,  $J = 3.5$  Hz), 20.66, 20.16.  $^{19}\text{F}$  NMR ( $\text{CDCl}_3$ ):  $\delta$   $-64.78$ . HRMS electrospray ( $m/z$ ):  $[\text{M}]^+$  calcd for  $\text{C}_{15}\text{H}_{12}\text{F}_3\text{NO}_2$ , 295.0820; found, 295.0814. IR (thin film)  $1768\text{ cm}^{-1}$ .

### 3.8 References

---

<sup>1</sup> For reviews, see: (a) Dick, A. R.; Sanford, M. S. *Tetrahedron* **2006**, *62*, 2439. (b) Daugulis, O.; Zaitsev, V. G.; Shabashov, D.; Pham, Q.-N.; Lazareva, A. *Synlett* **2006**, 3382. (c) Alberico, D.; Scott, M. E.; Lautens, M. *Chem. Rev.* **2007**, *107*, 174. (d) Li, B. J.; Yand, S. D.; Shi, Z. J., *Synlett*, **2008**, 949. (e) Chen, X.; Engle, K. M.; Wang, D. H.; Yu, J. Q. *Angew. Chem. Int. Ed.* **2009**, *48*, 5094 (f) Lyons, T. W.; Sanford, M. S. *Chem. Rev.* **2010**, *110*, 1147-1169. (g) Jazzar, R.; Hitce, J.; Renaudat, A.; Sofack-Kreutzer, J.; Baudoin, O. *Chem. Eur. J.* **2010**, *16*, 2654-2672.

<sup>2</sup> For examples, see: (a) Desai, L. V.; Hull, K. L.; Sanford, M. S. *J. Am. Chem. Soc.* **2004**, *126*, 9542. (b) Giri, R.; Liang, J.; Lei, J. G.; Li, J. J.; Wang, D. H.; Chen, X.; Naggar, I. C.; Guo, C.; Foxman, B. M.; Yu, J. Q. *Angew. Chem., Int. Ed.* **2005**, *44*, 7420. (c) Reddy, B. V. S.; Reddy, L. R.; Corey, E. J. *Org. Lett.* **2006**, *8*, 3391. (d) Neufeldt, S. R.; Sanford, M. S. *Org. Lett.* **2010**, *12*, 532-535. (e) Kubota, A.; Sanford, M. S. *Synthesis* **2011**, 2579. (f) Reddy, B. V. S.; Revathi, G.; Reddy, A.; Yadav, J. S. *Tetrahedron Lett.* **2011**, *52*, 5926.

<sup>3</sup> For examples, see: (a) Dick, A. R.; Hull, K. L.; Sanford, M. S. *J. Am. Chem. Soc.* **2004**, *126*, 2300. (b) Giri, R.; Chen, X.; Yu, J. Q. *Angew. Chem. Int. Ed.* **2005**, *44*, 2112. (c) Kalyani, D.; Dick, A. R.; Anani, W. Q.; Sanford, M. S. *Tetrahedron* **2006**, *62*, 11483. (d) Hull, K. L.; Anani, W. Q.; Sanford, M. S. *J. Am. Chem. Soc.* **2006**, *128*, 7134. (e) Wan, X.; Ma, Z.; Li, B.; Zhang, K.; Cao, S.; Zhang, S.; Shi, Z. *J. Am. Chem. Soc.* **2006**, *128*, 7416. (f) Wang, X.; Mei, T. S.; Yu, J. Q. *J. Am. Chem. Soc.* **2009**, *131*, 7520. (g) Kakiuchi, F.; Kochi, T.; Mutsutani, H.; Kobayashi, N.; Urano, S.; Sato, M.; Nishiyama, S.; Tanabe, T. *J. Am. Chem. Soc.* **2009**, *131*, 11310.

<sup>4</sup> For examples, see: (a) Thu, H. Y.; Yu, W. Y.; Che, C. M. *J. Am. Chem. Soc.* **2006**, *128*, 9048. (b) Jordon-Hore, J. A.; Johansson, C. C. C.; Gulia, M.; Beck, E. M.; Gaunt, M. J. *J. Am. Chem. Soc.* **2008**, *130*, 16184. (c) Mei, T. S.; Wang, X.; Yu, J. Q. *J. Am. Chem. Soc.* **2009**, *131*, 10806. (d) Yoo, E. J.; Ma, S.; Mei, T.-S.; Chan, K. S. L.; Yu, J.-Q. *J. Am. Chem. Soc.* **2011**, 7652. (e) Youn, S. W.; Bihn, J. H.; Kim, B. S. *Org. Lett.* **2011**, *13*, 3738.

<sup>5</sup> Zhao, X.; Dimitrijevic, E.; Dong, V. M. *J. Am. Chem. Soc.* **2009**, *131*, 3466.

<sup>6</sup> (a) Wasa, M.; Engle, K. M.; Yu, J. Q. *J. Am. Chem. Soc.* **2009**, *131*, 9886. (b) Vickers, C. J.; Mei, T.-S.; Yu, J.-Q. *Org. Lett.* **2010**, *12*, 2511. (c) Mei, T.-S.; Wang, D.-H.; Yu, J.-Q. *Org. Lett.* **2010**, *12*, 3140.

<sup>7</sup> (a) Hull, K. L.; Lanni, E. L.; Sanford, M. S. *J. Am. Chem. Soc.* **2007**, *128*, 14047. (b) Desai, L. V.; Stowers, K. J.; Sanford, M. S. *J. Am. Chem. Soc.* **2008**, *130*, 13285. (c) Hull, K. L.; Sanford, M. S. *J. Am. Chem. Soc.* **2009**, *131*, 9651. (d) Racowski, J. M.; Dick, A. R.; Sanford, M. S. *J. Am. Chem. Soc.* **2009**, *131*, 10974. (e) Deprez, N. R.; Sanford, M. S. *J. Am. Chem. Soc.* **2009**, *131*, 11234.

<sup>8</sup> (a) Chiong, H. A.; Pham, Q. N.; Daugulis, O. *J. Am. Chem. Soc.* **2007**, *129*, 9879. (b) Li, J. J.; Giri, R.; Yu, J. Q. *Tetrahedron* **2008**, *64*, 6979. (c) Powers, D.

---

C.; Ritter, T. *Nat. Chem.* **2009**, *1*, 302. (d) Powers, D. C.; Xiao, D.Y.; Geibel, M. A. L.; Ritter, T. *J. Am. Chem. Soc.* **2010**, *132*, 14540.

<sup>9</sup> The identity of the ancillary ligands at [Pd] is not currently known; as a result, these ligands are represented as sticks.

<sup>10</sup> For examples, see: (a) Deeming, A. J.; Rothwell, I. P. *J. Organomet. Chem.* **1981**, *205*, 117. (b) Ryabov, A. D.; Sakodinskaya, I. K.; Katsimirsky, A. K. *J. Chem. Soc., Dalton Trans.* **1985**, 2629. (c) Ryabov, A. D. *Chem. Rev.* **1990**, *90*, 403 and references therein.

<sup>11</sup> Kurzeev, S. A.; Kazankov, G. M.; Ryabov, A. D. *Inorg. Chim. Acta.* **2002**, *340*, 192.

<sup>12</sup> Vicente, J.; Saura-Llamas, I. *Comm. Inorg. Chem.* **2007**, *28*, 39.

<sup>13</sup> For examples of cyclometalation mechanisms analogous to path *a*, see ref. <sup>10c</sup> as well as: (a) Yatsimirsky, A. K. *Zh. Neorg. Khim.* **1979**, *24*, 2711. (b) Yagyu, T.; Aizawa, S.; Funahashi, S. *Bull. Chem. Soc. Jpn* **1998**, *71*, 619. (c) Yagyu, T.; Iwatsuki, S.; Aizawa, S.; Funahashi, S. *Bull. Chem. Soc. Jpn* **1998**, *71*, 1857. (d) Martin-Matute, B.; Mateo, C.; Cardenas, D. J.; Echavarren, A. M. *Chem. Eur. J.* **2001**, *7*, 2341.

<sup>14</sup> For examples of cyclometalation mechanisms analogous to path *b*, see: (a) Alsters, P. L.; Engel, P. F.; Hogerheide, M. P.; Copijn, M.; Spek, A. L.; van Koten, G. *Organometallics* **1993**, *12*, 1831. (b) Otto, S.; Chanda, A.; Samuleev, P. V.; Ryabov, A. D. *Eur. J. Inorg. Chem.* **2006**, 2561 and references therein.

<sup>15</sup> Utas, J. E.; Olofsson, B.; Akermark, B. *Synlett.* **2006**, *12*, 1965-1967.

<sup>16</sup> Connon, S. J.; Hegarty, A. F. *Tetrahedron Lett.* **2001**, *42*, 735-737.

<sup>17</sup> Harris, D. C. *Quantitative Chemical Analysis*. W. H. Freeman/Company; New York, **2003**; pp 55-83

## Chapter 4: Olefination of $sp^3$ C–H bonds

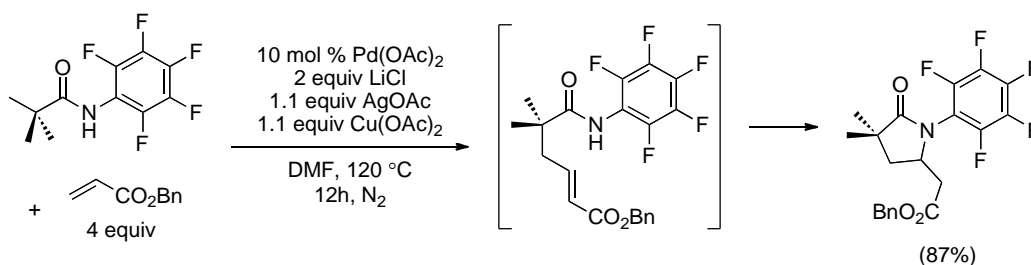
### 4.1 Introduction

Transition metal catalyzed C–H olefination reactions have been the subject of tremendous research activity over the past 20 years.<sup>1</sup> These transformations provide an atom economical method for replacing a simple carbon-hydrogen bond with a readily derivatizable alkene functional group. A variety of different metals (for example, Pd, Cu, Ni, Co, Rh, and Ru) catalyze the olefination of arenes,<sup>2</sup> and these transformations have been applied to the synthesis and functionalization of biologically active molecules.<sup>3</sup> Pd-based catalysts have been particularly well studied and effectively promote the reaction of alkenes with diverse arene and heteroarene-based substrates.<sup>4</sup>

While the olefination of  $sp^2$ -C–H bonds is a reliable and widely-used synthetic method, the analogous transformations that we sought to develop at unactivated  $sp^3$ -C–H sites remain extremely rare.<sup>5,6</sup> Expanding this chemistry to unactivated alkyl groups is challenging for several reasons. First, palladium-mediated cleavage of  $sp^3$ -C–H bonds is typically slow<sup>7,13b</sup> and is expected to be even slower in the presence of an alkene, which can compete for coordination sites at the metal center. Second, the key C–C bond-forming event requires carbometallation of a Pd-alkyl intermediate. Such reactions (particularly intermolecular variants) are difficult, because they are frequently plagued by competing  $\beta$ -hydride elimination.<sup>8,9</sup> Finally, the nucleophilic directing groups often required to promote  $sp^3$ -C–H activation can undergo intramolecular Michael addition into the olefinated products, thereby removing the versatile olefin functional group that was installed in the first step. Due to these challenges, at the time we published these studies there was only one report of the C–H olefination of unactivated  $sp^3$ -C–H bonds.<sup>5</sup> As shown in Scheme 4.1, this study

by Yu and coworkers described the Pd-catalyzed reaction of pentafluorophenyl-substituted amides with benzyl acrylate.<sup>5</sup> Although this was a landmark report, the transformation has numerous limitations, including a limited substrate scope, the requirement for stoichiometric Cu<sup>II</sup> and Ag<sup>I</sup> salts as oxidants, and the formation of cyclic products derived from irreversible Michael addition of the amide to the alkene.

**Scheme 4.1** Precedent for Pd-Catalyzed sp<sup>3</sup> C–H Olefination



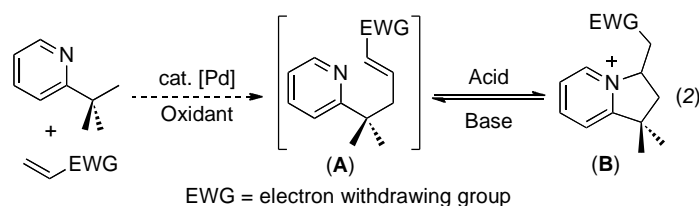
As part of a program aimed at developing Pd-catalyzed methods for the functionalization of unactivated C–H bonds,<sup>10</sup> we developed a new nitrogen heterocycle-directed sp<sup>3</sup>-C–H olefination reaction. This transformation utilizes air as the terminal oxidant and proceeds efficiently with diverse 2-alkyl pyridines and  $\alpha,\beta$ -unsaturated alkenes. The olefin-containing products can be elaborated using a variety of synthetic methods. In addition, this reaction provides a novel entry to bicyclic-nitrogen heterocycles, which constitute the core of numerous alkaloid natural products.<sup>11</sup>

## 4.2 Results

Our first efforts towards sp<sup>3</sup>-C–H olefination focused on the reaction of 2-*tert*-butylpyridine (2-*tbp*) with electron deficient alkenes. Previous work from our group<sup>10a,b</sup> and others<sup>12</sup> has shown that pyridine and quinoline derivatives are effective directing groups for the Pd-mediated cleavage of sp<sup>3</sup>-C–H bonds. The resulting palladacycles are generally slow to undergo  $\beta$ -hydride elimination, making them amenable to subsequent functionalization.<sup>7,13</sup> In addition, we

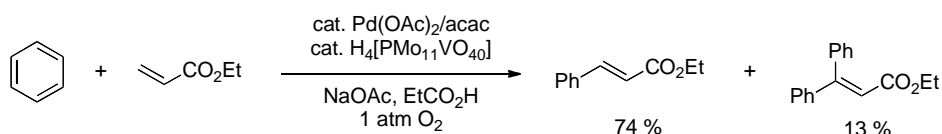
reasoned that a pyridine directing group could undergo *reversible* intramolecular Michael addition with the functionalized product, thereby providing access to either olefin (**A**) or a cyclic pyridinium salt (**B**), depending on the reaction conditions as shown in Scheme 4.2.

**Scheme 4.2** Hypothesized Equilibrium between Olefin Product (**A**) and Cyclized Product (**B**)



Dioxygen is the most cost effective and environmentally benign oxidant for this transformation; therefore, we were interested to use this as the terminal oxidant in our reactions. However, the use of oxygen for this type of oxidative Heck reaction is rare.<sup>14</sup> As such, we first examined the reaction of 2-tbp with ethyl acrylate under conditions reported by Ishii for the Pd/polyoxometalate co-catalyzed aerobic olefination of benzene derivatives (Scheme 4.3).<sup>15</sup> We hypothesized that this could be a good starting point for the C–H activation and olefination of unactivated  $sp^3$ -C–H bonds.

**Scheme 4.3** Ishii Conditions for Oxidative Heck Reactions with Acrylates

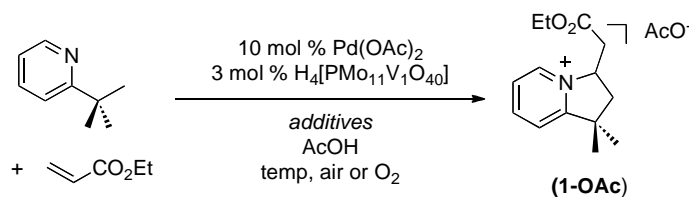


Gratifyingly, the use of 10 mol % of Pd(OAc)<sub>2</sub> and 10 mol % of acetylacetone (acac) along with 3 mol % of H<sub>4</sub>[PMo<sub>11</sub>VO<sub>40</sub>] in AcOH at 90 °C under 1 atm of O<sub>2</sub> (analogous conditions to those used by Ishii) provided 49% yield of product **1-OAc** (Table 4.1, entry 1). We were delighted to find that ambient air could be used in place of 1 atm of O<sub>2</sub> without any detrimental effect on the overall yield



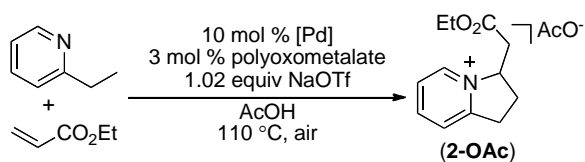
(entry 2). Increasing the temperature to 110 °C under 1 atm of O<sub>2</sub> or air significantly increased the yield to 81% (entries 3 and 4). Finally, simplifying the conditions somewhat by removing the acac ligand also increased the yield (entry 5).

**Table 4.1.** Optimization of catalyst, polyoxometalate, additives and O<sub>2</sub>

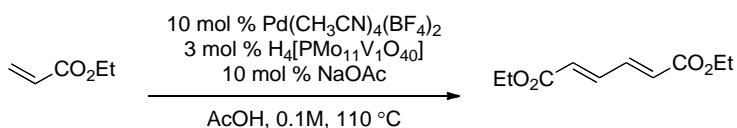


Entry	Additives	air or O <sub>2</sub>	Temp	Yield
1	10 mol% acac 8 mol% NaOAc	O <sub>2</sub>	90 °C	49%
2	10 mol% acac 8 mol% NaOAc	air	90 °C	40%
3	10 mol% acac 10 mol% NaOAc	O <sub>2</sub>	110 °C	81%
4	10 mol% acac 10 mol% NaOAc	air	110 °C	83%
5	None 10 mol% NaOAc	air	110 °C	89%

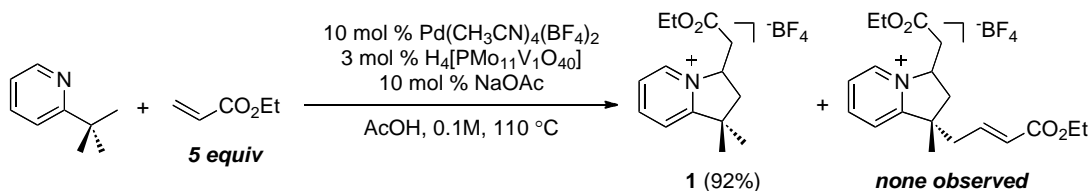
With these modified conditions in hand, we next studied the effects of Pd catalyst structure on the olefination reaction as summarized in Table 4.2. It was observed that the polyoxometallate was necessary for catalyst turnover (entry 1). Although a number of palladium sources were viable for product formation (entries 2-4), replacing Pd(OAc)<sub>2</sub> with the cationic catalyst Pd(MeCN)<sub>4</sub>(BF<sub>4</sub>)<sub>2</sub><sup>16</sup> enhanced the yield of olefination (entry 6) and limited the formation of byproducts derived from homo-coupling of the olefin starting material (Scheme 4.4).<sup>17</sup> These byproducts formed in large quantities and increased the difficulty of product purification, particularly for reactions performed on a larger scale.

**Table 4.2.** Optimization of Catalyst

Entry	[Pd]	Polyoxometalate	Yield
1	Pd(OAc) <sub>2</sub>	none	6%
2	PdCl <sub>2</sub>	H <sub>4</sub> [PMo <sub>11</sub> VO <sub>40</sub> ]	0%
3	Pd <sub>2</sub> (dba) <sub>3</sub>	H <sub>4</sub> [PMo <sub>11</sub> VO <sub>40</sub> ]	39%
4	Pd(OTf) <sub>2</sub>	H <sub>4</sub> [PMo <sub>11</sub> VO <sub>40</sub> ]	53%
5	Pd(OAc) <sub>2</sub>	H <sub>4</sub> [PMo <sub>11</sub> VO <sub>40</sub> ]	68%
6	Pd(MeCN) <sub>4</sub> (BF <sub>4</sub> ) <sub>2</sub>	H <sub>4</sub> [PMo <sub>11</sub> VO <sub>40</sub> ]	89%

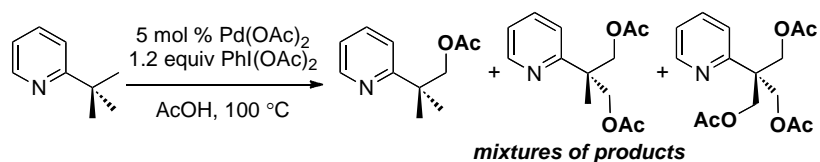
**Scheme 4.4** Homo-coupled byproduct of the Olefin Starting Material

Interestingly, despite the presence of an excess (5 equiv) of alkene, this reaction exclusively afforded the mono-functionalized product **1** in 92% isolated yield (Scheme 4.5).

**Scheme 4.5.** Observance of Selective Mono-Functionalization

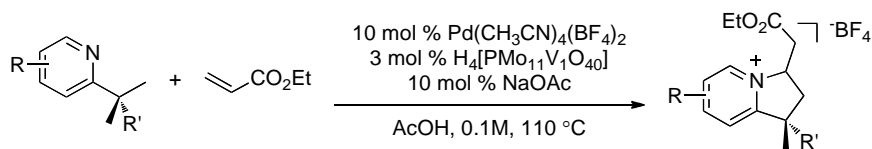
This result is in marked contrast to the C–H acetoxylation of 2-tbp with PhI(OAc)<sub>2</sub>, which forms mixtures of mono-, di-, and triacetoxyated products under all conditions examined (Scheme 4.6).<sup>10b</sup>

#### Scheme 4.6. Observance of Mixtures of Acetoxyated Products



As shown in Table 4.3, a variety of different 2-alkylpyridine derivatives participate in this  $sp^3$ -C–H olefination/cyclization reaction. Both electron-withdrawing and electron-donating substituents were tolerated on the pyridine ring (substrates **3-5**). Remarkably, despite the sterically crowded environment around the pyridine moiety, 2-methyl-6-*tert*-butylpyridine provided moderate (36%) yield of **6**. In addition, a tethered ester was also compatible with the reaction conditions although this substrate afforded a modest (49%) yield of **7**. Quinoline was also an effective directing group for  $sp^3$ -C–H olefination under these conditions to afford cyclized product **8**.

**Table 4.3.** Pd-Catalyzed Olefination and Cyclization Between Various Pyridines and Ethylacrylate.

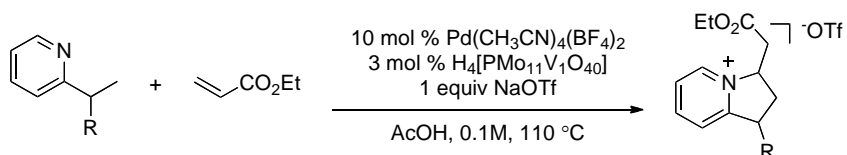


Entry	Substrate	Product	Yield
1			<b>3</b> (70%)
2			<b>4</b> (71%)
3			<b>5</b> (75%)
4			<b>6</b> (36%)
5			<b>7</b> (49%) dr = 1 : 1
6			<b>8</b> (39%)

Remarkably, geminal dimethyl groups are not necessary in these substrates as summarized in Table 4.4; both 2-ethyl and 2-*iso*-propyl pyridine afforded high yields of the desired products **2** and **9** respectively.<sup>18</sup> C–H activation/C–C coupling proceeded with high selectivity for 1° over 2° sp<sup>3</sup> C–H bonds as demonstrated in product **10**. A 2° C–H bond on the cyclopropane ring of 2-

cyclopropyl-3-methylpyridine could be functionalized to form tricyclic product **11** in modest yield.

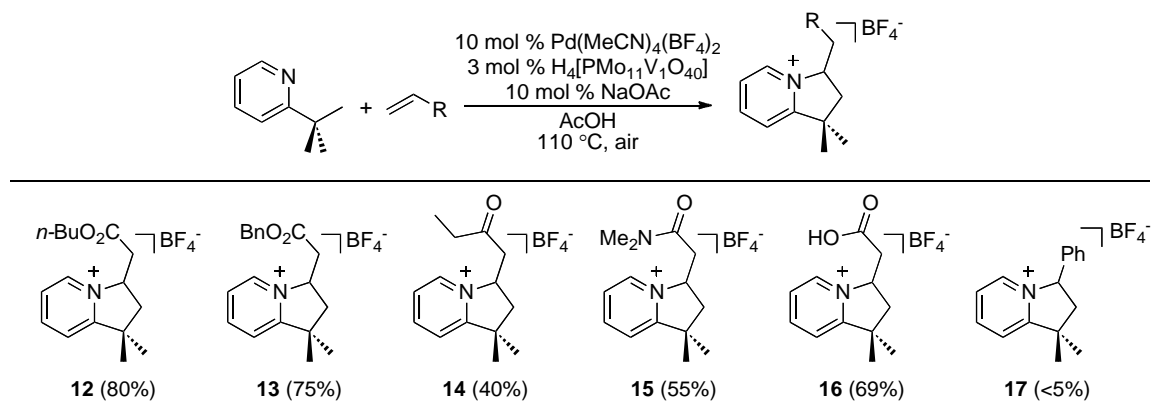
**Table 4.4.** Pd-Catalyzed Olefination and Cyclization Between Pyridines and Ethylacrylate.



Entry	Substrate	Product	Yield
1			<b>2</b> (89%)
2			<b>9</b> (81%) (dr = 1.2 : 1)
3			<b>10</b> (55%) (dr = 1.2 : 1)
4			<b>11</b> (43%) (dr = 2.4 : 1)

The reaction of 2-tbp was examined with a series of different olefinic substrates to form products **12-16**. As shown in Figure 4.3,  $\alpha,\beta$ -unsaturated esters, amides, and ketones were effective alkene coupling partners. Remarkably, the free carboxylic acid moiety of acrylic acid was also well tolerated to form **16**. In contrast, more electron rich olefins like styrene and 1-hexene exhibited low reactivity under the current conditions as in **17**. This result is a common limitation of Pd-catalyzed arene C–H alkenylation reactions.<sup>4</sup>

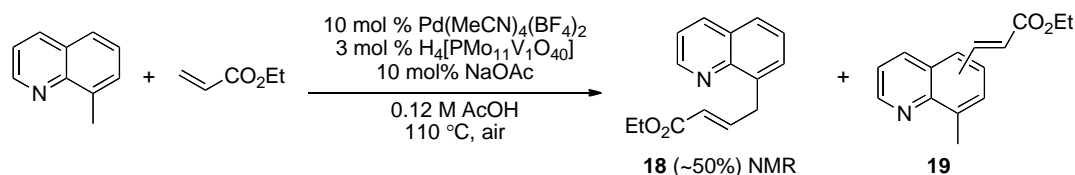
**Figure 4.1.** Alkene Scope for C–H Bond Alkenylation.



<sup>a</sup>Reported as NMR yields against internal standard. Olefin by product remained.

A number of additional substrates/directing groups were examined for C–H olefination, with mixed results. In a first example, 8-methylquinoline underwent sp<sup>3</sup>-C–H olefination with ethyl acrylate to form product **18** in a cyclized 50% yield (observed by <sup>1</sup>H NMR spectroscopy). The uncyclized product was isolated (~30%), however, analysis of the crude reaction mixture by <sup>1</sup>H NMR spectroscopy indicated that selectivity was poor, and some minor products of general structure **19** (20% yield as determined by <sup>1</sup>H NMR spectroscopy and GC/MS) were formed via C–C bond formation of the aryl ring itself.

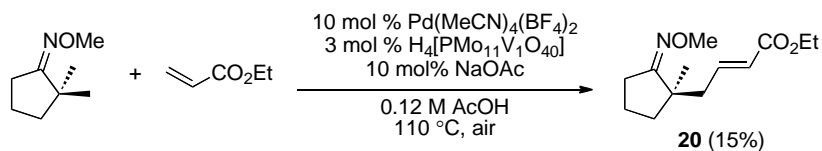
**Scheme 4.7** Olefination of 8-Methylquinoline to form olefinated product **18**



2,2-Dimethylcyclopentanone O-methyl oxime also reacted with ethyl acrylate to form an olefinated product in approximately 15% yield as observed by <sup>1</sup>H NMR spectroscopy (Scheme 4.8). This compound was isolated in very low yield, but was confirmed to be olefinated product **20**. However, all efforts to optimize the

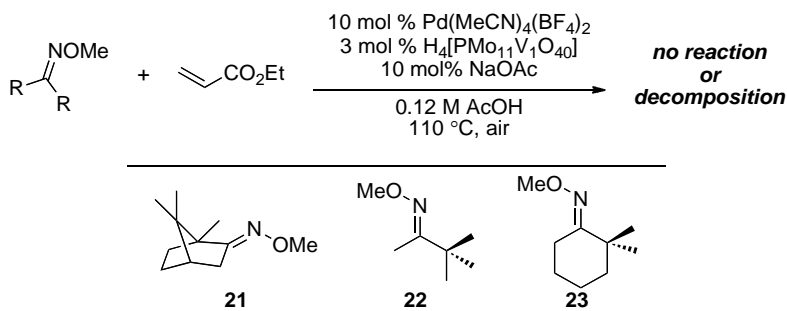
reaction conditions for this substrate did not significantly increase the yield of this product.

**Scheme 4.8** Olefination of 2,2-Dimethylcyclopentyl O-Methyloxime Ether



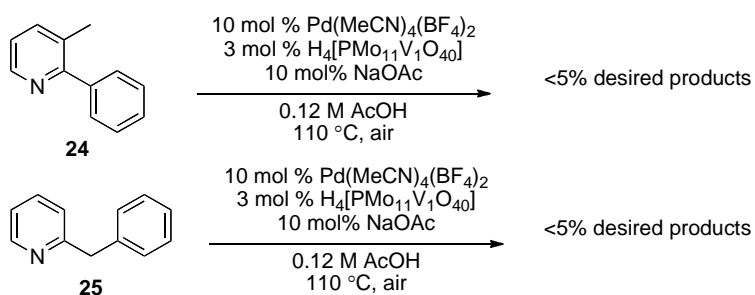
A few other methyl oxime ethers (**21-23**) were also submitted to the optimal reaction conditions with ethyl acrylate. Interestingly, in all of these cases no C–H olefinated products were detected (as determined by <sup>1</sup>H NMR spectroscopic analysis of the crude reaction mixtures). For substrate **21**, only starting material was detected. Substrates **22** and **23** underwent decomposition under these reaction conditions.

**Figure 4.2.** Other Methyl Oxime Ether Substrates.



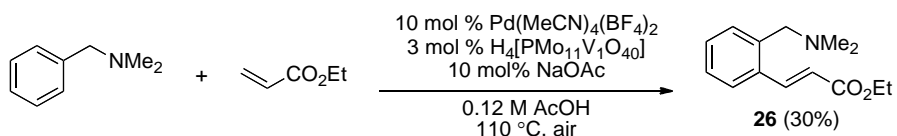
We also submitted substrates **24** and **25** (which could undergo pyridine-directed sp<sup>2</sup> C–H activation) to the reaction conditions and found that mostly starting material remained with very little other reactivity in both cases (<5%) (Figure 4.3).

**Figure 4.3.** Substrates with Pyridine Directing Groups for  $sp^2$  C–H Activation.



Interestingly, when *N,N*-dimethylbenzylamine was used as the substrate, we did observe approximately 30% of an  $sp^2$ -C–H olefination product was isolated and characterized by NMR spectroscopy (Scheme 4.9). However, the mass balance in this reaction was poor.

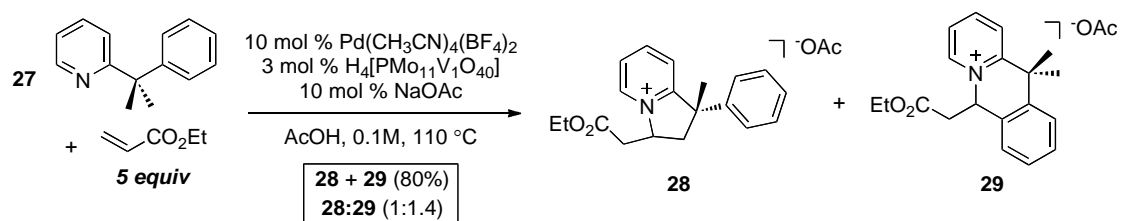
**Scheme 4.9** Olefination of *N,N*-dimethylbenzylamine



Due to the preference in reactivity of  $sp^3$ -C–H bonds over the traditionally more reactive  $sp^2$  C–H bond for olefination under our conditions, we hypothesized that we might be able to obtain selectivity for  $sp^3$ -C–H functionalization in a molecule with both  $sp^3$  and  $sp^2$ -C–H bonds in proximity to a directing group. Surprisingly, we observed that when the substrate **27** was submitted to the optimized reaction conditions, we observed a slightly higher preference for  $sp^2$  functionalization (forming cyclic compound **29**) as summarized in Scheme 4.10. The yields for this reaction were 80% for total olefinated products detected (**28** and **29**). Yield and selectivity was determined using NMR against the internal standard dichloroethane.



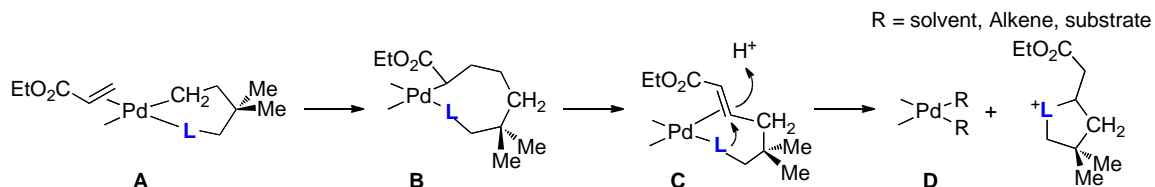
### Scheme 4.10 Selectivity for $sp^3$ and $sp^2$ C–H Olefination



### 4.3 Discussion

In the current system, based on a number of observations it seems that the intramolecular Michael addition appears to play several key roles. First, it operates to protect the product from over-functionalization. We also believe that this cyclization may be what allows high catalyst turnover with pyridine substrates, since the cyclized product does not coordinate to the catalyst as strongly as the acrylate starting material. The hypothesized mechanism for product inhibition is illustrated in Figure 4.4. After cyclopalladated complex **A** undergoes olefin insertion to form the new cyclopalladated complex **B**,  $\beta$ -hydride elimination forms a coordinated complex **C**. Without cyclization, the product could potentially irreversibly bind as an  $L_2$  type ligand through the pyridine and olefin (complex **C**), which would lead to product inhibition. However, this type of  $L_2$  ligand binding is not possible after cyclization to release the Pd complex **D**, which would then be catalytically active. As an example, the oxime ether, which is unlikely to undergo cyclization due to the low-nucleophilicity of the oxime, only proceeds in what is essentially stoichiometric olefination possibly due to formation of complex **C**.

**Figure 4.4.** Possible Mechanism for Product Inhibition

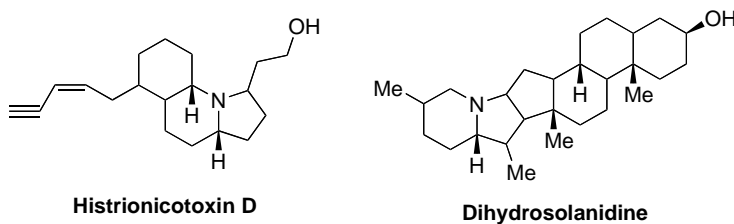


It was also observed that the counterion must be tuned in order to achieve efficient catalysis. For example, 2-ethylpyridine and other substrates that have a hydrogen  $\beta$  to the pyridine exhibited significantly higher reactivity with triflate as a counterion as opposed to the less coordinating tetrafluoroborate that is used for the 2-*tert*-butylpyridines. This non-generality of the counterion may also be due to the counterion's influence on product inhibition and/or the cyclization of the product.

#### 4.4 Application

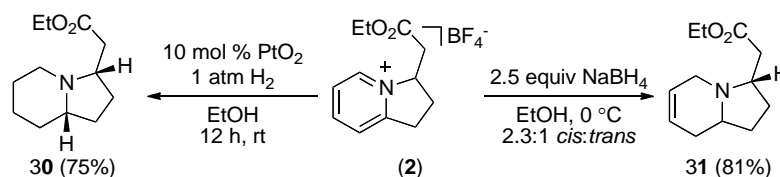
The cationic bicyclic products in Tables 1-3 are useful synthetic intermediates. This chemistry, if applied to a total synthesis, could provide an expedient route to 6,5-nitrogen heterocycles, which are a common structural motif in naturally occurring alkaloids as shown in Figure 4.5. Working with Dr. Kevin Fortner, a post-doctoral fellow in our laboratory, our next aim was to demonstrate some of the synthetic utility by conducting further synthetic manipulations of the olefinated products.

**Figure 4.5.** Examples of Naturally Occurring 6,5-Nitrogen Heterocycles



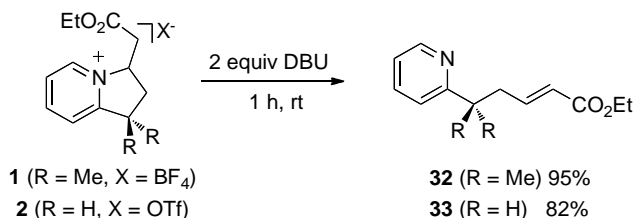
For example as summarized in Scheme 4.11, the  $\text{PtO}_2$ -catalyzed reduction of **2** with  $\text{H}_2$  formed piperidine **30** in 75% yield as a 28 : 1 mixture of *cis* and *trans* isomers.<sup>19</sup> In addition, partial reduction of **2** with  $\text{NaBH}_4$  in EtOH afforded 1,2,3,6-tetrahydropyridine **31** in 81% yield as a 2.3 : 1 mixture of readily separable *cis* and *trans* isomers.<sup>20</sup>

### Scheme 4.11. Reduction Reactions of **2**



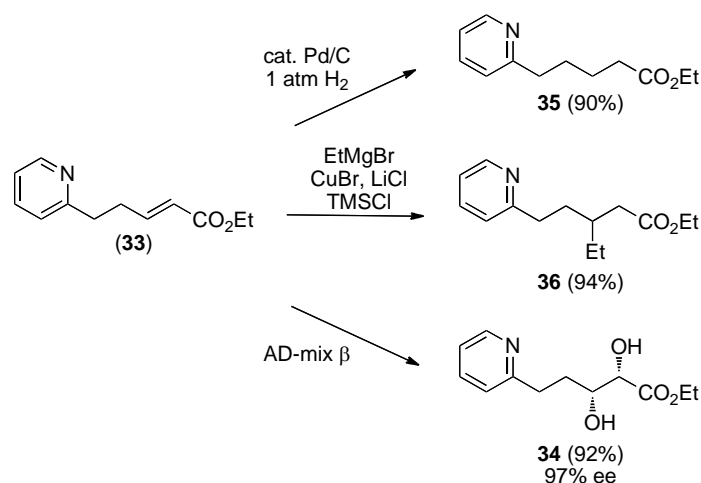
The pyridinium products of  $sp^3$  C–H olefination/cyclization can also be readily converted to the corresponding alkenes by treatment with base. For example, the reaction of **2** with 2 equiv of DBU in  $\text{CH}_2\text{Cl}_2$  for 1 h afforded olefin **33** in 95% yield (Scheme 4.12).

### Scheme 4.12 Deprotonation to Obtain the Alkene Product



The ability to readily generate the olefin-containing products allowed us to explore the further functionalization of these molecules. As shown in Figure 4.6, **33** underwent smooth and high yielding asymmetric dihydroxylation<sup>21</sup> (to form **34** in 97% ee), hydrogenation<sup>22</sup> (to form **35**), and Cu-catalyzed conjugate addition of  $\text{EtMgBr}$ <sup>23</sup> (to form **36**).

**Figure 4.6.** Functionalization of C–H Alkenylated Product **14**.<sup>a</sup>



<sup>a</sup>Conditions: (a) AD-mix β, MeSO<sub>2</sub>NH<sub>2</sub>, *t*-BuOH, H<sub>2</sub>O, 0 °C, 92%, 97% ee. (b) H<sub>2</sub>, Pd/C, EtOH, rt, 90%. (c) CuBr, LiCl, EtMgBr, TMSCl, THF, 0 °C, 94%.

## 4.5 Conclusions

In conclusion, this chapter describes a new Pd-catalyzed reaction for the pyridine-directed aerobic olefination of unactivated sp<sup>3</sup> C–H sites. This transformation provides a convenient route to 6,5-N-fused bicyclic cores as well as readily functionalizable alkene products. Ongoing work is focused on expanding the scope of this transformation with respect to both directing group and alkene substrate, and will be reported in due course.

## 4.6 Experimental

**Standard Procedure A.** In a 40 mL vial in air, NaOAc (2.1 mg, 0.025 mmol, 0.1 equiv), Pd(MeCN)<sub>4</sub>(BF<sub>4</sub>)<sub>2</sub> (11.11 mg, 0.025 mmol, 0.10 equiv) and H<sub>4</sub>[PMo<sub>11</sub>VO<sub>40</sub>] (13.36 mg, 0.0075 mmol, 0.03 equiv) were combined in AcOH (2 mL). The alkene (1.25 mmol, 5.0 equiv) was added, followed by addition of substrate (0.25 mmol, 1.0 equiv), after which the vial was sealed with a Teflon-lined cap, and the resulting solution was heated at 110 °C for 18 h. The reaction was then cooled to room temperature and filtered through a short celite plug, which was washed with MeOH (1 mL). The AcOH and MeOH were removed

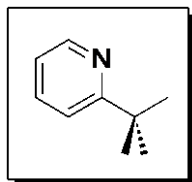
under reduced pressure, and the remaining salts were dried under vacuum. Water (1 mL) was added to dissolve the cyclized product and the solution was filtered through a short celite plug to remove the polyoxometalate and catalyst. The celite was rinsed with 1 mL of water. The water layers were combined and the water was removed under reduced pressure followed by addition of 1 mL of saturated aqueous solution of NaBF<sub>4</sub> to exchange the AcO<sup>-</sup> counterion. The organic BF<sub>4</sub><sup>-</sup> salt was then extracted into CH<sub>2</sub>Cl<sub>2</sub> (5 x 2 mL). The CH<sub>2</sub>Cl<sub>2</sub> layers were combined and dried with MgSO<sub>4</sub>. The solvent was removed under reduced pressure to provide the product.

**Standard Procedure B.** In a 40 mL vial in air, NaOTf (47.3 mg, 0.275 mmol, 1.1 equiv), Pd(MeCN)<sub>4</sub>(BF<sub>4</sub>)<sub>2</sub> (11.11 mg, 0.025 mmol, 0.10 equiv) and H<sub>4</sub>[PMo<sub>11</sub>VO<sub>40</sub>] (13.36 mg, 0.0075 mmol, 0.03 equiv) were combined in AcOH (2 mL). The alkene (1.25 mmol, 5.0 equiv) was added followed by addition of substrate (0.25 mmol, 1.0 equiv), after which the vial was sealed with a Teflon-lined cap, and the resulting solution was heated at 110 °C for 18 h. The reaction was then cooled to room temperature and filtered through a short celite plug, which was washed with MeOH (1 mL). The AcOH and MeOH were removed under reduced pressure, and the remaining salts were dried under vacuum. Water (1 mL) was added to dissolve the cyclized product and the solution was filtered through a short celite plug to remove the polyoxometalate and catalyst. The celite was rinsed with 1 mL of water. The water layers were combined and the water was removed under reduced pressure. The remaining salt was dissolved in a saturated NaHCO<sub>3</sub> solution and the TfO<sup>-</sup> salt of the product was extracted into CH<sub>2</sub>Cl<sub>2</sub> (5 x 2 mL). The CH<sub>2</sub>Cl<sub>2</sub> layers were combined and dried with MgSO<sub>4</sub>. The solvent was removed under reduced pressure to provide the product.

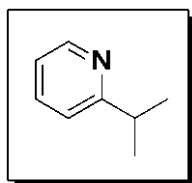
#### 4.7 Characterization

##### II. Synthesis and Characterization of Substrates S1, S3-S11

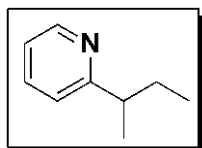
(Substrate S2 was commercially available through Sigma-Aldrich.)



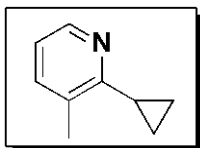
Substrate S1 was prepared by Cu-catalyzed coupling between 2-bromopyridine (Aldrich) and  $t$ BuMgCl (Alfa Aesar) using a literature procedure.<sup>24</sup> S1 was obtained as a yellow oil ( $R_f = 0.29$  in 95:5 pentanes/Et<sub>2</sub>O). Spectral data (<sup>1</sup>H NMR (CDCl<sub>3</sub>) and <sup>13</sup>C{<sup>1</sup>H} NMR (CDCl<sub>3</sub>)) for S1 matched those reported in the literature.<sup>25</sup>



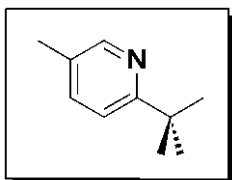
Substrate S3 was prepared by alkylation of 2-ethylpyridine (Aldrich) with iodomethane (Aldrich) according to a literature procedure.<sup>25</sup> S3 was obtained as a yellow oil ( $R_f = 0.16$  in 95:5 pentanes/Et<sub>2</sub>O). Spectral data (<sup>1</sup>H NMR (CDCl<sub>3</sub>) and <sup>13</sup>C{<sup>1</sup>H} NMR (CDCl<sub>3</sub>)) for S3 matched those reported in the literature.<sup>25</sup>



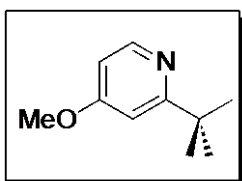
Substrate S4 was prepared by alkylation of 2-*n*-propylpyridine (Lancaster Synthesis Inc.) with iodomethane (Aldrich) using a literature procedure.<sup>25</sup> S4 was obtained as a yellow oil ( $R_f = 0.3$  in 90:10 hexanes/ethyl acetate). <sup>1</sup>H NMR (CDCl<sub>3</sub>):  $\delta$  8.54 (d,  $J = 4.0$  Hz, 1H), 7.59 (dd,  $J = 7.9, 7.8$  Hz, 1H), 7.13-7.07 (multiple peaks, 2H), 2.78 (tq,  $J = 7.2, 6.8$  Hz, 1H), 1.76 (d app. quin,  $J = 13.6, 7.2$  Hz, 1H), 1.63 (d app. quin,  $J = 13.6, 7.2$  Hz, 1H), 1.28 (d,  $J = 6.8$  Hz, 3H), 0.84 (t,  $J = 7.2$  Hz, 3H). <sup>13</sup>C{<sup>1</sup>H} NMR (CDCl<sub>3</sub>):  $\delta$  166.71, 149.37, 136.39, 121.78, 121.19, 43.90, 30.20, 20.60, 12.33. HRMS electrospray ( $m/z$ ):  $[M+H]^+$  calcd for C<sub>9</sub>H<sub>14</sub>N<sup>+</sup> 136.1121; found 136.1120.



Substrate S5 was prepared from 3-methyl-2-bromopyridine (Matrix Scientific) and cyclopropylboronic acid (Frontier Scientific) according to the literature procedure<sup>26</sup> with extended reaction time (overnight). After the reaction was complete, 3 M HCl solution was added to acidify the reaction mixture and the aqueous layer was extracted with EtOAc. The aqueous layer was basified with 3 M NaOH solution and the product was extracted with Et<sub>2</sub>O. The products were then purified by flash chromatography using 90:10 petroleum ether/Et<sub>2</sub>O. This product (S5) was obtained as a yellow oil ( $R_f = 0.28$  in 90:10 hexanes/ethyl acetate). <sup>1</sup>H NMR (CDCl<sub>3</sub>):  $\delta$  8.28 (d,  $J = 4.8$  Hz, 1H), 7.36 (d,  $J = 7.2$  Hz, 1H), 6.93 (dd,  $J = 7.2, 4.8$  Hz, 1H), 2.41 (s, 3H), 2.08 (tt,  $J = 9.6, 5.2$  Hz, 1H), 1.06 (m, 2H), 0.95 (m, 2H). <sup>13</sup>C{<sup>1</sup>H} NMR (CDCl<sub>3</sub>):  $\delta$  160.67, 146.77, 136.97, 131.20, 120.29, 19.06, 13.75, 9.00. HRMS electrospray (m/z): [M-H]<sup>+</sup> calcd for C<sub>9</sub>H<sub>10</sub>N<sup>+</sup> 132.0813; found 132.0816.

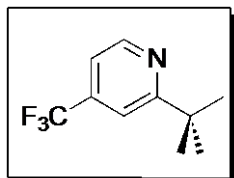


Substrate S6 was prepared by Cu-catalyzed coupling between 2-bromo-5-methylpyridine (Matrix Scientific) and <sup>t</sup>BuMgCl using a literature procedure.<sup>24</sup> S6 was obtained as a pale yellow oil ( $R_f = 0.32$  in 95:5 pentanes/Et<sub>2</sub>O). <sup>1</sup>H NMR (CDCl<sub>3</sub>):  $\delta$  8.38 (d,  $J = 2.4$  Hz, 1H), 7.41 (dd,  $J = 8.0, 2.4$  Hz, 1H), 7.22 (d,  $J = 8.0$  Hz, 1H), 2.28 (s, 3H), 1.35 (s, 9H). <sup>13</sup>C{<sup>1</sup>H} NMR (CDCl<sub>3</sub>):  $\delta$  166.67, 149.20, 136.88, 129.87, 118.70, 37.16, 30.47, 18.14. HRMS electrospray (m/z): [M+H]<sup>+</sup> calcd for C<sub>10</sub>H<sub>16</sub>N<sup>+</sup> 150.1277; found 150.1275.

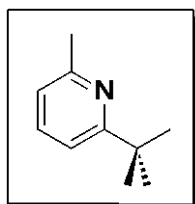


Substrate S7 was prepared by double alkylation<sup>25</sup> using iodomethane (Aldrich) of 2-ethyl-4-methoxypyridine prepared according to a literature procedure.<sup>27</sup> S7 was obtained as a yellow oil ( $R_f = 0.30$  in 90:10

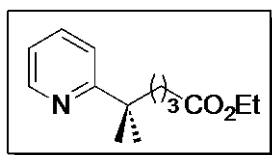
hexanes/ethyl acetate).  $^1\text{H}$  NMR ( $\text{CDCl}_3$ ):  $\delta$  8.40 (d,  $J = 5.6$  Hz, 1H), 6.85 (s, 1H) 6.63 (d,  $J = 5.6$  Hz, 1H), 3.84 (s, 3H), 1.35 (s, 9H).  $^{13}\text{C}\{^1\text{H}\}$  NMR ( $\text{CDCl}_3$ ):  $\delta$  171.33, 166.18, 150.19, 106.42, 105.94, 55.15, 37.55, 30.32. HRMS electrospray (m/z):  $[\text{M}+\text{H}]^+$  calcd for  $\text{C}_{10}\text{H}_{16}\text{NO}^+$  166.1226; found 166.1224.



Substrate S8 was prepared by Cu-catalyzed coupling between 2-bromo-4-trifluoromethylpyridine (Matrix Scientific) and  $t\text{BuMgCl}$  using a literature procedure.<sup>24</sup> S8 was obtained as a yellow oil ( $R_f = 0.3$  in 97:3 pentanes/ $\text{Et}_2\text{O}$ ).  $^1\text{H}$  NMR ( $\text{CDCl}_3$ ):  $\delta$  8.73 (d,  $J = 4.8$  Hz, 1H), 7.53 (s, 1H), 7.31 (d,  $J = 4.8$  Hz, 1H), 1.40 (s, 9H).  $^{13}\text{C}\{^1\text{H}\}$  NMR ( $\text{CDCl}_3$ ):  $\delta$  171.34, 149.85, 138.70 (q,  $^2J_{\text{CF}} = 34.0$  Hz), 123.42 (q,  $^1J_{\text{CF}} = 271.0$  Hz), 116.52 (q,  $^3J_{\text{CF}} = 4.0$  Hz) 114.94 (q,  $^3J_{\text{CF}} = 4.0$  Hz), 38.13, 30.26.  $^{19}\text{F}\{^1\text{H}\}$  NMR ( $\text{CDCl}_3$ ):  $\delta$  -64.84. HRMS electrospray (m/z):  $[\text{M}+\text{H}]^+$  calcd for  $\text{C}_{10}\text{H}_{13}\text{F}_3\text{N}^+$  204.0995; found 204.0994.



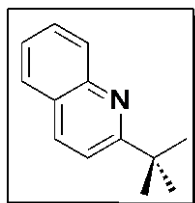
Substrate S9 was prepared by Cu-catalyzed coupling between 2-bromo-6-methylpyridine (Matrix Scientific) and  $t\text{BuMgCl}$  using a literature procedure.<sup>24</sup> S9 was obtained as a yellow oil ( $R_f = 0.32$  in 95:5 pentanes/ $\text{Et}_2\text{O}$ ).  $^1\text{H}$  NMR ( $\text{CDCl}_3$ ):  $\delta$  7.47 (app. t,  $J = 7.6$ , Hz, 1H), 7.12 (d,  $J = 7.6$  Hz, 1H), 6.92 (d,  $J = 7.6$ , 1H), 2.28 (s, 3H), 1.35 (s, 9H).  $^{13}\text{C}\{^1\text{H}\}$  NMR ( $\text{CDCl}_3$ ):  $\delta$  168.84, 157.22, 136.32, 120.12, 115.83, 37.46, 30.45, 25.00. HRMS electrospray (m/z):  $[\text{M}+\text{H}]^+$  calcd for  $\text{C}_{10}\text{H}_{16}\text{N}^+$  150.1277; found 150.1276.



Substrate S10 was prepared by hydrogenation (10 mol% Pd/C, 0.2 M EtOH, rt, 8 h, 90% yield) of 14. S10 was obtained as a colorless oil



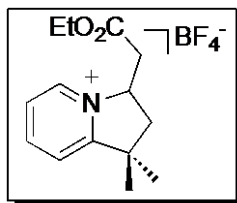
( $R_f = 0.25$  in 90:10 hexanes/ethyl acetate).  $^1\text{H}$  NMR ( $\text{CDCl}_3$ ):  $\delta$  8.57 (m, 1H), 7.60 (ddd,  $J = 7.4, 6.0, 1.2$  Hz, 1H), 7.29 (dd,  $J = 8.0, 1.6$  Hz, 1H), 7.08 (ddd,  $J = 7.6, 4.8, 1.2$ , 1H), 4.09 (q,  $J = 7.2$  Hz, 2H), 2.21 (t,  $J = 7.6$  Hz, 2H), 1.74 (m, 2H), 1.40 (m, 2H), 1.36 (s, 6H), 1.23 (t,  $J = 7.2$  Hz, 3H).  $^{13}\text{C}\{^1\text{H}\}$  NMR ( $\text{CDCl}_3$ ):  $\delta$  173.92, 168.06, 148.95, 136.26, 120.85, 120.09, 60.36, 42.93, 40.53, 35.01, 28.02, 20.58, 14.44. IR (thin film):  $1735\text{ cm}^{-1}$ . HRMS electrospray ( $m/z$ ):  $[\text{M}+\text{H}]^+$  calcd for  $\text{C}_{14}\text{H}_{22}\text{NO}_2^+$  236.1645; found 236.1653.



Substrate S11 was prepared by triple alkylation of quinaldine (Alfa Aesar) with iodomethane (Aldrich) using a literature procedure.<sup>25</sup> S11 was obtained as a yellow oil ( $R_f = 0.3$  in 90:10 hexanes/ethyl acetate).  $^1\text{H}$  NMR ( $\text{CDCl}_3$ ):  $\delta$  8.07 (d,  $J = 8.8$  Hz, 1H), 8.06 (d,  $J = 8.4$  Hz, 1H), 7.76 (dd,  $J = 8.2, 1.2$  Hz, 1H), 7.69 (ddd,  $J = 8.4, 6.8, 1.6$  Hz, 1H), 7.53 (d,  $J = 8.4$  Hz, 1H), 7.47 (ddd,  $J = 8.4, 6.8, 1.2$  Hz, 1H), 1.48 (s, 9H).  $^{13}\text{C}\{^1\text{H}\}$  NMR ( $\text{CDCl}_3$ ):  $\delta$  169.47, 147.64, 136.05, 129.63, 129.18, 127.43, 126.65, 125.82, 118.44, 38.34, 30.36. HRMS electrospray ( $m/z$ ):  $[\text{M}+\text{H}]^+$  calcd for  $\text{C}_{13}\text{H}_{16}\text{N}^+$  186.1277; found 186.1276.

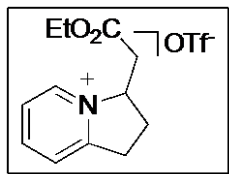
#### IV. Synthesis and Characterization of Cyclized Products 1-11, P1-P5

Products 3-5 were isolated as inseparable mixtures of diastereomers. Analysis by COSY and HSQC allowed for assignment of the  $^1\text{H}$  and  $^{13}\text{C}$  NMR resonances associated with each diastereomer.

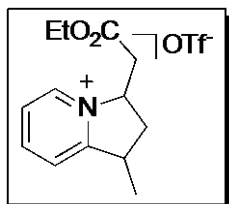


Product 1 was prepared from S1 and ethyl acrylate using standard procedure A and was obtained in 90% yield as an orange oil.  $^1\text{H}$  NMR ( $\text{CDCl}_3$ ):  $\delta$  8.80 (d,  $J = 6.4$  Hz, 1H), 8.38 (app. t,  $J = 7.6$  Hz, 1H), 7.87 (dd,  $J = 7.6, 6.4$  Hz, 1H), 7.76 (d,  $J = 7.6$  Hz, 1H), 5.46 (m, 1H), 4.09 (q,  $J = 7.2$  Hz, 2H), 3.31 (dd,  $J = 17.2, 3.8$  Hz, 1H), 3.27 (dd,  $J = 17.2, 4.6$  Hz, 1H), 2.60 (dd,  $J =$

13.1, 7.7 Hz, 1H), 2.24 (dd,  $J = 13.1, 9.4$  Hz, 1H), 1.56 (s, 3H), 1.42 (s, 3H), 1.19 (t,  $J = 7.2$  Hz, 3H).  $^{13}\text{C}\{^1\text{H}\}$  NMR ( $\text{CDCl}_3$ ):  $\delta$  169.67, 165.46, 146.34, 140.34, 126.81, 122.50, 65.15, 61.74, 44.46, 42.39, 37.02, 28.48, 27.36, 14.22.  $^{19}\text{F}\{^1\text{H}\}$  NMR ( $\text{CDCl}_3$ ):  $\delta$  -152.15, -152.20. IR (thin film): 1731  $\text{cm}^{-1}$ . HRMS electrospray (m/z):  $[\text{M}]^+$  calcd for  $\text{C}_{14}\text{H}_{20}\text{NO}_2^+$  234.1489; found 234.1488.

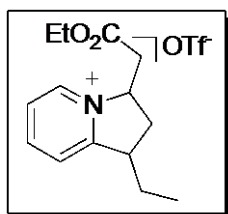


Product 2 was prepared from S2 and ethyl acrylate using standard procedure B and was obtained in 89% yield as a pale yellow oil.  $^1\text{H}$  NMR ( $\text{CDCl}_3$ ):  $\delta$  8.89 (d,  $J = 6.2$  Hz, 1H), 8.29 (app. t,  $J = 7.8$  Hz, 1H), 7.85-7.80 (multiple peaks, 2H), 5.50 (m, 1H), 4.10 (dq,  $J = 10.8, 7.2$  Hz, 1H), 4.07 (dq,  $J = 10.8, 7.2$  Hz, 1H), 3.61 (dd,  $J = 19.2, 7.6$  Hz, 1H), 3.54 (dd,  $J = 19.2, 7.2$  Hz, 1H), 3.26 (dd,  $J = 17.8, 5.8$  Hz, 1H), 3.20 (dd,  $J = 17.8, 4.6$  Hz, 1H), 2.82 (m, 1H), 2.30 (m, 1H), 1.18 (t,  $J = 7.2$  Hz, 3H).  $^{13}\text{C}\{^1\text{H}\}$  NMR ( $\text{CDCl}_3$ ):  $\delta$  169.55, 159.24, 145.53, 140.64, 126.35, 125.03, 120.77 (q,  $^1J_{\text{CF}} = 318$  Hz), 67.56, 61.62, 38.10, 31.53, 26.93, 14.09.  $^{19}\text{F}\{^1\text{H}\}$  NMR ( $\text{CDCl}_3$ ):  $\delta$  -78.43. IR (thin film): 1730  $\text{cm}^{-1}$ . HRMS electrospray (m/z):  $[\text{M}]^+$  calcd for  $\text{C}_{12}\text{H}_{16}\text{NO}_2^+$  206.1176; found 206.1172.

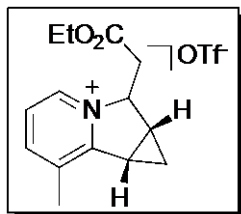


Product 9 was prepared from S3 and ethyl acrylate using standard procedure B and was obtained in 81% yield as an orange oil. This compound was isolated as a 1.2:1 mixture of inseparable diastereomers.  $^1\text{H}$  NMR ( $\text{CDCl}_3$ ) *major diastereomer*:  $\delta$  8.93 (d,  $J = 5.6$  Hz, 1H), 8.35 (dd,  $J = 8.0, 7.6$  Hz, 1H), 7.88-7.80 (multiple peaks, 2H), 5.51 (m, 1H), 4.08 (q,  $J = 7.2$  Hz, 2H), 3.89 (m, 1H), 3.18-3.06 (multiple peaks, 2H), 2.54 (m, 1H), 2.44 (m, 1H), 1.48 (d,  $J = 7.2$  Hz, 3H), 1.19 (t,  $J = 7.2$  Hz, 3H). *minor diastereomer*:  $\delta$  8.83 (d,  $J = 5.6$  Hz, 1H), 8.35 (app. t,  $J = 7.6$  Hz, 1H), 7.85-7.80 (multiple peaks, 2H), 5.39 (m, 1H), 4.08 (q,  $J = 7.2$  Hz, 2H), 3.79 (m, 1H), 3.35-3.22 (multiple peaks, 2H),

2.97 (m, 1H), 1.94 (m, 1H), 1.52 (d,  $J = 6.8$  Hz, 3H), 1.19 (t,  $J = 7.2$  Hz, 3H).  $^{13}\text{C}\{^1\text{H}\}$  NMR ( $\text{CDCl}_3$ ) *major diastereomer*:  $\delta$  169.72, 162.43, 146.26, 140.83, 126.66, 124.06, 120.81 (q,  $^1J_{\text{CF}} = 318$  Hz), 66.54, 61.66, 38.40, 38.24, 35.65, 18.11, 14.14. *minor diastereomer*: 169.49, 162.46, 145.78, 140.02, 126.44, 123.74, 120.81 (q,  $^1J_{\text{CF}} = 318$  Hz), 66.26, 61.66, 38.18, 37.06, 36.15, 17.67, 14.14.  $^{19}\text{F}\{^1\text{H}\}$  NMR ( $\text{CDCl}_3$ ):  $\delta$  -78.35. IR (thin film): 1732  $\text{cm}^{-1}$ . HRMS electrospray (m/z):  $[\text{M}]^+$  calcd for  $\text{C}_{13}\text{H}_{18}\text{NO}_2^+$  220.1332; found 220.1331.

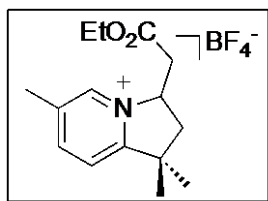
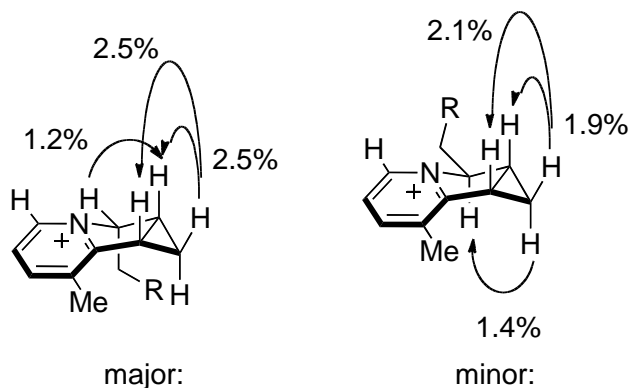


Product 10 was prepared from S4 and ethyl acrylate using standard procedure B and was obtained in 55% yield as an orange oil. This compound was isolated as a 1.2:1 mixture of inseparable diastereomers.  $^1\text{H}$  NMR ( $\text{CDCl}_3$ ) *major diastereomer*:  $\delta$  8.93 (d,  $J = 6.0$  Hz, 1H), 8.41 (app. t,  $J = 8.0$  Hz, 1H), 7.91-7.84 (multiple peaks, 2H), 5.52 (m, 1H), 4.11 (d app. q,  $J = 7.2, 5.6$  Hz, 2H), 3.77 (m, 1H), 3.17-3.15 (multiple peaks, 2H), 2.53-2.49 (multiple peaks, 2H), 2.07 (m, 1H), 1.70 (m, 1H), 1.22 (t,  $J = 7.2$  Hz, 3H), 1.08 (t,  $J = 4.8$  Hz, 3H). *minor diastereomer*:  $\delta$  8.85 (d,  $J = 6.4$  Hz, 1H), 8.39 (app. t,  $J = 7.6$  Hz, 1H), 7.91-7.84 (multiple peaks, 2H), 5.40 (m, 1H), 4.11 (d app. q,  $J = 7.2, 5.6$  Hz, 2H), 3.69 (m, 1H), 3.32-3.30 (multiple peaks, 2H), 2.97 (dt,  $J = 12.8, 8.4$  Hz, 1H), 2.19 (m, 1H), 1.97 (m, 1H), 1.70 (m, 1H), 1.22 (t,  $J = 7.2$  Hz, 3H), 1.05 (t,  $J = 4.9$  Hz, 3H).  $^{13}\text{C}\{^1\text{H}\}$  NMR ( $\text{CDCl}_3$ ) *major diastereomer*:  $\delta$  169.73, 161.58, 145.91, 140.50, 126.77, 124.17, 120.80 (q,  $^1J_{\text{CF}} = 318$  Hz), 66.57, 61.68, 44.67, 38.46, 33.45, 25.64, 14.14, 11.40. *minor diastereomer*: 169.39, 161.48, 145.50, 141.23, 126.50, 123.82, 120.80 (q,  $^1J_{\text{CF}} = 318$  Hz), 66.31, 61.68, 44.85, 37.03, 33.06, 26.35, 14.14, 11.50.  $^{19}\text{F}\{^1\text{H}\}$  NMR ( $\text{CDCl}_3$ ):  $\delta$  -78.40. IR (thin film): 1733  $\text{cm}^{-1}$ . HRMS electrospray (m/z):  $[\text{M}]^+$  calcd for  $\text{C}_{14}\text{H}_{20}\text{NO}_2^+$  234.1486; found 234.1489.



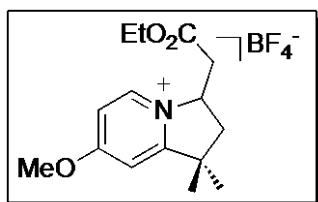
Product 11 was prepared from S5 and ethyl acrylate using standard procedure B and was obtained in 43% yield as a green oil. This compound was isolated as a 2.4:1 mixture of inseparable diastereomers. The stereochemical assignment was determined by nOe as shown in Figure 1.  $^1\text{H}$  NMR ( $\text{CDCl}_3$ ) *major diastereomer*:  $\delta$  8.77 (d,  $J = 6.0$  Hz, 1H), 8.12 (d,  $J = 7.6$  Hz, 1H), 7.70 (app. t,  $J = 7.6$  Hz, 1H), 5.51 (m, 1H), 4.08 (q,  $J = 7.2$  Hz, 2H), 3.24 (dd,  $J = 17.0, 6.0$  Hz, 1H), 3.14 (dd,  $J = 17.0, 4.4$  Hz, 1H), 3.06 (m, 1H), 2.61 (s, 3H), 2.41 (app. q,  $J = 5.2$  Hz, 1H), 1.68 (app. q,  $J = 8.0$  Hz, 1H), 1.19 (t,  $J = 7.2$  Hz, 3H), 0.93 (m, 1H). *minor diastereomer*: 8.64 (d,  $J = 6.0$  Hz, 1H), 8.12 (d,  $J = 7.4$  Hz, 1H), 7.68 (app. t,  $J = 7.4$  Hz, 1H), 5.66 (m, 1H), 4.20 (dd,  $J = 7.0, 2.0$  Hz, 1H), 4.17 (dd,  $J = 7.0, 2.0$  Hz, 1H), 3.46 (m, 1H), 3.06 (m, 1H), 2.94 (dd,  $J = 16.8, 8.8$  Hz, 1H), 2.78 (m, 1H), 2.60 (s, 3H), 1.52 (app. q,  $J = 6.0$  Hz, 1H), 1.29 (t,  $J = 7.2$  Hz, 3H), 0.93 (m, 1H).  $^{13}\text{C}\{^1\text{H}\}$  NMR ( $\text{CDCl}_3$ ) *major diastereomer*:  $\delta$  169.02, 159.30, 145.91, 139.02, 134.80, 125.44, 120.78 (q,  $^1J_{\text{CF}} = 318$  Hz), 69.71, 61.58, 39.98, 23.06, 20.74, 18.21, 17.07, 14.13, *minor diastereomer*:  $\delta$  169.62, 159.30, 145.91, 138.74, 135.45, 125.63, 120.78 (q,  $^1J_{\text{CF}} = 318$  Hz), 68.07, 61.85, 37.44, 22.01, 20.59, 18.11, 14.20 13.56.  $^{19}\text{F}\{^1\text{H}\}$  NMR ( $\text{CDCl}_3$ ):  $\delta$  -78.50. IR (thin film):  $1734\text{ cm}^{-1}$ . HRMS electrospray (m/z):  $[\text{M}]^+$  calcd for  $\text{C}_{14}\text{H}_{18}\text{NO}_2^+$  232.1332; found 232.1332.

Figure 1. Observed nOes for 5:



Product 3 was prepared from S6 and ethyl acrylate using

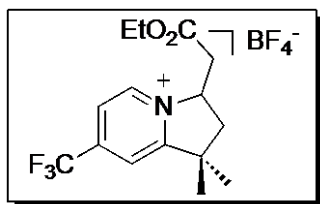
standard procedure A and was obtained in 70% yield as an orange oil.  $^1\text{H}$  NMR ( $\text{CDCl}_3$ ):  $\delta$  8.69 (s, 1H), 8.19 (d,  $J = 8.2$  Hz, 1H), 7.68 (d,  $J = 8.2$  Hz, 1H), 5.47 (m, 1H), 4.13 (q,  $J = 7.2$  Hz, 2H), 3.36 (dd,  $J = 18.1, 6.0$  Hz, 1H), 3.32 (dd,  $J = 18.1, 4.6$  Hz, 1H), 2.62 (dd,  $J = 13.2, 7.6$  Hz, 1H), 2.57 (s, 3H), 2.25 (dd,  $J = 13.2, 9.6$  Hz, 1H), 1.59 (s, 3H), 1.43 (s, 3H), 1.24 (t,  $J = 7.2$  Hz, 3H).  $^{13}\text{C}\{^1\text{H}\}$  NMR ( $\text{CDCl}_3$ ):  $\delta$  169.65, 162.61, 147.18, 139.31, 138.17, 121.87, 64.94, 61.60, 44.01, 42.45, 37.04, 28.47, 27.40, 18.40, 14.19.  $^{19}\text{F}\{^1\text{H}\}$  NMR ( $\text{CDCl}_3$ ):  $\delta$  -151.97, -152.03. IR (thin film):  $1733\text{ cm}^{-1}$ . HRMS electrospray ( $m/z$ ):  $[\text{M}]^+$  calcd for  $\text{C}_{15}\text{H}_{22}\text{NO}_2^+$  248.1645; found 248.1646.



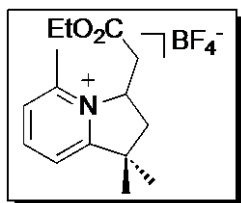
Product 4 was prepared from S7 and ethyl acrylate

using standard procedure A and was obtained in 71% yield as an orange oil.  $^1\text{H}$  NMR ( $\text{CDCl}_3$ ):  $\delta$  8.55 (d,  $J = 7.2$  Hz, 1H), 7.30 (dd,  $J = 7.2, 2.8$  Hz, 1H), 7.11 (d,  $J = 2.8$  Hz, 1H), 5.24 (m, 1H), 4.13 (q,  $J = 7.2$  Hz, 2H), 4.10 (s, 3H), 3.21 (dd,  $J = 17.6, 4.8$  Hz, 1H), 3.15 (dd,  $J = 17.6, 6.0$  Hz, 1H), 2.57 (dd,  $J = 13.2, 7.2$  Hz, 1H), 2.18 (dd,  $J = 13.2, 9.2$  Hz, 1H), 1.55 (s, 3H), 1.41 (s, 3H), 1.23 (t,  $J = 7.2$  Hz, 3H).  $^{13}\text{C}\{^1\text{H}\}$  NMR ( $\text{CDCl}_3$ ):  $\delta$  172.51, 169.82, 167.32, 140.90, 113.06, 107.10, 63.06,

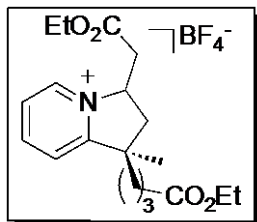
61.72, 58.16, 44.17, 43.07, 37.34, 28.32, 27.24, 14.19.  $^{19}\text{F}\{^1\text{H}\}$  NMR ( $\text{CDCl}_3$ ):  $\delta$  – 152.48, –152.54. IR (thin film):  $1733\text{ cm}^{-1}$ . HRMS electrospray ( $m/z$ ):  $[\text{M}]^+$  calcd for  $\text{C}_{15}\text{H}_{22}\text{NO}_3^+$  264.1594; found 264.1596.



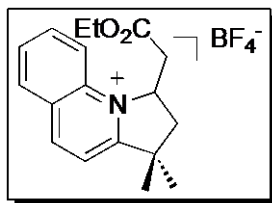
Product 5 was prepared from S8 and ethyl acrylate using standard procedure A and was obtained in 75% yield as an orange oil.  $^1\text{H}$  NMR ( $\text{CDCl}_3$ ):  $\delta$  9.02 (d,  $J = 6.4\text{ Hz}$ , 1H), 8.04 (d,  $J = 6.0\text{ Hz}$ , 1H), 7.92 (s, 1H), 5.49 (m, 1H), 4.05 (q,  $J = 7.2\text{ Hz}$ , 2H), 3.30 (dd,  $J = 17.8, 4.4\text{ Hz}$ , 1H), 3.24 (dd,  $J = 17.8, 6.8\text{ Hz}$ , 1H), 2.62 (dd,  $J = 13.2, 8.0\text{ Hz}$ , 1H), 2.23 (dd,  $J = 13.2, 9.6\text{ Hz}$ , 1H), 1.72 (s, 3H), 1.60 (s, 3H), 1.21 (t,  $J = 7.2\text{ Hz}$ , 3H).  $^{13}\text{C}\{^1\text{H}\}$  NMR ( $\text{CDCl}_3$  with minimal  $\text{CD}_3\text{OD}$  added for solubility):  $\delta$  169.60, 167.69, 146.42 (q,  $^2J_{\text{CF}} = 36.1\text{ Hz}$ ), 142.55 (q,  $^3J_{\text{CF}} = 3.1\text{ Hz}$ ), 123.36, 121.13 (q,  $^1J_{\text{CF}} = 273.2\text{ Hz}$ ), 119.04 (q,  $^3J_{\text{CF}} = 3.4\text{ Hz}$ ), 66.26, 61.80, 44.99, 42.25, 36.53, 28.02, 27.00, 13.94.  $^{19}\text{F}\{^1\text{H}\}$  NMR ( $\text{CDCl}_3$ ):  $\delta$  –65.24, –152.68, –152.74. IR (thin film):  $1733\text{ cm}^{-1}$ . HRMS electrospray ( $m/z$ ):  $[\text{M}]^+$  calcd for  $\text{C}_{15}\text{H}_{19}\text{F}_3\text{NO}_2^+$  302.1362; found 302.1362.



Product 6 was prepared from S9 and ethyl acrylate using standard procedure A and was obtained in 36% yield as an orange oil.  $^1\text{H}$  NMR ( $\text{CDCl}_3$ ):  $\delta$  8.28 (dd,  $J = 8.0, 7.6\text{ Hz}$ , 1H), 7.66-7.61 (multiple peaks, 2H), 5.59 (m, 1H), 4.18 (q,  $J = 7.2\text{ Hz}$ , 2H), 3.08 (dd,  $J = 16.6, 2.4\text{ Hz}$ , 1H), 2.94 (dd,  $J = 16.4, 9.6\text{ Hz}$ , 1H), 2.85 (s, 3H), 2.77 (dd,  $J = 14.0, 9.6\text{ Hz}$ , 1H), 2.19 (dd,  $J = 14.0, 2.4\text{ Hz}$ , 1H), 1.56 (s, 3H), 1.52 (s, 3H), 1.27 (t,  $J = 7.2\text{ Hz}$ , 3H).  $^{13}\text{C}\{^1\text{H}\}$  NMR ( $\text{CDCl}_3$ ):  $\delta$  168.98, 165.89, 152.74, 146.25, 128.52, 120.70, 64.47, 61.87, 44.80, 41.32, 39.28, 30.28, 29.49, 19.97, 14.23.  $^{19}\text{F}\{^1\text{H}\}$  NMR ( $\text{CDCl}_3$ ):  $\delta$  –153.22, –153.27. IR (thin film):  $1733\text{ cm}^{-1}$ . HRMS electrospray ( $m/z$ ):  $[\text{M}]^+$  calcd for  $\text{C}_{15}\text{H}_{22}\text{NO}_2^+$  248.1645; found 248.1645.

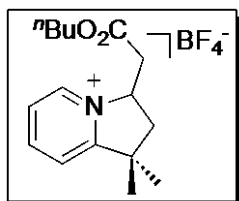


Product 7 was prepared from S10 and ethyl acrylate using standard procedure A and was obtained in 49% yield as a 1:1 mixture of diastereomers as an orange oil. However, the assignment of specific NMR peaks to each diastereomer was not possible due to the number of overlapping resonances.  $^1\text{H}$  NMR ( $\text{CDCl}_3$ , 500 MHz):  $\delta$  8.83 (d,  $J = 4.8$  Hz, 1H), 8.80 (d,  $J = 4.8$  Hz, 1H), 8.40 (app t,  $J = 6.4$  Hz, 2H), 7.89 (m, 2H), 7.80 (d,  $J = 6.4$  Hz, 1H), 7.77 (d,  $J = 6.8$  Hz, 1H), 5.46-5.41 (multiple peaks, 2H), 4.11-4.04 (multiple peaks, 8H), 3.29-3.27 (multiple peaks, 4H), 2.75 (dd,  $J = 10.8, 6.4$  Hz, 1H), 2.49 (dd,  $J = 10.8, 6.4$  Hz, 1H), 2.33 (m, 2H), 2.26 (t,  $J = 5.6$  Hz, 2H), 2.15 (dd,  $J = 11.0, 7.4$  Hz, 1H), 1.95-1.82 (multiple peaks, 2H), 1.76-1.38 (multiple peaks, 13H), 1.23-1.18 (multiple peaks, 12H).  $^{13}\text{C}\{^1\text{H}\}$  NMR ( $\text{CDCl}_3$ , 125 MHz):  $\delta$  173.15, 173.06, 169.56 (2C), 169.38, 164.57, 146.46, 146.32, 140.36 (2C), 127.04, 126.91, 123.27, 122.98, 65.40, 65.04, 61.66, 60.67, 47.91, 47.86, 39.99, 39.94, 39.37, 38.37, 37.46, 36.73, 33.82, 33.68, 26.09, 25.24, 23.03, 19.91, 19.75, 14.38, 14.36, 14.17, 14.16.  $^{19}\text{F}\{^1\text{H}\}$  NMR ( $\text{CDCl}_3$ ):  $\delta$  -151.92, -151.97. IR (thin film):  $1727\text{ cm}^{-1}$ . HRMS electrospray ( $m/z$ ):  $[\text{M}]^+$  calcd for  $\text{C}_{19}\text{H}_{28}\text{NO}_4^+$  334.2013; found 334.2008.

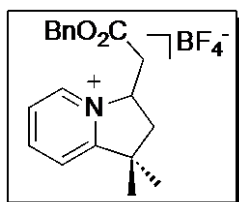


Product 8 was prepared from S11 and ethyl acrylate using standard procedure A and was obtained in 39% yield as a yellow oil.  $^1\text{H}$  NMR ( $\text{CDCl}_3$ ):  $\delta$  8.99 (d,  $J = 8.4$  Hz, 1H), 8.26 (d,  $J = 8.0$  Hz, 1H), 8.22-8.14 (multiple peaks, 2H), 7.92-7.88 (multiple peaks, 2H), 6.13 (m, 1H), 4.17-4.07 (multiple peaks, 2H), 3.28 (dd,  $J = 16.8, 2.4$  Hz, 1H), 3.07 (dd,  $J = 16.4, 9.6$  Hz, 1H), 2.96 (dd,  $J = 13.6, 9.6$  Hz, 1H), 2.37 (dd,  $J = 13.6, 2.0$  Hz, 1H), 1.69 (s, 3H), 1.65 (s, 3H), 1.27 (t,  $J = 6.8$  Hz, 3H).  $^{13}\text{C}\{^1\text{H}\}$  NMR ( $\text{CDCl}_3$ ):  $\delta$  169.24 (2C), 148.92,

136.05, 135.88, 131.12, 129.94, 129.46, 118.76, 117.96, 63.93, 61.99, 46.62, 41.34, 39.47, 29.57 (2C), 14.26.  $^{19}\text{F}\{^1\text{H}\}$  NMR ( $\text{CDCl}_3$ ):  $\delta$  -153.22, -153.27. IR (thin film):  $1733\text{ cm}^{-1}$ . HRMS electrospray ( $m/z$ ):  $[\text{M}]^+$  calcd for  $\text{C}_{18}\text{H}_{22}\text{NO}_2^+$  284.1645; found 284.1645.



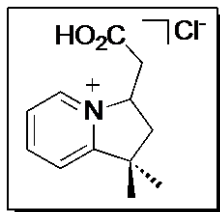
Product 12 was prepared from S1 and *n*-butyl acrylate using standard procedure A and was obtained in 80% yield as an orange oil.  $^1\text{H}$  NMR ( $\text{CDCl}_3$ ):  $\delta$  8.84 (d,  $J = 6.2$  Hz, 1H), 8.43 (dd,  $J = 8.0, 7.6$  Hz, 1H), 7.91 (dd,  $J = 7.2, 6.2$  Hz, 1H), 7.81 (d, 8.0 Hz, 1H), 5.50 (m, 1H), 4.07 (app. t,  $J = 10.8$  Hz, 2H), 3.33 (app. d,  $J = 4.8$  Hz, 2H), 2.64 (dd,  $J = 13.2, 7.6$  Hz, 1H), 2.27 (dd,  $J = 13.2, 9.4$  Hz, 1H), 1.61-1.55 (multiple peaks, 5H), 1.46 (s, 3H), 1.38-1.31 (multiple peaks, 2H), 0.92 (t,  $J = 6.8$  Hz, 3H).  $^{13}\text{C}\{^1\text{H}\}$  NMR ( $\text{CDCl}_3$ ):  $\delta$  169.74, 165.45, 146.36, 140.27, 126.78, 122.54, 65.60, 65.14, 44.46, 42.37, 36.96, 30.58, 28.45, 27.34, 19.20, 13.83.  $^{19}\text{F}\{^1\text{H}\}$  NMR ( $\text{CDCl}_3$ ):  $\delta$  -152.51, -152.57. IR (thin film):  $1731\text{ cm}^{-1}$ . HRMS electrospray ( $m/z$ ):  $[\text{M}]^+$  calcd for  $\text{C}_{16}\text{H}_{24}\text{NO}_2^+$  262.1802; found 262.1802.



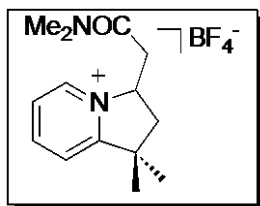
Product 13 was prepared from S1 and benzyl acrylate using standard procedure A and was obtained in 75% yield as a yellow oil.  $^1\text{H}$  NMR ( $\text{CDCl}_3$ ):  $\delta$  8.77 (d,  $J = 6.4$  Hz, 1H), 8.28 (dd,  $J = 8.0, 7.6$  Hz, 1H), 7.79 (app. t,  $J = 6.4$  Hz, 1H), 7.65 (d, 8.0 Hz, 1H), 7.31-7.22 (multiple peaks, 5H), 5.46 (m, 1H), 5.05 (s, 2H), 3.35 (dd,  $J = 15.8, 3.4$  Hz, 1H), 3.32 (dd,  $J = 15.8, 2.6$  Hz, 1H), 2.54 (dd,  $J = 13.2, 7.6$  Hz, 1H), 2.19 (dd,  $J = 13.2, 9.6$  Hz, 1H), 1.49 (s, 3H), 1.38 (s, 3H).  $^{13}\text{C}\{^1\text{H}\}$  NMR ( $\text{CDCl}_3$ ):  $\delta$  169.42, 165.34, 146.26, 140.35, 135.19, 128.89, 128.83, 128.81, 126.74, 122.37, 67.48, 65.12, 44.39, 42.29, 36.96, 28.42, 27.24.



$^{19}\text{F}\{^1\text{H}\}$  NMR ( $\text{CDCl}_3$ ):  $\delta$  -152.00, -152.05. IR (thin film):  $1735\text{ cm}^{-1}$ . HRMS electrospray ( $m/z$ ):  $[\text{M}]^+$  calcd for  $\text{C}_{19}\text{H}_{22}\text{NO}_2^+$  296.1645; found 296.1646.

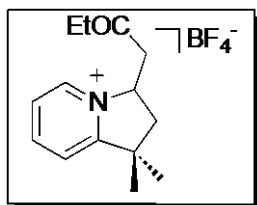


Product 16 was prepared from S1 and acrylic acid (Aldrich) using standard procedure A. After removal of the acetic acid and methanol, NMR analysis of crude mixture shows 69% yield; however, the carboxylic acid product was inseparable from acrylic acid oligomers. A pure sample of P3 for characterization was obtained as the chloride salt through hydrolysis of 1.<sup>28</sup>  $^1\text{H}$  NMR ( $\text{CD}_3\text{OD}$ ) for P3:  $\delta$  8.84 (d,  $J = 6.0$  Hz, 1H), 8.44 (app. t,  $J = 7.6$  Hz, 1H), 7.99 (d,  $J = 8.0$  Hz, 1H), 7.87 (app. t,  $J = 6.4$  Hz, 1H), 5.37 (m, 1H), 3.27 (dd,  $J = 18.6, 4.8$  Hz, 1H), 3.14 (dd,  $J = 17.6, 6.8$  Hz, 1H), 2.60 (dd,  $J = 14.2, 5.6$  Hz, 1H), 2.19 (dd,  $J = 13.2, 8.8$  Hz, 1H), 1.53 (s, 3H), 1.39 (s, 3H).  $^{13}\text{C}\{^1\text{H}\}$  NMR ( $\text{CD}_3\text{OD}$ ):  $\delta$  171.09, 165.76, 146.29, 139.69, 126.16, 122.82, 65.28, 43.99, 42.14, 36.98, 27.01, 26.22. IR (thin film):  $2971, 1732\text{ cm}^{-1}$ . HRMS electrospray ( $m/z$ ):  $[\text{M}]^+$  calcd for  $\text{C}_{12}\text{H}_{16}\text{NO}_2^+$  206.1176; found 206.1172.

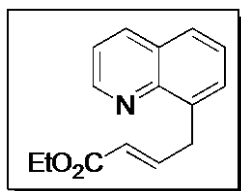


Product 15 was prepared from S1 and N,N-dimethyl acrylamide (Aldrich) using standard procedure A. After removal of the acetic acid and methanol, NMR analysis of crude mixture shows 55% yield. Water was added and the solution was washed with (5 x 2 mL) of  $\text{CH}_2\text{Cl}_2$  to remove the acrylamide oligomers, polyoxometalate and catalyst. The water was removed under reduced pressure and 1 mL of saturated  $\text{NaBF}_4$  solution was added. The product was extracted with (5 x 1 mL)  $\text{CH}_2\text{Cl}_2$  as a  $\text{BF}_4^-$  salt. The  $\text{CH}_2\text{Cl}_2$  layers were combined, dried with  $\text{MgSO}_4$ , filtered and evaporated to afford the product in 40% yield as a yellow oil.  $^1\text{H}$  NMR ( $\text{CDCl}_3$ ):  $\delta$  8.80 (d,  $J = 6.0$  Hz, 1H), 8.38 (app. t,  $J = 7.6$  Hz, 1H), 7.82-7.78 (multiple peaks, 2H), 5.47 (m, 1H), 3.42 (dd,  $J$

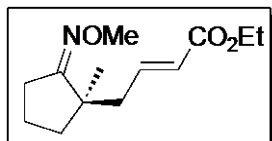
= 17.6, 5.2 Hz, 1H), 3.23 (dd,  $J = 17.6, 5.2$  Hz, 1H), 3.04 (s, 3H), 2.91 (s, 3H), 2.57 (dd,  $J = 13.0, 7.6$  Hz, 1H), 2.36 (dd,  $J = 13.0, 10.0$  Hz, 1H), 1.59 (s, 3H), 1.41 (s, 3H).  $^{13}\text{C}\{^1\text{H}\}$  NMR ( $\text{CDCl}_3$ ):  $\delta$  168.66, 165.51, 146.12, 140.22, 126.55, 122.47, 65.78, 44.23, 42.80, 37.28, 36.68, 35.65, 28.33, 27.03.  $^{19}\text{F}\{^1\text{H}\}$  NMR ( $\text{CDCl}_3$ ):  $\delta$  -152.07, -152.13. IR (thin film): 1652  $\text{cm}^{-1}$ . HRMS electrospray ( $m/z$ ):  $[\text{M}]^+$  calcd for  $\text{C}_{14}\text{H}_{21}\text{N}_2\text{O}^+$  233.1648; found 233.1648.



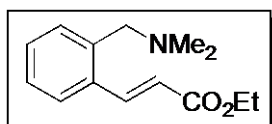
Product 14 was prepared from S1 and ethyl vinyl ketone (Aldrich, freshly distilled prior to use) using standard procedure A and was obtained in 40% yield as a yellow solid. Mp = 102-105  $^{\circ}\text{C}$ .  $^1\text{H}$  NMR ( $\text{CDCl}_3$ ):  $\delta$  8.74 (d,  $J = 6.4$  Hz, 1H), 8.41 (app. t,  $J = 7.2$  Hz, 1H), 7.85 (app t.,  $J = 7.6$  Hz, 1H), 7.82 (d,  $J = 8.0$  Hz, 1H), 5.39 (m, 1H), 3.60 (dd,  $J = 19.2, 4.8$  Hz, 1H), 3.38 (dd,  $J = 18.8, 6.4$  Hz, 1H), 2.64 (dd,  $J = 13.2, 7.6$  Hz, 1H), 2.56 (m, 2H), 2.19 (dd,  $J = 13.2, 9.6$  Hz, 1H), 1.59 (s, 3H), 1.43 (s, 3H), 1.02 (t,  $J = 7.2$  Hz, 3H).  $^{13}\text{C}\{^1\text{H}\}$  NMR ( $\text{CDCl}_3$ ):  $\delta$  208.34, 165.39, 146.30, 140.09, 126.82, 122.59, 64.90, 44.89, 44.46, 42.80, 36.21, 28.30, 27.34, 7.55.  $^{19}\text{F}\{^1\text{H}\}$  NMR ( $\text{CDCl}_3$ ):  $\delta$  -152.12, -152.17. IR (thin film): 1714  $\text{cm}^{-1}$ . HRMS electrospray ( $m/z$ ):  $[\text{M}]^+$  calcd for  $\text{C}_{14}\text{H}_{20}\text{NO}^+$  218.1539; found 218.1537.



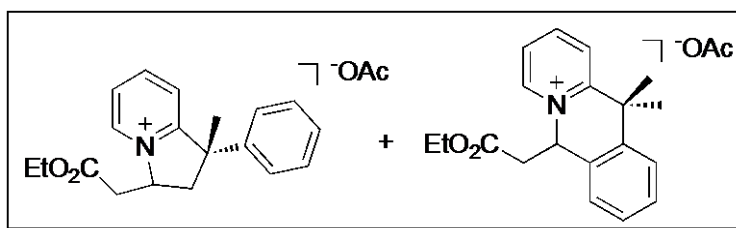
Product 18 was prepared from 8-methylquinoline and ethyl acrylate using standard procedure A and was obtained in 20% isolated yield as the uncyclized product.  $^1\text{H}$  NMR ( $\text{CDCl}_3$ ):  $\delta$  8.95 (dd,  $J = 4.4, 1.6$  Hz, 1H), 8.16 (m, 1H), 7.75 (m, 1H), 7.57-7.47 (multiple peaks, 2H), 7.43 (dd,  $J = 8.4, 4.4$  Hz, 1H), 7.34 (dt,  $J = 16.0, 7.2$  Hz, 1H), 5.84 (dt,  $J = 15.6, 1.6$  Hz, 1H), 4.22 (d, 6.8 Hz, 2H), 4.16 (q,  $J = 7.2$  Hz, 2H), 1.34 (m, 1H), 1.26 (t,  $J = 7.2$  Hz, 3H).



Product 20 was prepared from 2,2-dimethyl cyclopentanone oxime ether and ethyl acrylate using standard procedure A and was obtained in 15% isolated yield as the uncyclized product.  $^1\text{H NMR}$  ( $\text{CDCl}_3$ ):  $\delta$  6.96 (quin,  $J = 7.6$  Hz, 1H), 5.86 (dt,  $J = 15.6, 1.6$  Hz, 1H), 4.20 (q,  $J = 6.8$  Hz, 2H), 3.85 (s, 3H), 2.52 (m, 1H), 2.43-2.38 (multiple peaks, 2H), 1.76-1.69 (multiple peaks, 2H), 1.57 (m, 1H), 1.30 (t,  $J = 6.8$  Hz, 3H), 1.14 (s, 3H).

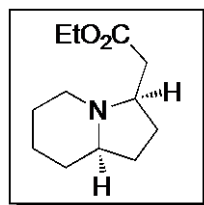


Product 26 was prepared from *N,N*-dimethylbenzylamine and ethyl acrylate using standard procedure A and was obtained in 30% isolated yield as the uncyclized product.  $^1\text{H NMR}$  ( $\text{CDCl}_3$ ):  $\delta$  8.20 (d,  $J = 16.0$  Hz, 1H), 7.34-7.29 (multiple peaks, 4H), 6.38 (d,  $J = 16.0$  Hz, 1H), 4.28 (q, 7.2 Hz, 2H), 3.50 (s, 2H), 2.26 (s, 6H), 1.35 (t,  $J = 7.2$  Hz, 3H).



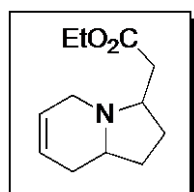
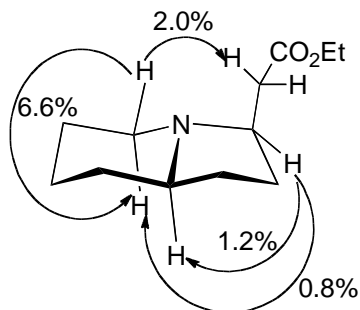
Products 28 and 29 were prepared from 2-(2-phenylpropan-2-yl)pyridine and ethyl acrylate using standard procedure A and was obtained in 80% isolated yield as mixtures of the cyclized products. Product **29**  $^1\text{H NMR}$  ( $\text{CDCl}_3$ ):  $\delta$  8.56 (dd,  $J = 2.8, 1.6$  Hz, 1H), 7.66 (d,  $J = 8.0$  Hz, 1H), 7.53 (td,  $J = 7.6, 1.6$  Hz, 1H), 7.45-7.7.39 (multiple peaks, 2H), 7.27 (t,  $J = 7.6$  Hz, 1H), 7.22 (s, 1H), 7.08-7.06 (multiple peaks, 2H), 5.91 (d,  $J = 15.6$  Hz, 1H), 4.10 (q,  $J = 6.8$  Hz, 2H), 1.74 (s, 6H), 1.24 (t,  $J = 6.8$  Hz, 3H). Product **28**  $^1\text{H NMR}$  ( $\text{CDCl}_3$ ):  $\delta$  8.56 (dd,  $J = 2.8, 1.6$  Hz, 1H), 7.66 (d,  $J = 8.0$  Hz, 1H), 7.53 (td,  $J = 7.6, 1.6$  Hz, 1H), 7.45-7.7.39 (multiple peaks, 2H), 7.27 (t,  $J = 7.6$  Hz, 1H), 7.22 (s, 1H), 7.10 (m, 1H), 7.00 (d, 8.0 Hz), 6.70 (quin,  $J = 7.6$  Hz, 1H), 5.80 (d,  $J = 15.6$  Hz, 1H), 3.28 (dd,  $J = 14.4, 8.0$  Hz, 1H), 3.04 (dd,  $J = 14.4, 8.0$  Hz, 1H), 4.10 (q,  $J = 6.8$  Hz, 2H), 1.68 (s, 3H), 1.24 (t,  $J = 6.8$  Hz, 3H).

## V. Reductions of Pyridinium Salts

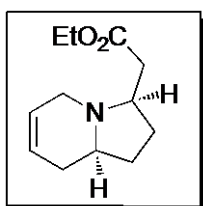


To a 25 mL flask were added **2** (147 mg, 0.50 mmol), PtO<sub>2</sub> (11 mg, 0.048 mmol, 10 mol%, Aldrich), and ethanol (5 mL). Hydrogen was bubbled through the resulting suspension for 5 min, and then the mixture was stirred at room temperature for 14 h under a balloon of hydrogen. The resulting suspension was filtered through a plug of glass wool, and the solvent was removed under vacuum. The crude product was dissolved in CH<sub>2</sub>Cl<sub>2</sub> (30 mL) and washed with 1 M aqueous NaOH (1 x 20 mL). The aqueous layer was extracted with CH<sub>2</sub>Cl<sub>2</sub> (2 x 30 mL), and the CH<sub>2</sub>Cl<sub>2</sub> extracts were combined, dried over Na<sub>2</sub>SO<sub>4</sub>, and concentrated under vacuum. <sup>1</sup>H NMR spectroscopic analysis of the crude product showed a 28:1 ratio of two diastereomeric products. The crude product was purified by chromatography on basic alumina by gradient elution starting with 95:5 and ending with 90:10 hexanes/ethyl acetate to provide diastereomerically pure **30** as a colorless oil (79 mg, 75% yield, R<sub>f</sub> = 0.31 in 90:10 hexanes/ethyl acetate on an alumina TLC plate). The stereochemistry of **12** was determined by nOe analysis (Figure 2). <sup>1</sup>H NMR (CDCl<sub>3</sub>): δ 4.13 (q, *J* = 7.2 Hz, 2H), 3.05 (m, 1H), 2.68 (dd, *J* = 14.8, 4.0 Hz, 1H), 2.53 (dtd, *J* = 9.2, 7.8, 4.0 Hz, 1H), 2.26 (dd, *J* = 14.8, 9.2 Hz, 1H), 1.99-1.86 (multiple peaks, 2H), 1.86 (ddd, *J* = 12.4, 10.8, 3.2 Hz, 1H), 1.80-1.71 (multiple peaks, 3H), 1.65 (m, 1H), 1.53-1.41 (multiple peaks, 2H), 1.35 (qd, *J* = 11.2, 6.8 Hz, 1H), 1.25 (t, *J* = 7.2 Hz, 3H), 1.23-1.15 (multiple peaks, 2H). <sup>13</sup>C{<sup>1</sup>H} NMR (CDCl<sub>3</sub>): δ 172.66, 65.31, 61.51, 60.40, 51.46, 39.18, 31.39, 29.24, 28.81, 25.62, 24.46, 14.42. IR (thin film): 1736 cm<sup>-1</sup>. HRMS electrospray (*m/z*): [M+H]<sup>+</sup> calcd for C<sub>12</sub>H<sub>22</sub>NO<sub>2</sub><sup>+</sup> 212.1645; found 212.1647.

Figure 2. Observed nOes for **30**:



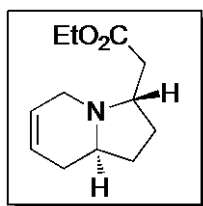
To a 25 mL flask were added **2** (147 mg, 0.50 mmol) and ethanol (5 mL). The solution was cooled to 0°C in an ice bath and NaBH<sub>4</sub> (49 mg, 1.3 mmol, 2.6 equiv, Aldrich) was added slowly over 5 min. The reaction mixture was stirred at 0 °C for 6 h, warmed to room temperature, and stirred for an additional 4 h. Water (1 mL) was added, and the reaction was concentrated to ~2 mL. The resulting white slurry was partitioned between CH<sub>2</sub>Cl<sub>2</sub> (15 mL) and water (15 mL), and the pH of the aqueous layer was adjusted to ~10 by addition of K<sub>2</sub>CO<sub>3</sub>. The layers were separated, and the aqueous layer was extracted with CH<sub>2</sub>Cl<sub>2</sub> (2 x 15 mL). The CH<sub>2</sub>Cl<sub>2</sub> extracts were combined, dried with Na<sub>2</sub>SO<sub>4</sub>, and concentrated under vacuum to give a colorless oil. <sup>1</sup>H NMR analysis of the crude product showed a 2.3:1 ratio of two diastereomeric products. The crude products were purified by chromatography on basic alumina by gradient elution starting with 98:2 and ending with 90:10 hexanes/ethyl acetate to provide the products **31A** and **31B**.



Product **31A** was isolated as a colorless oil (60 mg, 57% yield, *R<sub>f</sub>* = 0.33 in 95:5 CH<sub>2</sub>Cl<sub>2</sub>/MeOH on a silica gel TLC plate). <sup>1</sup>H NMR (CDCl<sub>3</sub>): δ 5.75 (m, 1H), 5.71 (m, 1H), 4.14 (q, *J* = 7.2 Hz, 2H), 3.44 (ddd, *J* = 16.0, 4.0, 2.4 Hz, 1H), 2.73 (m, 1H), 2.72 (dd, *J* = 14.4, 4.8 Hz, 1H), 2.67

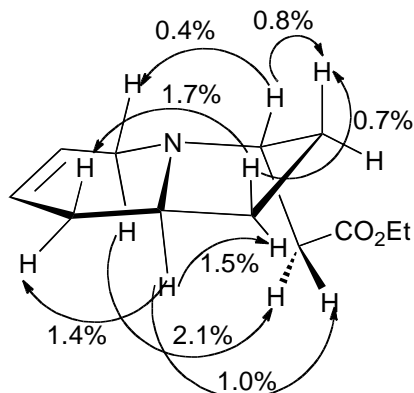
(dddd,  $J = 12.4, 8.8, 8.0, 4.4$  Hz, 1H), 2.32 (dd,  $J = 14.4, 8.8$  Hz, 1H), 2.36-2.21 (multiple peaks, 2H), 2.08-1.90 (multiple peaks, 3H), 1.53 (dddd,  $J = 12.4, 10.8, 6.4, 4.8$  Hz, 1H), 1.42 (dddd,  $J = 12.4, 10.8, 8.4, 6.4$  Hz, 1H), 1.26 (t,  $J = 7.2$  Hz, 3H).  $^{13}\text{C}\{^1\text{H}\}$  NMR ( $\text{CDCl}_3$ ):  $\delta$  172.54, 125.57, 125.29, 62.32, 60.53, 60.50, 51.50, 39.55, 33.07, 29.64, 29.05, 14.45. IR (thin film): 3033, 1734, 1656  $\text{cm}^{-1}$ . HRMS electrospray ( $m/z$ ):  $[\text{M}+\text{H}]^+$  calcd for  $\text{C}_{12}\text{H}_{20}\text{NO}_2^+$  210.1489; found 210.1487.

The stereochemistry of 31A was confirmed by hydrogenation to form 12 in the following manner: To a 25 mL flask were added 31A (21 mg, 0.10 mmol),  $\text{PtO}_2$  (2 mg, 0.009 mmol, 9 mol%), and ethanol (1 mL). Hydrogen was bubbled through the resulting suspension, and then the mixture was stirred at room temperature for 14 h under a balloon of hydrogen. The suspension was filtered through a plug of glass wool, and the solvent was removed under vacuum. The  $^1\text{H}$  NMR spectrum of the crude product matched that of 30.



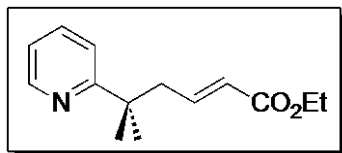
Product 31B was isolated as a colorless oil (25 mg, 24% yield,  $R_f = 0.32$  in 90:10  $\text{CH}_2\text{Cl}_2/\text{MeOH}$  on a silica gel TLC plate). The stereochemistry of 31B was determined by nOe analysis (Figure 3).  $^1\text{H}$  NMR ( $\text{C}_6\text{D}_6$ ):  $\delta$  5.65 (dddd,  $J = 10.0, 4.0, 2.8, 2.4, 2.0$  Hz, 1H), 5.55 (ddq,  $J = 10.0, 4.0, 2.0$  Hz, 1H), 3.97 (q,  $J = 7.2$  Hz, 2H), 3.70 (dddd,  $J = 9.2, 8.0, 4.8, 3.2$  Hz, 1H), 3.16 (dddt,  $J = 16.8, 4.0, 3.6, 2.0$  Hz, 1H), 3.08 (ddq,  $J = 16.8, 4.0, 2.0$  Hz, 1H), 2.68 (ddt,  $J = 8.8, 6.8, 5.6$  Hz, 1H), 2.46 (dd,  $J = 14.4, 4.8$  Hz, 1H), 2.04 (dd,  $J = 14.4, 9.2$  Hz, 1H), 2.03 (dddd,  $J = 12.8, 10.4, 8.0, 6.8$  Hz, 1H), 1.87-1.82 (multiple peaks, 2H), 1.78 (ddt,  $J = 12.4, 10.0, 6.8$  Hz, 1H), 1.56 (dddd,  $J = 12.8, 10.0, 4.4, 3.2$  Hz, 1H), 1.24 (dddd,  $J = 12.4, 10.4, 5.6, 4.4$  Hz, 1H), 0.97 (t,  $J = 7.2$  Hz, 3H).  $^{13}\text{C}\{^1\text{H}\}$  NMR ( $\text{CDCl}_3$ ):  $\delta$  173.05, 125.44, 125.21, 60.59, 57.75, 54.84, 46.19, 35.53, 31.75, 29.84, 28.56, 14.45. IR (thin film): 3030, 1733, 1659  $\text{cm}^{-1}$ . HRMS electrospray ( $m/z$ ):  $[\text{M}+\text{H}]^+$  calcd for  $\text{C}_{12}\text{H}_{20}\text{NO}_2^+$  210.1489; found 210.1488.

Figure 3. Observed nOes for 31B:



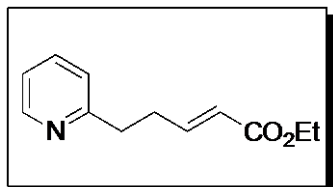
## VI. Formation of the Linear Heck Products

To a 25 mL flask charged with the appropriate pyridinium salt (0.50 mmol, 1.0 equiv) under nitrogen was added 10 mL of dry  $\text{CH}_2\text{Cl}_2$  followed by 1,8-diazabicyclo[5.4.0]undec-7-ene (150  $\mu\text{L}$ , 1.0 mmol, 2.0 equiv, Aldrich). The reaction was stirred for 1h at room temperature, after which the solution was diluted with  $\text{CH}_2\text{Cl}_2$  (30 mL). The  $\text{CH}_2\text{Cl}_2$  solution was washed with saturated aqueous  $\text{NaHCO}_3$  (2 x 20 mL), and the combined aqueous layers were extracted once with  $\text{CH}_2\text{Cl}_2$  (20 mL). The  $\text{CH}_2\text{Cl}_2$  layers were combined, washed with 20 mL of brine, dried over  $\text{Na}_2\text{SO}_4$ , concentrated under vacuum, and chromatographed as indicated below.



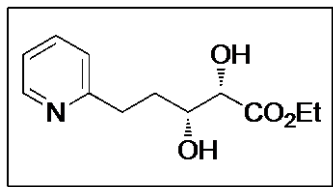
Product 32 was made from pyridinium salt 1 and was purified by chromatography on basic alumina, which had been flushed with 99:1 hexanes/triethylamine, eluting with 69:30:1 hexanes/ethyl acetate/triethylamine to provide the product 14 as a colorless oil (96 mg, 82% yield,  $R_f = 0.39$  in 78:20:2 hexanes/ethyl acetate/triethylamine on an alumina TLC plate to which 98:2 hexanes/triethylamine had been applied and allowed to evaporate prior to spotting with the sample).  $^1\text{H}$  NMR ( $\text{CDCl}_3$ ):  $\delta$  8.57 (ddd,  $J = 4.8, 2.0, 0.8$  Hz, 1H), 7.61 (ddd,  $J = 8.0, 7.6, 2.0$  Hz, 1H), 7.27 (d,  $J = 8.0$  Hz, 1H), 7.10 (ddd,  $J = 7.6, 4.8, 0.8$  Hz, 1H), 6.74 (dt,  $J = 15.6, 7.6$  Hz, 1H), 5.77 (dt,  $J = 15.6, 1.2$  Hz, 1H), 4.13 (q,  $J = 7.2$  Hz, 2H), 2.65 (dd,  $J = 7.6$  Hz, 1.2 Hz, 2H), 1.36 (s, 6H), 1.24

(t,  $J = 7.2$  Hz, 3H).  $^{13}\text{C}\{^1\text{H}\}$  NMR ( $\text{CDCl}_3$ ):  $\delta$  167.06, 166.66, 149.07, 146.52, 136.50, 123.69, 121.23, 119.88, 60.31, 45.72, 40.93, 27.96, 14.45. IR (thin film): 3052, 1718, 1652  $\text{cm}^{-1}$ . HRMS electrospray ( $m/z$ ):  $[\text{M}+\text{H}]^+$  calcd for  $\text{C}_{14}\text{H}_{20}\text{NO}_2^+$  234.1489; found 234.1486.



Product 33 was made from pyridinium salt 2 and was purified by chromatography on basic alumina eluting with 70:30 hexanes/ethyl acetate to provide the product 15 as a colorless oil (98 mg, 95% yield,  $R_f = 0.28$  in 80:20 hexanes/ethyl acetate on an alumina TLC plate).  $^1\text{H}$  NMR ( $\text{CDCl}_3$ ):  $\delta$  8.53 (ddd,  $J = 4.8, 1.6, 1.2$  Hz, 1H), 7.59 (ddd,  $J = 8.0, 7.6, 2.0$  Hz, 1H), 7.13 (d,  $J = 8.0$  Hz, 1H), 7.12 (ddd,  $J = 7.6, 4.8, 1.2$  Hz, 1H), 7.00 (dt,  $J = 15.6, 6.8$  Hz, 1H), 5.84 (dt,  $J = 15.6, 1.6$  Hz, 1H), 4.16 (q,  $J = 7.2$  Hz, 2H), 2.94 (dd,  $J = 8.0, 7.2$  Hz, 2H), 2.66 (dddd, 8.0, 7.2, 6.8, 1.6 Hz, 2H), 1.27 (t,  $J = 7.2$  Hz, 3H).  $^{13}\text{C}\{^1\text{H}\}$  NMR ( $\text{CDCl}_3$ ):  $\delta$  166.78, 160.53, 149.64, 148.09, 136.62, 123.06, 122.12, 121.56, 60.40, 36.74, 32.12, 14.45. IR (thin film): 3064, 1718, 1654  $\text{cm}^{-1}$ . HRMS electrospray ( $m/z$ ):  $[\text{M}+\text{H}]^+$  calcd for  $\text{C}_{12}\text{H}_{16}\text{NO}_2^+$  206.1176; found 206.1174.

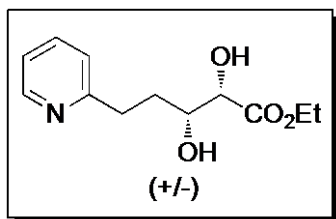
#### VII. Derivatizations of the Linear Heck Product



To a 20 mL vial was added AD-mix  $\beta$  (700 mg, Aldrich), methanesulfonamide (95 mg, 1.00 mmol, 2.0 equiv, Aldrich),  $t$ -BuOH (1 mL), and water (1 mL). The mixture was stirred and cooled to 0  $^\circ\text{C}$  in an ice bath. 33 (103 mg, 0.50 mmol) was added, and the mixture was stirred at 0  $^\circ\text{C}$  for 24 h. A 10% aqueous solution of  $\text{Na}_2\text{SO}_3$  (5 mL) was added with stirring followed by the addition of another 5 mL of water. The mixture was extracted with  $\text{CH}_2\text{Cl}_2$  (8 x 10 mL), and the  $\text{CH}_2\text{Cl}_2$  extracts were combined and concentrated under vacuum. The crude product was purified by chromatography on silica gel, eluting



with 95:5 CH<sub>2</sub>Cl<sub>2</sub>/MeOH to provide the product 34 as a colorless oil (110 mg, 92% yield, 97% ee as determined by Mosher ester analysis, R<sub>f</sub> = 0.19 in 95:5 CH<sub>2</sub>Cl<sub>2</sub>/MeOH). The absolute stereochemistry of the diol was assumed based on the mnemonic rule for the facial selectivity of the Sharpless dihydroxylation reaction.<sup>29</sup> <sup>1</sup>H NMR (CDCl<sub>3</sub>): δ 8.46 (d, *J* = 5.4 Hz, 1H), 7.63 (td, *J* = 7.6, 2.0 Hz, 1H), 7.20 (d, *J* = 7.6 Hz, 1H), 7.14 (dd, *J* = 7.6, 5.4 Hz, 1H), 5.98 (br s, 1H), 4.30 (dq, *J* = 10.4, 7.2 Hz, 1H), 4.28 (dq, *J* = 10.4, 7.2 Hz, 1H), 4.11-4.04 (multiple peaks, 2H), 3.29 (br d, *J* = 5.6 Hz, 1H), 3.10 (ddd, *J* = 15.2, 7.6, 4.8 Hz, 1H), 3.06 (ddd, *J* = 15.2, 7.2, 5.2 Hz, 1H), 2.15 (m, 1H), 2.06 (m, 1H), 1.32 (t, *J* = 7.2 Hz, 3H). <sup>13</sup>C{<sup>1</sup>H} NMR (CDCl<sub>3</sub>): δ 173.61, 161.24, 148.54, 137.24, 123.53, 121.52, 74.19, 72.80, 61.84, 34.76, 32.46, 14.36. IR (thin film): 3368, 1734 cm<sup>-1</sup>. HRMS electrospray (*m/z*): [M+H]<sup>+</sup> calcd for C<sub>12</sub>H<sub>18</sub>NO<sub>4</sub><sup>+</sup> 240.1230; found 240.1228. [α]<sub>D</sub><sup>25</sup> = -11.8 (*c* = 2.00, CHCl<sub>3</sub>).



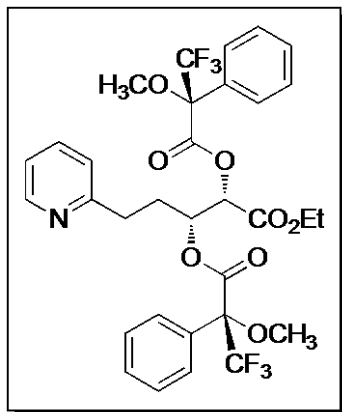
To a solution of 33 (103 mg, 0.50 mmol) in 9:1 acetone/water (4 mL) in a 20 mL vial was added 4-methylmorpholine *N*-oxide (117 mg, 1.00 mmol, 2.0 equiv, Aldrich) and aqueous 4% OsO<sub>4</sub> (32 μL, 0.0050 mmol, 1.0 mol%, Aldrich). The mixture was stirred at room temperature for 12 h. A 10% aqueous solution of Na<sub>2</sub>SO<sub>3</sub> (5 mL) was added with stirring followed by the addition of another 5 mL of water. The mixture was extracted with CH<sub>2</sub>Cl<sub>2</sub> (8 x 10 mL), and the CH<sub>2</sub>Cl<sub>2</sub> extracts were combined and concentrated under vacuum. The crude product was purified by chromatography on silica gel, eluting with 95:5 CH<sub>2</sub>Cl<sub>2</sub>/MeOH to provide the racemic product *rac*-34 as a colorless oil (105 mg, 88% yield). The spectroscopic data matched that of the diol 16 made by Sharpless asymmetric dihydroxylation.

Mosher analysis<sup>30</sup> of 34:

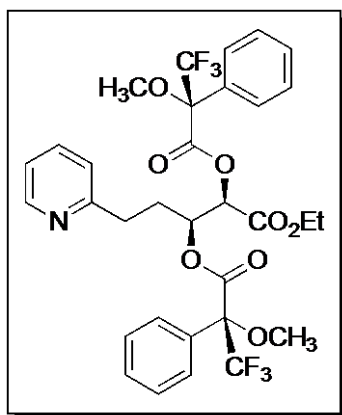
The (*R*)-Mosher diester of 34 was prepared from 34 and (*R*)-(+)-α-methoxy-α-trifluoromethylphenylacetic acid ((*R*)-(+)-MTPA) as follows: To a 25 mL flask was

added *rac*-34 (24 mg, 0.10 mmol). Toluene (5 mL) was added and evaporated under high vacuum to remove water as an azeotrope. (*R*)-MTPA, (70 mg, 0.30 mmol, 3.0 equiv, Matrix Scientific) and dry CH<sub>2</sub>Cl<sub>2</sub> (1 mL) were added under nitrogen. 1-Ethyl-3-(3-dimethylaminopropyl) carbodiimide hydrochloride (58 mg, 0.30 mmol, 3.0 equiv, TCI America), 4-(dimethylamino)pyridine (3.0 mg, 0.025 mmol, 0.25 equiv, Aldrich), and *N*-ethyldiisopropylamine (85 μL, 0.50 mmol, 5.0 equiv, Alfa Aesar) were added sequentially. The reaction mixture was stirred at room temperature for 24 h, diluted with 10 mL of CH<sub>2</sub>Cl<sub>2</sub>, and then this CH<sub>2</sub>Cl<sub>2</sub> solution was washed with saturated aqueous NH<sub>4</sub>Cl (10 mL), water (10 mL), saturated aqueous NaHCO<sub>3</sub> (10 mL), and brine (10 mL). The CH<sub>2</sub>Cl<sub>2</sub> solution was dried over Na<sub>2</sub>SO<sub>4</sub>, and the solvent was evaporated under vacuum. The crude product was purified by chromatography on silica gel, eluting with 98:2 CH<sub>2</sub>Cl<sub>2</sub>/MeOH, and collecting all of the fractions that contained the Mosher ester products according to TLC. The fractions were concentrated to provide the product mixture (bis-(*R*)-MTPA esters of *rac*-34) as a colorless oil (63 mg, 94% yield, R<sub>f</sub> = 0.29 in 98:2 CH<sub>2</sub>Cl<sub>2</sub>/MeOH).

The Mosher esterification reaction above was performed on diol 34 made by Sharpless asymmetric dihydroxylation to provide predominantly the bis-(*R*)-MTPA ester of (2*S*, 3*R*)-34. Integration of the doublets at 5.41 ppm and 5.49 ppm in the <sup>1</sup>H NMR spectrum of the product mixture indicated that the ee of 34 was 97% (Figure 4).



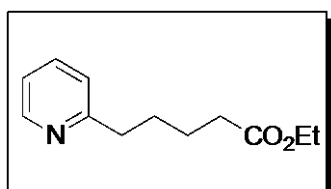
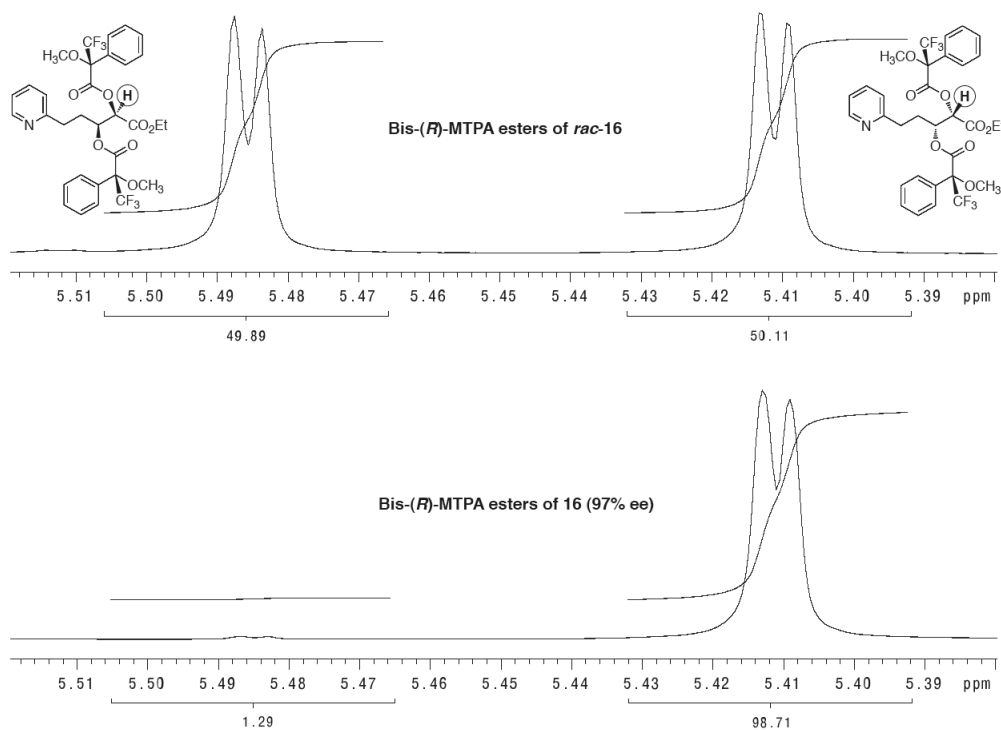
Bis-(*R*)-MTPA ester of (*2S*, *3R*)-34:  $^1\text{H}$  NMR (500 MHz,  $\text{CDCl}_3$ ):  $\delta$  8.51 (br d,  $J = 5.0$  Hz, 1H), 7.58 (br d,  $J = 7.5$  Hz, 2H), 7.57 (td,  $J = 7.5$ , 1.5 Hz, 1H), 7.51 (br d,  $J = 7.5$  Hz, 2H), 7.41-7.31 (multiple peaks, 6H), 7.12 (dd,  $J = 7.5$ , 5.0 Hz, 1H), 6.94 (d,  $J = 7.5$  Hz, 1H), 5.68 (td,  $J = 7.0$ , 2.0 Hz, 1H), 5.41 (d,  $J = 2.0$  Hz, 1H), 4.18 (dq,  $J = 11.0$ , 7.0 Hz, 1H), 4.16 (dq,  $J = 11.0$ , 7.0 Hz, 1H), 3.48 (s, 3H), 3.38 (s, 3H), 2.65 (dt,  $J = 14.0$ , 7.5 Hz, 1H), 2.62 (dt,  $J = 14.0$ , 7.5 Hz, 1H), 2.16 (q,  $J = 7.0$  Hz, 2H), 1.23 (t,  $J = 7.0$  Hz, 3H).  $^{13}\text{C}\{^1\text{H}\}$  NMR ( $\text{CDCl}_3$ ):  $\delta$  166.42, 166.34, 166.13, 159.55, 149.68, 136.73, 132.02, 131.38, 129.98, 129.87, 128.60, 128.58, 128.06, 127.55, 123.33 (q,  $^1J_{\text{CF}} = 288.5$  Hz), 123.27 (q,  $^1J_{\text{CF}} = 288.5$  Hz), 123.07, 121.76, 85.14 (q,  $^2J_{\text{CF}} = 28.0$  Hz), 84.70 (q,  $^2J_{\text{CF}} = 27.7$  Hz), 74.24, 73.98, 62.76, 55.73 (2C), 33.33, 30.33, 14.04.  $^{19}\text{F}\{^1\text{H}\}$  NMR ( $\text{CDCl}_3$ ):  $\delta$  -71.64, -72.21. IR (thin film): 1754  $\text{cm}^{-1}$ . HRMS electrospray (m/z):  $[\text{M}+\text{H}]^+$  calcd for  $\text{C}_{32}\text{H}_{32}\text{F}_6\text{NO}_8^+$  672.2027; found 672.2020.



Bis-(*R*)-MTPA ester of (*2R*, *3S*)-34:  $^1\text{H}$  NMR (500 MHz,  $\text{CDCl}_3$ ):  $\delta$  8.52 (br d,  $J = 5.0$  Hz, 1H), 7.66 (br d,  $J = 7.5$  Hz, 2H), 7.58 (td,  $J = 7.5$ , 1.5 Hz, 1H), 7.51 (br d,  $J = 7.5$  Hz, 2H), 7.41-7.31 (multiple peaks, 6H),

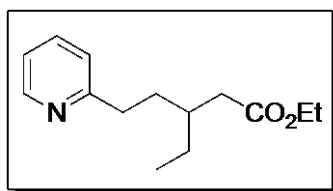
7.13 (dd,  $J = 7.5, 5.0$  Hz, 1H), 6.98 (d,  $J = 7.5$  Hz, 1H), 5.64 (td,  $J = 7.0, 2.0$  Hz, 1H), 5.49 (d,  $J = 2.0$  Hz, 1H), 4.08 (q,  $J = 7.0$  Hz, 2H), 3.60 (s, 3H), 3.42 (s, 3H), 2.72 (ddd,  $J = 14.5, 8.0, 7.0$  Hz, 1H), 2.69 (ddd,  $J = 14.5, 8.0, 7.0$  Hz, 1H), 2.11 (ddt,  $J = 15.0, 7.5, 7.0$  Hz, 1H), 2.01 (ddt,  $J = 15.0, 7.5, 7.0$  Hz, 1H), 1.19 (t,  $J = 7.0$  Hz, 3H).  $^{13}\text{C}\{^1\text{H}\}$  NMR ( $\text{CDCl}_3$ ):  $\delta$  166.21, 166.18, 165.78, 159.47, 149.62, 136.74, 131.90, 131.58, 129.88, 129.87, 128.62, 128.54, 127.73, 127.67, 123.36 (q,  $^1J_{\text{CF}} = 288.9$  Hz, 1C), 123.26 (q,  $^1J_{\text{CF}} = 288.5$  Hz, 1C), 122.98, 121.77, 84.76 (q,  $^2J_{\text{CF}} = 28.0$  Hz, 1C), 84.74 (q,  $^2J_{\text{CF}} = 27.7$  Hz, 1C), 74.56, 73.68, 62.63, 55.88, 55.50, 33.47, 29.72, 14.01.  $^{19}\text{F}\{^1\text{H}\}$  NMR ( $\text{CDCl}_3$ ):  $\delta$  -71.79, -72.06.

**Figure 4.** Comparison of (*R*)-MTPA esters of *rac*-**34** and (*R*)-MTPA esters of **34** made by Sharpless dihydroxylation.



To a 20 mL scintillation vial was added palladium on carbon (10.6 mg, 10 wt% Pd/C, 0.01 mmol, 10 mol% Pd, Aldrich), **33** (20.7 mg, 0.1 mmol) and MeOH (0.5 mL). The vial was fitted with a 24/40 septum and was

stirred at room temperature for 10 h under a balloon of hydrogen. The solvent was evaporated, and the product was purified by chromatography on silica gel, eluting with 60:40 hexanes/ethyl acetate. Compound **35** was obtained as a colorless oil (9.6 mg, 90% yield,  $R_f = 0.3$  in 60:40 hexanes/ethyl acetate).  $^1\text{H}$  NMR ( $\text{CDCl}_3$ ):  $\delta$  8.52 (dd,  $J = 4.8, 0.8$  Hz, 1H), 7.59 (app. td,  $J = 7.6, 2.0$  Hz, 1H), 7.14 (d,  $J = 7.6$  Hz, 1H), 7.10 (dd,  $J = 7.6, 5.2$  Hz, 1H), 4.12 (q,  $J = 7.2$  Hz, 2H), 2.81 (t,  $J = 7.2$  Hz, 2H), 2.34 (t,  $J = 7.6$  Hz, 2H), 1.80-1.68 (multiple peaks, 4H), 1.25 (t,  $J = 7.2$  Hz, 3H).  $^{13}\text{C}\{^1\text{H}\}$  NMR ( $\text{CDCl}_3$ ):  $\delta$  173.84, 161.99, 149.47, 136.50, 122.94, 121.21, 60.44, 38.19, 34.40, 29.44, 24.86, 14.45. IR (thin film): 1732  $\text{cm}^{-1}$ . HRMS electrospray ( $m/z$ ):  $[\text{M}+\text{H}]^+$  calcd for  $\text{C}_{12}\text{H}_{18}\text{NO}_2^+$  208.1332; found 208.1331.



Copper(I) bromide (7 mg, 0.05 mmol, 10 mol %, Fisher) and lithium chloride (4 mg, 0.1 mmol, 20 mol %, Fisher) were added to an oven-dried 5 mL Schlenk tube under nitrogen. The tube was evacuated, heated with a heat gun, allowed to cool to room temperature under vacuum, and filled with nitrogen. Dry THF (1 mL) was added, and the mixture stirred for 10 min. The tube was placed in an ice bath, and after 10 min, a solution of **33** (103 mg, 0.50 mmol, 1 equiv) in dry THF (1 mL) was added followed by TMSCl (70  $\mu\text{L}$ , 0.55 mmol, 1.1 equiv, Aldrich). The solution was stirred at 0  $^\circ\text{C}$  for 15 min, and then 3 M EtMgBr in Et<sub>2</sub>O (250  $\mu\text{L}$ , 0.75 mmol, 1.5 equiv, Aldrich) was added dropwise. The solution was stirred for 1 h at 0  $^\circ\text{C}$  and then poured into 10 mL of saturated aqueous  $\text{NH}_4\text{Cl}$ . The mixture was extracted with Et<sub>2</sub>O (3 x 20 mL). The Et<sub>2</sub>O extracts were combined, washed with brine, dried over  $\text{Na}_2\text{SO}_4$ , and concentrated under vacuum. The crude product was purified by chromatography on silica gel, eluting with 80:20 hexanes/ethyl acetate, to provide product **36** as a colorless oil (222 mg, 94% yield,  $R_f = 0.22$  in 70:30 hexanes/ethyl acetate).  $^1\text{H}$  NMR ( $\text{CDCl}_3$ ):  $\delta$  8.51 (ddd,  $J = 4.8, 2.0, 0.8$  Hz, 1H), 7.58 (app. td,  $J = 7.6, 2.0$

Hz, 1H), 7.14 (d,  $J = 7.6$  Hz, 1H), 7.09 (ddd,  $J = 7.6, 4.8, 1.2$  Hz, 1H), 4.12 (q,  $J = 7.2$  Hz, 2H), 2.79 (t,  $J = 4.0$  Hz, 2H), 2.31 (d,  $J = 6.8$  Hz, 2H), 1.90 (tq,  $J = 6.8, 6.4$  Hz, 1H), 1.82-1.66 (multiple peaks, 2H), 1.51-1.34 (multiple peaks, 2H), 1.24 (t,  $J = 7.2$  Hz, 3H), 0.90 (t,  $J = 7.2$  Hz, 3H).  $^{13}\text{C}\{^1\text{H}\}$  NMR ( $\text{CDCl}_3$ ):  $\delta$  173.57, 162.36, 149.41, 136.48, 122.83, 121.14, 60.33, 38.83, 36.43, 35.75, 33.75, 26.37, 14.44, 10.89. IR (thin film):  $1734\text{ cm}^{-1}$ . HRMS electrospray ( $m/z$ ):  $[\text{M}+\text{H}]^+$  calcd for  $\text{C}_{14}\text{H}_{22}\text{NO}_2^+$  236.1645; found 236.1645.

## 4.8 References

---

<sup>1</sup> Oestreich, M., Ed., *The Mizoroki-Heck Reaction*. John Wiley and Sons, Chichester, U.K. 2009.

<sup>2</sup> (a) Satoh, T.; Miura, M. *Chem. Eur. J.* **2010**, *16*, 11212. (b) Ref 1, p. 383-400.

<sup>3</sup> (a) Trost, B. M.; Godleski, S. A.; Genet, J. P. *J. Am. Chem. Soc.* **1978**, *100*, 3930. (b) Baran, P. S.; Corey, E. J. *J. Am. Chem. Soc.* **2002**, *124*, 7904. (c) Garg, N. K.; Caspi, D. D.; Stoltz, B. M. *J. Am. Chem. Soc.* **2004**, *126*, 9552. (d) Beck, E. M.; Hatley, R.; Gaunt, M. J. *Angew. Chem. Int. Ed.* **2008**, *47*, 3004. (e) Wang, D. H.; Engle, K. M.; Shi, B. F.; Yu, J.-Q. *Science* **2010**, *327*, 315.

<sup>4</sup> Ref. 1, p. 345-378.

<sup>5</sup> Wasa, M.; Engle, K. M.; Yu, J. Q. *J. Am. Chem. Soc.* **2010**, *132*, 3680.

<sup>6</sup> For examples of olefination and alkylation at  $\text{sp}^3$  C–H sites activated by a-heteroatoms or aromatic rings, see: (a) Chatani, N.; Asaumi, T.; Yorimitsu, S.; Ikeda, T.; Kakiuchi, F.; Murai, S. *J. Am. Chem. Soc.* **2001**, *123*, 10935 and references therein. (b) DeBoef, B.; Pastine, S. J.; Sames, D. *J. Am. Chem. Soc.* **2004**, *126*, 6556. (c) Song, C.-X.; Cai, G.-X.; Farrell, T. R.; Jiang, Z.-P.; Li, H.; Gan, L.-B.; Shi, Z.-J. *Chem. Commun.* **2009**, 6002. (d) Li, H.; Li, B.-J.; Shi, Z.-J. *Catal. Sci. Tech.* **2011**, *1*, 191-206.

<sup>7</sup> Jazzar, R.; Hitce, J.; Renaudat, A.; Sofack-Kreutzer, J.; Baudoin, O. *Chem. Eur. J.* **2010**, *16*, 2654.

<sup>8</sup> Shultz, L. H.; Tempel, D. J.; Brookhart, M. *J. Am. Chem. Soc.* **2001**, *123*, 11539.

<sup>9</sup> (a) Firmansjah, L.; Fu, G. C. *J. Am. Chem. Soc.* **2007**, *129*, 11340. (b) Bloome, K. S.; Alexanian, E. J. *J. Am. Chem. Soc.* **2010**, *132*, 12823.

- 
- <sup>10</sup> (a) Dick, A. R.; Hull, K. L.; Sanford, M. S. *J. Am. Chem. Soc.* **2004**, *126*, 2300. (b) Desai, L. V.; Hull, K. L.; Sanford, M. S. *J. Am. Chem. Soc.* **2004**, *126*, 9542. (c) Dick, A. R.; Sanford, M. S. *Tetrahedron* **2006**, *62*, 2439. (d) Neufeldt, S. R.; Sanford, M. S. *Org. Lett.* **2010**, *12*, 532. (e) Lyons, T. W.; Sanford, M. S. *Chem. Rev.* **2010**, *110*, 1147.
- <sup>11</sup> A Scifinder search on Feb. 16, 2011 showed >5000 alkaloid derivatives containing 6,5-N-fused bicyclic scaffolds.
- <sup>12</sup> For examples, see: (a) Zaitsev, V. G.; Shabashov, D.; Daugulis, O. *J. Am. Chem. Soc.* **2005**, *127*, 13154. (b) Shabashov, D.; Daugulis, O. *Org. Lett.* **2005**, *7*, 3657. (c) Reddy, B. V. S.; Reddy, L. R.; Corey, E. J. *Org. Lett.* **2006**, *8*, 3391. (d) Shabashov, D.; Daugulis, O. *J. Am. Chem. Soc.* **2010**, *132*, 3965. (e) Zhang, S.; Luo, F.; Wang, W.; Jia, X.; Hu, M.; Cheng, J. *Tetrahedron Lett.* **2010**, *51*, 3317.
- <sup>13</sup> (a) Baldwin, J. E.; Jones, R. H.; Najera, C.; Yus, M. *Tetrahedron*, **1985**, *4*, 699-711. (b) Ryabov, A. D. *Chem. Rev.* **1990**, *90*, 403-424.
- <sup>14</sup> (a) Gligorich, K. M.; Sigman, M. S. *Chem. Commun.* **2009**, 3854-3867. (b) Stahl, S. *Angew. Chem., Int. Ed.* **2004**, *43*, 3400-3420.
- <sup>15</sup> Obora, Y.; Ishii, Y. *Molecules*, **2010**, *15*, 1487.
- <sup>16</sup> Nishikata, T.; Lipshutz, B. H. *Org. Lett.* **2010**, *12*, 1972.
- <sup>17</sup> Hatamoto, Y.; Sakaguchi, S.; Ishii, Y. *Org. Lett.* **2004**, *6*, 4623-4625.
- <sup>18</sup> The addition of 1 equiv of NaOTf significantly increased the yield where indicated and in these cases the product was isolated with a <sup>-</sup>OTf counterion.
- <sup>19</sup> Azzouz, R.; Fruit, C.; Bischoff, L.; Marsais, F. *J. Org. Chem.* **2008**, *73*, 1154.
- <sup>20</sup> Sinigaglia, I.; Nguyen, T. M.; Wypych, J. C.; Delpech, B.; Marazano, C. *Chem. Eur. J.* **2010**, *16*, 3594.
- <sup>21</sup> Kolb, H. C.; VanNieuwenhze, M. S.; Sharpless, K. B. *Chem. Rev.* **1994**, *94*, 2483.
- <sup>22</sup> Dias, L. C.; de Oliveira, L. G.; Vilcachagua, J. D.; Nigsch, F. *J. Org. Chem.* **2005**, *70*, 2225.
- <sup>23</sup> Reetz, M. T.; Kindler, A. *J. Organomet. Chem.* **1995**, *502*, C5.
- <sup>24</sup> Bell, T. W.; Hu, L. Y.; Patel, S. V. *J. Org. Chem.* **1987**, *52*, 3847-3850.
- <sup>25</sup> Pasquinet, E.; Rocca, P.; Marsais, F.; Godard, A.; Quéguiner, G. *Tetrahedron* **1998**, *54*, 8771-8782.

- 
- <sup>26</sup> Wallace, D. J.; Chen, C. Y. *Tetrahedron Lett.* **2002**, *43*, 6987-6990.
- <sup>27</sup> Zhang, C. X.; Liang, H. C.; Kim, E.; Shearer, J.; Helton, M. E.; Kim, E.; Kaderli, S.; Incarvito, C. D.; Rheingold, A. L.; Zuberbuhler, A. D.; Karlin, K. D. *J. Am. Chem. Soc.* **2003**, *125*, 634-635.
- <sup>28</sup> Baldwin, J. E.; Fryer, A. M.; Pritchard, G. J. *J. Org. Chem.* **2001**, *66*, 2588-2596.
- <sup>29</sup> Kolb, H. C.; VanNieuwenhze, M. S.; Sharpless, K. B. *Chem. Rev.* **1994**, *94*, 2483-2547.
- <sup>30</sup> Dale, J. A.; Mosher, H. S. *J. Am. Chem. Soc.* **1968**, *90*, 3732-3738.



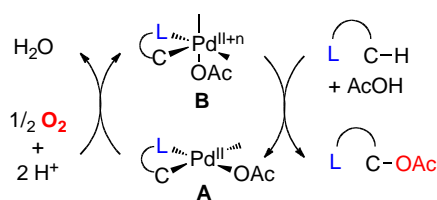
## Chapter 5: Acetoxylation using Oxygen

### 5.1 Introduction

The use of metal-catalyzed C–H activation to install C–O bonds directly into unfunctionalized molecules has received increased attention and interest over the last decade.<sup>1</sup> Historically the oxygenation of unactivated 1° sp<sup>3</sup> C–H bonds has proven particularly challenging.<sup>2</sup> (For the purposes of this chapter, unactivated refers to C–H bonds that are not alpha to an aromatic ring, alkene, or electron donating atom like oxygen or nitrogen). Only over the past 10 years have efficient methods been developed for the ligand directed C–H oxygenation of this class of substrates. These transformations generally involve Pd catalysts in conjunction with oxidants such as PhI(OAc)<sub>2</sub>,<sup>1h,3</sup> IOAc,<sup>4</sup> Oxone®,<sup>5</sup> or TBHP.<sup>6</sup> However, there are a number of distinct disadvantages to these oxidants, including the formation of stoichiometric quantities of byproducts, the requirement for expensive or non-commercial reagents, poor atom economy, and limited functional group tolerance.

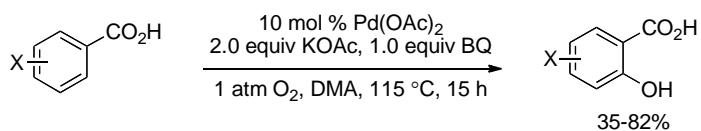
From all of these perspectives, it would be ideal to use O<sub>2</sub> as the terminal oxidant in Pd-catalyzed sp<sup>3</sup>-C–H oxygenation. A potential catalytic cycle for this type of a reaction is shown in Figure 5.1. Notably, it is expected that the acetate ligand on high oxidation state Pd intermediate **B** would come from the solvent by ligand association or exchange. The major challenge for achieving this transformation is that the vast majority of palladacycles with general structure **A** are highly kinetically inert towards O<sub>2</sub>.<sup>7</sup> Therefore, the use of O<sub>2</sub> as oxidant is expected to require extremely high temperatures and high pressures for most substrates.

**Figure 5.1.** Potential Catalytic Cycle for Oxygenation Using O<sub>2</sub>



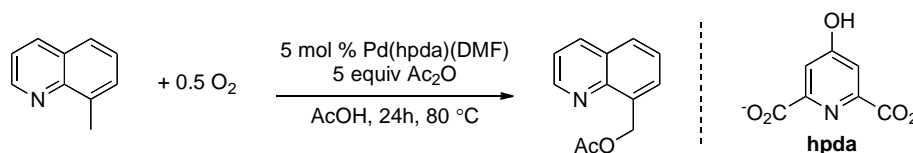
To this end, a single report demonstrates that oxygen can be used as the sole oxidant to afford Pd-catalyzed ligand directed C–H oxygenation of arenes (Scheme 5.1).<sup>8</sup> While this hydroxylation proceeds efficiently with a variety of electron poor and electron rich benzoic acid derivatives, there are a number of drawbacks. First, the catalyst loading is high at 10 mol %. Second, the reaction is only compatible with a limited set of functional groups (such as F, OMe, Me). Other functionalities, such as ketones, nitro groups, and CF<sub>3</sub> substituents, resulted in a decrease in the product yield. Higher pressures of O<sub>2</sub> (5 atm) were required to increase the yield for these electron poor arenes. Finally, the substrate scope does not include examples of oxygenation of unactivated sp<sup>3</sup> C–H bonds.

**Scheme 5.1.** Pd-Catalyzed Benzoic Acid-Directed Aerobic C–H Oxygenation of Arenes



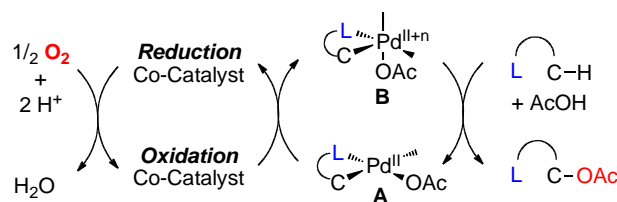
In addition, it has been demonstrated that O<sub>2</sub> can be used as the terminal oxidant for the Pd-catalyzed ligand-directed C–H acetoxylation of benzylic C–H bonds in 8-methylquinoline derivatives (Figure 5.2).<sup>9</sup> Here a specialized supporting ligand (hpda, Figure 5.2) was required for the desired reactivity. This report shows the feasibility of using oxygen for the functionalization of activated (benzylic) sp<sup>3</sup> C–H bonds. However, the substrate scope is extremely narrow, including just derivatives of 8-methylquinoline (at substitution *para* to the 8-methyl).

**Figure 5.2.** Pd-Catalyzed Quinoline-Directed Aerobic Oxygenation of Benzylic C–H Bonds



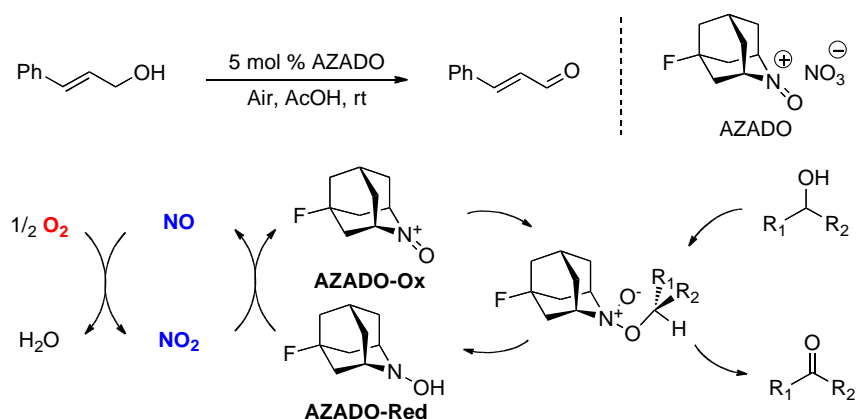
Despite exhibiting low kinetic reactivity towards most palladacycles, O<sub>2</sub> is a thermodynamically strong oxidant, with comparable oxidation potential to PhI(OAc)<sub>2</sub> (+1.23 V for O<sub>2</sub> [at pH = 0] versus +1.15 V for PhI(OAc)<sub>2</sub>).<sup>10</sup> Thus, we reasoned that the use of a redox co-catalyst with high kinetic reactivity towards both O<sub>2</sub> and palladacycles like **A** might enable aerobic oxidations of unactivated C–H substrates (Figure 5.3). Notably, this concept of a redox co-catalysis is used widely for Wacker oxidations, where sub-stoichiometric Cu(II)<sup>11</sup> or polyoxometalate<sup>12</sup> is used in conjunction with O<sub>2</sub> as the terminal oxidant.

**Figure 5.3.** Redox Catalyst Cycle to harness oxidation potential of dioxygen.



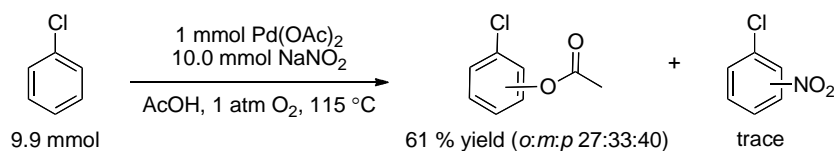
We were most interested in identifying a co-catalyst that would be inexpensive, readily available, and generate minimal waste. Recent reports have demonstrated that NO<sub>3</sub><sup>−</sup> is effective for aerobic oxidation of alcohols in conjunction with amine oxide co-catalysts.<sup>13</sup> In this catalytic cycle illustrated in Figure 5.4, **AZADO-Ox** oxidizes the alcohol. The electrons are transferred from **AZADO-Red** to the NO<sub>x</sub> redox cycle which cooperate with O<sub>2</sub> as the terminal oxidant. The NO/NO<sub>2</sub> required for this reaction to be conducted under ambient conditions is generated from the small % of NO<sub>3</sub><sup>−</sup> (5 mol%) from the AZADO nitrate salt reagent.

**Figure 5.4.** Organocatalytic Aerobic Oxidation of Alcohols



In a 1969 report by Tisue and Downs, nitrate salts were examined as nucleophiles for the Pd-catalyzed nitration of benzene in acetic acid using O<sub>2</sub> as the oxidant. Interestingly, mixtures of phenyl acetate along with the desired product, nitrobenzene, were obtained (14 total turnovers of catalyst).<sup>14</sup> Since then, nitrates or nitrites have been used in a number of reactions as reagents for nitration of arenes. While selectivity was significantly improved in many of these systems, oxygenated products were often formed in competition with the nitrated products.<sup>15</sup> During optimization of the Pd-catalyzed acetoxylation of chlorobenzene, Eberson and Jonsson reported that only minor amounts of nitrated products are detected when using sodium nitrite and oxygen in acetic acid (Scheme 5.2).<sup>16</sup>

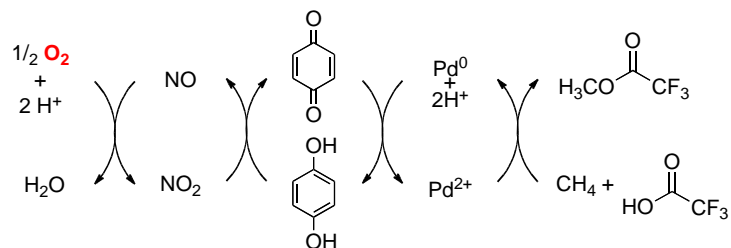
**Scheme 5.2.** Acetoxylation of Chlorobenzene



The most recent report demonstrating co-catalytic oxygenation uses a palladium catalyst, oxygen, *p*-benzoquinone (Q) and sodium nitrate for the functionalization of methane (Figure 5.5).<sup>17</sup> An electron-transfer chain

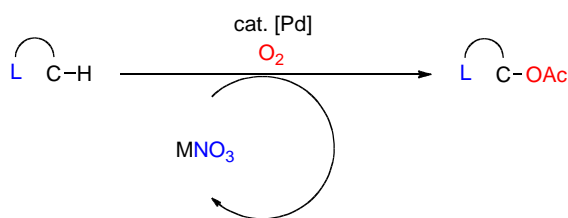
mechanism is thought to be operative as the  $O_2$ , NO/NO<sub>2</sub>, Q/H<sub>2</sub>Q cycles work cooperatively to oxidize methane at low temperatures (80 °C).

**Figure 5.5.** Redox Couples for Oxidation of Methane



Due to the ease of handling, we wondered whether nitrates could be compatible as a redox shuttle for a higher oxidation state palladium catalysis manifold. This chapter describes the use of substoichiometric nitrate salts in conjunction with  $O_2$  to perform C–H oxygenation of both activated and unactivated  $sp^3$  C–H bonds (Figure 5.6).

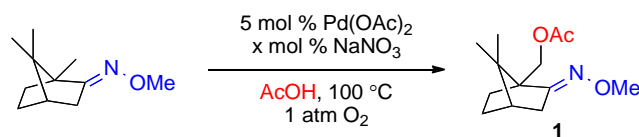
**Figure 5.6.** Acetoxylation with Nitrates and Oxygen as the Terminal Oxidant



## 5.2 Results

We began our investigation studying the Pd-catalyzed conversion of an unactivated  $sp^3$ -C–H bond of camphor oxime ether **1** to an OAc bond (Scheme 5.3).

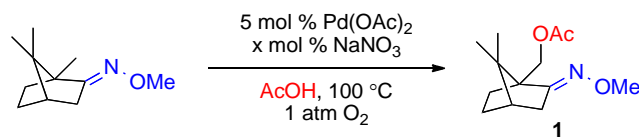
### Scheme 5.3. Acetoxylation with Nitrates and Oxygen as the Terminal Oxidant



Initial studies employed 5 mol % of Pd(OAc)<sub>2</sub> in conjunction with 10 mol % of NaNO<sub>3</sub> under air. Gratifyingly, we found that these simple reaction conditions provided 45% of the acetoxyated product (entry 1). Without the nitrate source acting as a co-catalyst, in the presence of O<sub>2</sub>, we observed <2% of the desired product (entry 2). To ensure that the nitrate is responsible for cooperating with the O<sub>2</sub> in air for catalytic turnover, we excluded air from the reaction. This afforded 11% product, which is presumably formed from a single turnover of the Pd/nitrate (entry 3). In order to improve catalyst turnover, 1 atm of O<sub>2</sub> was used in place of air, and the product yield increased to 53% (entry 4). By increasing the amount of NaNO<sub>3</sub> to 25 mol % we were able to further enhance the product yield to 75% (entry 5). We found that oxidation state of the nitrogen in the co-catalyst source (NO<sub>3</sub><sup>-</sup> versus NO<sub>2</sub><sup>-</sup>) had a negligible effect on product yield (entries 5 and 6).

In testing the effect of the nitrate counterion, it was determined that sodium and potassium showed similar reactivity (entries 6 and 7). In contrast, silver and ammonium nitrate provided poor results (entries 8 and 9). By increasing the temperature slightly (110 °C) we found that the yield increased to 85% (entry 10). With these optimized conditions in hand, we examined a variety of other substrates containing directing groups that are proximal to unactivated sp<sup>3</sup> C-H bonds.

**Table 5.1.** Optimization of nitrate salt as a co-catalyst for palladium catalyzed oxygenation.

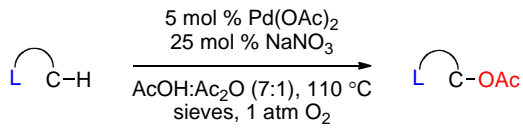


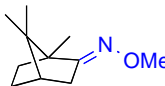
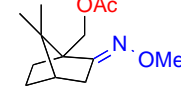
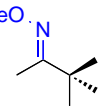
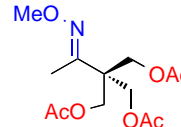
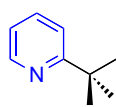
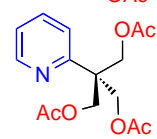
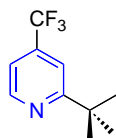
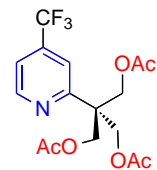
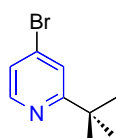
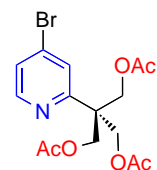
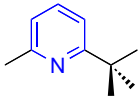
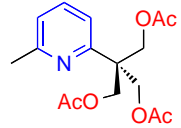
Entry	Salt	x mol %	Yield (GC)
1	NaNO <sub>3</sub>	10 <sup>a</sup>	49
2	None	0 <sup>a</sup>	2
3	NaNO <sub>3</sub>	10 <sup>b</sup>	11
4	NaNO <sub>3</sub>	10	53
5	NaNO <sub>3</sub>	25	75
6	NaNO <sub>2</sub>	25	75
7	KNO <sub>3</sub>	25	73
8	AgNO <sub>3</sub>	25	42
9	NH <sub>4</sub> NO <sub>3</sub>	25	25
10	NaNO <sub>3</sub>	25 <sup>c</sup>	85

a air, b N<sub>2</sub>, c 110 °C

Using 5 mol % of Pd(OAc)<sub>2</sub> and 25 mol % of NaNO<sub>3</sub> with 1 atm of O<sub>2</sub> in 0.12 M AcOH/Ac<sub>2</sub>O (7:1), a number of substrates with different directing groups were examined. In addition to the oxime ethers **1** and **2** of Table 5.2, pyridine directing groups were also effective for selective 1° sp<sup>3</sup> C–H acetoxylation under the reaction conditions (entries 3-6). Due to triacetoxylation of the *t*-butyl group adjacent to the ligand, an increase in the amount of NaNO<sub>3</sub> (to 50 mol %) was necessary to drive the reaction to completion (products **3-6**). Entry 5 includes a bromide-substituted pyridine that is tolerated under the reaction conditions affording a 77% isolated yield. The compatibility with this functional group is suggestive of a mechanism involving high oxidation state Pd.<sup>18</sup> A very sterically hindered pyridine also can be acetoxylation selectively at the *t*-butyl group without competing oxygenation of the activated methyl group; however, an increase in nitrate salt (1 equiv) was required for complete triacetoxylation (entry 6).

**Table 5.2.** Substrate Scope for Oxygenation.



Entry	Substrate	Product	Yield
1			<b>1</b> (80%)
2			<b>2</b> (83%)
3			<b>3<sup>b,c</sup></b> (79%)
4			<b>4<sup>b,c</sup></b> (78%)
5			<b>5<sup>b,c</sup></b> (77%)
6			<b>6<sup>b,d</sup></b> (68%)

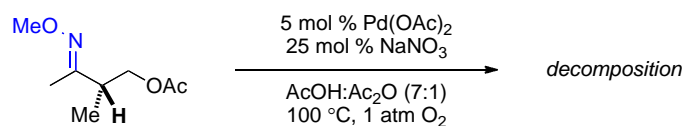
b) 270 mg/mmol 3 A molecular sieves added, c) 50 mol % NaNO<sub>3</sub> used, d) 1 equiv NaNO<sub>3</sub> used.

When applying these reaction conditions to other substrates commonly used for sp<sup>3</sup> C-H oxygenation, such as other oxime ethers (**7-11**) we found that reoptimization was required, as the conditions in Table 5.2 led to either decomposition or poor mass balance. For example, we found that the products of oxime ethers with a single site of  $\alpha$ -branching readily decompose in acetic acid; therefore, these systems required propionic acid as the solvent (Scheme 5.4). Even in propionic acids the yields of the desired products **7** and **8** remain modest

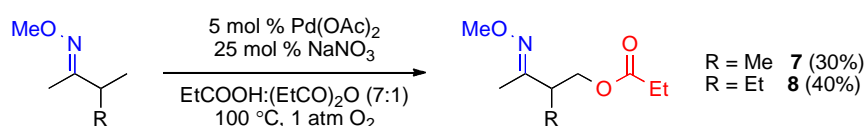


despite variation of oxidant equivalents, temperature, solvent, catalyst and reaction time (Scheme 5.5).

**Scheme 5.4.** Decomposition of Acetoxylation Product



**Scheme 5.5.** C–H Oxygenation to form **7** and **8**



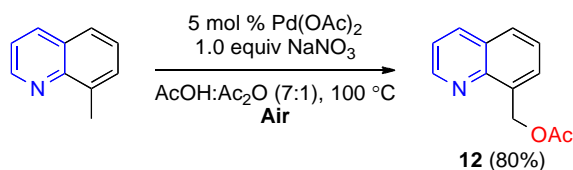
Other oxime ethers underwent the desired transformation, albeit in modest yields. 2,2-dimethylcyclopentanone O-methyl oxime **9** undergoes selective monoacetoxylation (Table 5.3, entry 1). However, it was found that an increase in catalyst loading was required (to 15 mol % Pd(OAc)<sub>2</sub>). For substrate **10**, an unactivated 2° C–H bond was shown to undergo acetoxylation albeit in modest yield with the remaining mass balance as starting material (entry 2). Interestingly, 2,2-dimethylcyclohexanone O-methyl oxime **11** undergoes diacetoxylation in good yield without an increase in catalyst or sodium nitrate.

**Table 5.3.** Substrate Scope for Acetoxylation of Sterically Hindered Oxime Ethers.

Entry	Substrate	Product	Yield
1			<b>9</b> (67%)
2			<b>10</b> (33%)
3			<b>11</b> (71%)

However, when applying 5 mol % of Pd(OAc)<sub>2</sub> and 25 mol % of NaNO<sub>3</sub> with 1 atm of O<sub>2</sub> in 0.12 M AcOH/Ac<sub>2</sub>O (7:1), to 8-methylquinoline **12** the reaction did not go to completion and seemed to stall at ~50% conversion. Upon optimization, this reaction can be conducted with 1 equivalent of NaNO<sub>3</sub> in air as opposed to 25 mol% under 1 atm O<sub>2</sub> (Scheme 5.6). Although more nitrate is required as oxidant, these conditions are still desirable since the molar price of Pd(OAc)<sub>2</sub> is 400 times that of NaNO<sub>3</sub> and there is no organic waste generated when using nitrate.

**Scheme 5.6** Acetoxylation of 8-methylquinoline with Nitrate and Air

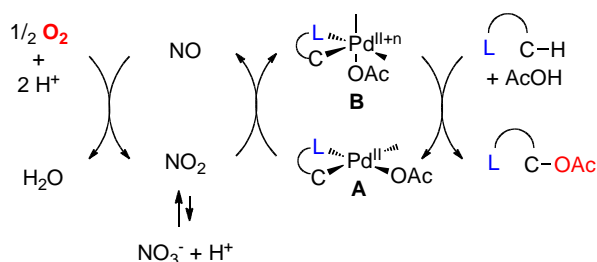


### 5.3 Discussion

It is known that nitrates will undergo thermal decomposition to form NO and NO<sub>2</sub>.<sup>19</sup> On this basis, we hypothesize that NO<sub>2</sub> is generated *in situ* and is acting

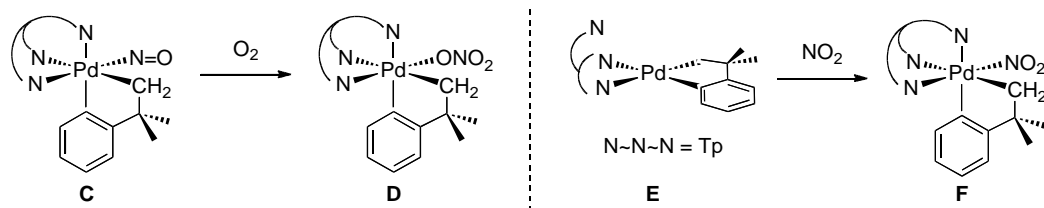
as the oxidant to Pd complex **A** to generate **B** in the presence of an a carboxylic acid solvent. Complex **B** then undergoes C–O bond-forming reductive elimination to release the acetoxyated product. The overall proposed catalytic cycle with NO/NO<sub>2</sub> cooperatively reacting with O<sub>2</sub> for the Pd(II/IV) redox cycle is illustrated in Figure 5.7.

**Figure 5.7.** Potential Redox Cycle for Nitrate Assisted Acetoxylation



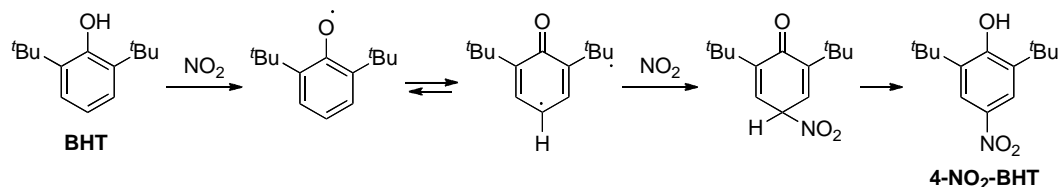
Palladium(IV) NO<sub>x</sub> complexes are somewhat rare in the literature, but one example shows the feasibility and reactivity of such complexes (Figure 5.8).<sup>20</sup> In this report the NO ligand of complex **C** reacted with O<sub>2</sub> to form complex **D** that now contains a nitrate ligand. Furthermore, a palladium (II) complex **E** reacts with NO<sub>2</sub> to form the new palladium (IV) complex **F**. This latter reaction in particular demonstrates the potential feasibility of oxidizing catalytic intermediate **A** with NO<sub>2</sub> to generate high oxidation state Pd complex **B**.

**Figure 5.8** Oxidation of a Pd(II) Complex **E** to form Pd(IV) Nitrosyl Complex **F**



We sought preliminary insight into the mechanism. It is well known that NO<sub>2</sub><sup>21</sup> reacts rapidly with 2,5-di-*tert*-butylphenol (BHT) to afford 4-nitro-2,5-di-*tert*-butylphenol.<sup>22</sup>

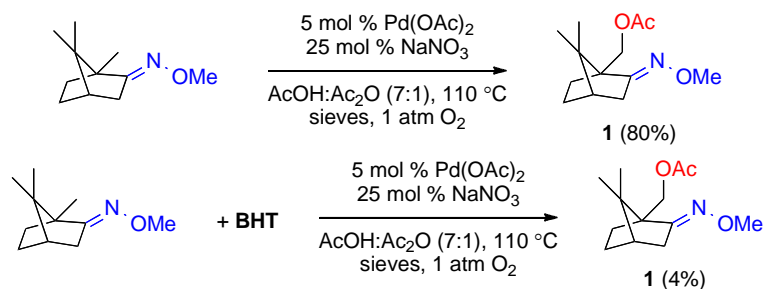
**Figure 5.9** Nitration of **BHT** with  $\text{NO}_2$  to form **4-NO<sub>2</sub>-BHT**



Thus, if this species is formed during catalysis (and is a key intermediate) it should be scavenged by BHT, thereby shutting down catalytic turnover.

The addition of 0.25 equiv of BHT under otherwise analogous reaction conditions to the optimized conditions provided a yield of only 4% of the desired acetoxylation (Scheme 5.7). We are currently working to confirm whether 4-nitro-2,5-di-*tert*-butylphenol was formed. This experiment preliminarily suggests that and NO/NO<sub>2</sub> radical formed in the reaction is immediately scavenged by the 2,5-di-*tert*-butylphenol thus ceasing catalysis.

**Scheme 5.7.** Addition of BHT to the optimized reaction conditions.



Finally, the exclusion of O<sub>2</sub> from the reaction resulted in near stoichiometric product formation (Table 5.1, entry 3). There is still much work to be done to elucidate the mechanistic details of this reaction.

## 5.4 Application

During our investigations, we were interested to see whether other nucleophiles could be incorporated into the starting material using the same Pd/



## 5.5 Conclusions

In this chapter, we have demonstrated the feasibility and advantages of using nitrate salts for *in situ* generation of nitrogen dioxide that serves as a co-catalyst for aerobic ligand directed palladium catalyzed acetoxylation of unactivated  $sp^3$  C–H bonds. Thus far nitrate salts have been underutilized as oxidants and/or catalysts for C–O bond formation at a higher oxidation state of palladium. Based on literature precedent, the mechanism is thought to proceed through oxidation of cyclopalladated complexes by nitrogen dioxide; however, we have not yet been able to gather definitive evidence for this proposal. Efforts toward understanding the mechanism of this reaction and using that information to determine how general this oxidant will be for further C–H functionalization reactions are currently underway.

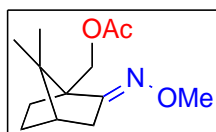
## 5.6 Experimental

*Acetoxylation Procedure:* Substrates 1-11 were prepared in the following manner: In a schlenk flask,  $Pd(OAc)_2$  (0.025 mmol, 0.05 equiv) and  $NaNO_3$  (0.125 mmol, 0.25 equiv) were weighed. Substrate (0.5 mmol, 1 equiv) was weighed into a separate vial and added to the schlenk tube using the appropriate solvent ( $AcOH:Ac_2O/7:1$ , 0.125 M). 270 mg/mmol of oven dried 4 A molecular sieves were added and the tube was fitted with a teflon stopcock. The reaction in the schlenk flask was then charged with 1 atm of  $O_2$  using the methods described in a previous report (ref). The flask was then heated and stirred at 110 °C in an oil bath for 18 hrs. The reaction was removed from heat, filtered, and then concentrated under reduced pressure to remove most of the solvent. The residual mixture was neutralized with saturated  $NaHCO_3$  solution and extracted with ether. The ether was then washed with brine and the organic layers were combined and dried with  $MgSO_4$ . The acetoxyated products were purified by silica gel column chromatography.

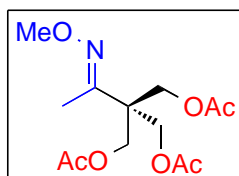
*Chlorination Procedure:* In a vial,  $Pd(OAc)_2$  (0.025 mmol, 0.05 equiv) and  $NaNO_3$  (0.05 mmol, 0.15 equiv) and  $NaCl$  (0.25 mmol, 10 equiv) were weighed. Substrate (0.5 mmol, 1 equiv) was weighed into a separate vial and added to the

schlenk tube using the appropriate solvent (AcOH, 0.125 M). The vial was closed with a teflon lined cap then heated and stirred at 80 °C in an aluminum heating block for 24 hrs. The reaction was removed from heat, filtered, and then concentrated under reduced pressure to remove most of the solvent. The residual mixture was neutralized with saturated NaHCO<sub>3</sub> solution and extracted with ether. The ether was then washed with brine and the organic layers were combined and dried with MgSO<sub>4</sub>. The chlorinated products were purified by silica gel column chromatography and then separated using high pressure liquid chromatography.

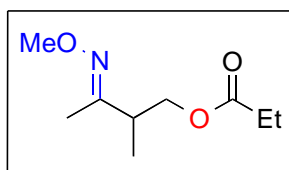
## 5.7 Characterization



(1) was obtained as a pale yellow oil ( $R_f = 0.25$  in 1:9 ethyl acetate/hexanes). Spectral data ( $^1\text{H NMR}$  ( $\text{CDCl}_3$ ) and  $^{13}\text{C}\{^1\text{H}\}$  NMR ( $\text{CDCl}_3$ )) matched published data.<sup>2</sup>

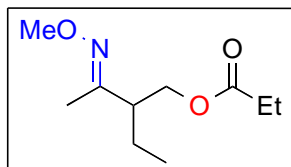


(2) was obtained as a colorless oil in 83 % isolated yield ( $R_f = 0.25$  in 1:9 ethyl acetate/hexanes). Spectral data ( $^1\text{H NMR}$  ( $\text{CDCl}_3$ ) and  $^{13}\text{C}\{^1\text{H}\}$  NMR ( $\text{CDCl}_3$ )) matched published data.<sup>2</sup>

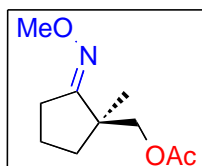


(7) was obtained as a colorless oil ( $R_f = 0.25$  in 1:9 diethyl ether/pentanes). Major isomer reported:  $^1\text{H NMR}$  ( $\text{CDCl}_3$ ):  $\delta$  4.12 (dd,  $J = 11.0, 7.5$  Hz, 1H), 4.02 (dd,  $J = 11.0, 6.5$  Hz, 1H), 3.79 (s, 3H), 2.65 (sextet,  $J = 7.0$  Hz, 1H), 2.29 (q,  $J = 8.0$  Hz, 2H), 1.76 (s, 3H), 1.10 (t,  $J = 8.0$  Hz, 3H), 1.07 (d,  $J = 7.5$  Hz, 3H).

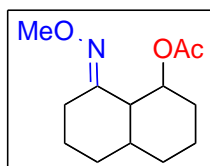
$^{13}\text{C}\{^1\text{H}\}$  NMR ( $\text{CDCl}_3$ ):  $\delta$  174.53, 158.06, 66.09, 61.47, 39.20, 27.76, 14.94, 11.77, 9.35. HRMS electrospray ( $m/z$ ):  $[\text{M}+\text{H}]^+$  calcd for  $\text{C}_9\text{H}_{18}\text{NO}_3$  predicted: 188.1281, measured: 188.1279.



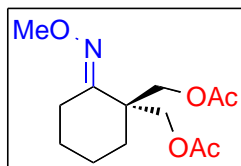
**(8)** was obtained as a colorless oil ( $R_f = 0.25$  in 1:9 diethyl ether/pentanes). Major isomer reported:  $^1\text{H}$  NMR ( $\text{CDCl}_3$ ):  $\delta$  4.13 (d,  $J = 7.2$  Hz, 2H), 3.84 (s, 3H), 2.52 (quin,  $J = 7.2$  Hz, 1H), 2.32 (q,  $J = 7.2$  Hz, 2H), 1.77 (s, 3H), 1.54 – 1.49 (multiple peaks, 2H), 1.13 (t,  $J = 7.2$  Hz, 3H), 0.90 (t,  $J = 7.2$  Hz, 3H).  $^{13}\text{C}\{^1\text{H}\}$  NMR ( $\text{CDCl}_3$ ):  $\delta$  174.49, 157.19, 64.90, 61.51, 46.19, 27.81, 22.07, 11.54, 11.50, 9.35. HRMS electrospray ( $m/z$ ):  $[\text{M}+\text{H}]^+$  calcd for  $\text{C}_{10}\text{H}_{18}\text{NO}_3$  predicted: 202.1438, measured: 202.1434.



**(9)** was obtained as a pale yellow oil ( $R_f = 0.25$  in 3:7 diethyl ether/pentanes). Spectral data ( $^1\text{H}$  NMR ( $\text{CDCl}_3$ ) and  $^{13}\text{C}\{^1\text{H}\}$  NMR ( $\text{CDCl}_3$ )) matched published data.<sup>2</sup>

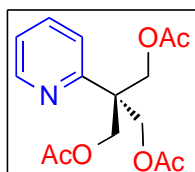


**(10)** was obtained as a yellow oil ( $R_f = 0.25$  in 1:4 ethyl acetate/ hexanes). Spectral data ( $^1\text{H}$  NMR ( $\text{CDCl}_3$ ) and  $^{13}\text{C}\{^1\text{H}\}$  NMR ( $\text{CDCl}_3$ )) matched published data.<sup>2</sup>

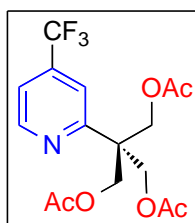




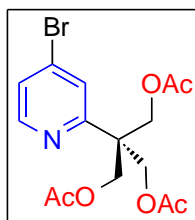
(11) was obtained as a pale yellow oil ( $R_f = 0.25$  in 1:4 ethyl acetate/ hexanes).  $^1\text{H}$  NMR ( $\text{CDCl}_3$ ) ( $\text{C}_6\text{H}_6$ ):  $\delta$  4.64 (d,  $J = 11.5$  Hz, 2H), 4.19 (d,  $J = 11.0$  Hz, 2H), 3.70 (s, 3H), 2.51 (t,  $J = 6.0$  Hz, 2H), 1.65 (two peaks, s, 6H), 1.42 (t,  $J = 6.5$  Hz, 2H), 1.20 (m, 2H), 1.13 (m, 2H).  $^{13}\text{C}\{^1\text{H}\}$  NMR ( $\text{CDCl}_3$ ):  $\delta$  192.86, 169.97, 157.98, 64.90, 61.37, 44.16, 32.37, 25.32, 21.66, 21.06, 20.32. HRMS electrospray ( $m/z$ ):  $[\text{M}+\text{H}]^+$  calcd for  $\text{C}_{13}\text{H}_{21}\text{NO}_5$  predicted: 272.1492, measured: 272.1491.



(3-OAc<sub>3</sub>) was obtained as a colorless oil in 79 % isolated yield ( $R_f = 0.2$  in 3:7 ethyl acetate/hexanes). Spectral data ( $^1\text{H}$  NMR ( $\text{CDCl}_3$ ) and  $^{13}\text{C}\{^1\text{H}\}$  NMR ( $\text{CDCl}_3$ )) matched published data.<sup>2</sup>

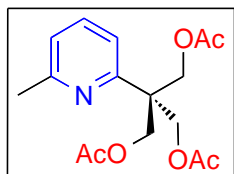


(4) was obtained as a colorless oil in 78 % isolated yield ( $R_f = 0.2$  in 1:9 ethyl acetate/hexanes).  $^1\text{H}$  NMR ( $\text{CDCl}_3$ ):  $\delta$  8.74 (d,  $J = 4.8$  Hz, 1H), 7.44 (s, 1H), 7.41 (d,  $J = 4.8$  Hz, 1H), 7.53 (s, 1H), 4.52 (s, 6H), 1.96 (s, 9H).  $^{13}\text{C}\{^1\text{H}\}$  (125 MHz) NMR ( $\text{CDCl}_3$ ):  $\delta$  170.61, 160.06, 150.49, 138.82 (q,  $J_2 = 33.7$  Hz), 122.95 (q,  $J_1 = 271.8$  Hz), 118.26 (q,  $J_3 = 3.4$  Hz) 117.53 (q,  $J_3 = 3.5$  Hz), 64.12, 48.50, 20.84.  $^{19}\text{F}$  NMR ( $\text{CDCl}_3$ ):  $\delta$  -64.77. HRMS electrospray ( $m/z$ ):  $[\text{M}+\text{H}]^+$  calcd for  $\text{C}_{16}\text{H}_{19}\text{F}_3\text{NO}_6$  predicted: 378.1159, measured: 378.1163.

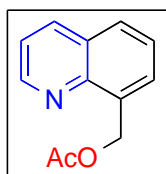


(5) was obtained as a colorless oil in 75 % isolated yield ( $R_f = 0.2$  in 3:7 ethyl acetate/hexanes).  $^1\text{H}$  NMR ( $\text{CDCl}_3$ ):  $\delta$  8.41 (d,  $J = 5.2$  Hz, 1H), 7.45 (d,  $J = 2.0$

Hz, 1H), 7.39 (dd,  $J = 5.2, 2.0$  Hz, 1H), 4.52 (s, 6H), 2.02 (s, 9H).  $^{13}\text{C}\{^1\text{H}\}$  NMR ( $\text{CDCl}_3$ ):  $\delta$  170.53, 159.75, 150.04, 133.12, 125.81, 125.09, 64.00, 48.01, 20.77. HRMS electrospray ( $m/z$ ):  $[\text{M}+\text{H}]^+$  calcd for  $\text{C}_{15}\text{H}_{18}\text{BrNO}_6$  predicted: 388.0390, measured: 388.0396.



(**6**) was obtained as a colorless oil in 68 % isolated yield ( $R_f = 0.2$  in 3:7 ethyl acetate/hexanes).  $^1\text{H}$  NMR ( $\text{CDCl}_3$ ):  $\delta$  7.50 (app t,  $J = 7.6$  Hz, 1H), 7.01 (d,  $J = 7.6$  Hz, 1H), 6.99 (d,  $J = 7.6$  Hz, 1H), 4.51 (s, 6H), 2.47 (s, 3H), 1.96 (s, 9H).  $^{13}\text{C}\{^1\text{H}\}$  NMR ( $\text{CDCl}_3$ ):  $\delta$  170.88, 158.33, 157.39, 136.50, 121.92, 118.39, 64.79, 47.92, 24.73, 21.00. HRMS electrospray ( $m/z$ ):  $[\text{M}+\text{H}]^+$  calcd for  $\text{C}_{16}\text{H}_{21}\text{NO}_6$  predicted: 324.1442, measured: 324.1446.



(**12**) was obtained as a colorless oil ( $R_f = 0.25$  in 1:9 ethyl acetate/hexanes). Spectral data ( $^1\text{H}$  NMR ( $\text{CDCl}_3$ ) and  $^{13}\text{C}\{^1\text{H}\}$  NMR ( $\text{CDCl}_3$ )) matched published data.<sup>2</sup>

## 5.8 References

<sup>1</sup> (a) Rousseaux, S.; Liegault, B.; Fagnou, K. *Chem. Sci.* **2012**, *3*, 244-248. (b) Piechowska, J.; Gryko, D. T. *J. Org. Chem.* **2011**, *76*, 10220-10228. (c) Huang, C.; Ghavtadze, N.; Chattopadhyay, B.; Gevorgyan, V. *J. Am. Chem. Soc.* **2011**, *133*, 17630-17633. (d) Kubota, A.; Sanford, M. S. *Synthesis* **2011**, 2579-2589. (e) Wang, C.; Flanigan, D. M.; Zakharov, L. N.; Blakemore, P. R. *Org. Lett.* **2011**, *13*, 4024-4027. (f) Richter, H.; Beckendorf, S.; Macheno, O. G. *Adv. Synth. Cat.* **2011**, *353*, 295-302. (g) Chernyak, N.; Dudnik, A. S.; Huang, C.; Gevorgyan, V. *J. Am. Chem. Soc.* **2010**, *132*, 8270-8272. (h) Lyons, T.; Sanford, M. S. *Chem. Rev.*, **2010**, *110*, 1147-1169 and references contained within.

---

<sup>2</sup> (a) Li, H.; Li, B.-J.; Shi, Z.-J. *Catal. Sci. Technol.*, **2011**, *1*, 191–206 (b) Jazzar, R.; Hitce, J.; Renaudat, A.; Sofack-Kreutzer, J.; Baudoin, O. *Chem. Eur. J.* **2010**, *16*, 2654-2672. (b) Li, H.; Li, B.-J.; Shi, Z.-J. *Cat. Sci. Tech.* **2011**, *1*, 191-206.

<sup>3</sup> For recent examples see: (a) Reddy, B. V. S.; Revathi, G.; Reddy, A. S.; Yadav, J. S. *Tetrahedron Letters* **2011**, *52*, 5926-5929. (b) Reddy, B. V. S.; Ramesh, K.; Yadav, J. S. *Synlett* **2011**, 169-172. (c) Wang, L.; Xia, X.-D.; Guo, W.; Chen, J.-R.; Xiao, W.-J. *Org. Biomol. Chem.* **2011**, *9*, 6895-6898. (d) Leng, Y.; Yang, F.; Zhu, W.; Wu, Y.; Li, X. *Org. Biomol. Chem.* **2011**, *9*, 5288-5296

<sup>4</sup> For a specific example see: Wang, D.-H.; Hao, X.-S.; Wu, D.-F.; Yu, J.-Q. *Org. Lett.* **2006**, *8*, 3387-3390.

<sup>5</sup> For examples see: (a) Wang, G.-W.; Yuan, T.-T.; Wu, X.-L. *J. Org. Chem.* **2008**, *73*, 4714-4720. (b) Desai, L. V.; Malik, H.; Sanford, M. S. *Org. Lett.* **2006**, *8*, 1141-1143. (c) Reddy, B. V. S.; Reddy, L. R.; Corey, E. J. *Org. Lett.* **2006**, *8*, 3391-3394.

<sup>6</sup> For a specific example see: Vickers, C. J.; Mei, T.-S.; Yu, J. Q. *Org. Lett.* **2010**, *12*, 2511-2513.

<sup>7</sup> Vedernikov, A. N. *Acc. Chem. Res.* **2011**, *asap*

<sup>8</sup> Zhang, Y. H.; Yu, J. Q. *J. Am. Chem. Soc.* **2009**, *131*, 14654-14655.

<sup>9</sup> Zhang, J.; Khaskin, E.; Anderson, N. P.; Zabaliy, P. Y.; Vedernikov, A. N. *Chem. Commun.* **2008**, 3625-3627.

<sup>10</sup> For O<sub>2</sub>: Oxtoby, D. W.; Gillis, H. P.; Nachtrieb, N. H.; *Principles of Modern Chemistry*, 5<sup>th</sup> ed.; Thomson, Brooks, Cole: London, 2002; p A.42. For PhI(OAc)<sub>2</sub>: Giffard, M.; Mabon, G.; Leclair, E.; Mercier, N.; Allain, M.; Gorgues, A.; Molinie, P.; Neilands, O.; Krief, P.; Khodorkovsky, V. *J. Am. Chem. Soc.* **2001**, *123*, 3852-3853.

<sup>11</sup> (a) Keith, J. A. and Henry, P. M. *Angew. Chem., Int. Ed.* **2009**, *48*, 2-14. (b) Cornell, C. N. and Sigman, M. S. *Inorg. Chem.* **2007**, *46*, 1903-1910. (c) Takacs, J. M. and Jiang, X.-T. *Curr. Org. Chem.* **2003**, *7*, 369-389. (d) Negishi, E.-i., Ed. *Handbook of Organopalladium Chemistry for Organic Synthesis*; Wiley: New York, 2002; Vol. 2.

<sup>12</sup> (a) Lambert, E. G.; Derouane, E. G.; Kozhevnikov, I. V. *J. Catalysis* **2002**, *211*, 445–450. (b) Nowinska, K.; Dudko, D. *React. Kinet. and Cat. Lett.* **1997**, *61*, 187-192. (c) Grate, J. H.; Hamm, D. R.; Mahajan, S. *Cat. Org. React.* **1994**, *53*, 213-264.

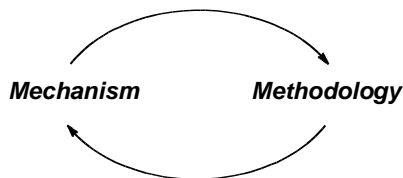
<sup>13</sup> (a) Shibuya, M.; Osada, Y.; Sasano, Y.; Tomizawa, M.; Iwabuchi, Y. *J. Am. Chem. Soc.* **2011**, *133*, 6457-6500. (b) Liu, R.; Liang, X.; Dong, C.; Hu, X. *J. Am. Chem. Soc.* **2004**, *126*, 4112-4113.

- 
- <sup>14</sup> Tissue, T.; Downs, W. *J. Chem. Soc., Chem. Commun.* **1969**, 410.
- <sup>15</sup> (a) Itahara, T.; Ebihara, R.; Kawasaki, K. *Bull. Chem. Soc. Jpn.* **1983**, *56*, 2171-2172. (b) Norman, R. O. C; Parr, W. J. E.; Thomas, C. B. *J. Chem. Soc., Perkin Trans. I*, **1974**, 369-372. (c) Henry, P. M. *J. Org. Chem.* **1971**, *36*, 1886-1890.
- <sup>16</sup> Ebersson, L.; Jonsson, E. *Acta Chem. Scan. B.* **1974**, *28*, 771-776.
- <sup>17</sup> An, Z.; Pan, X.; Liu, X.; Han, X.; Bao, X. *J. Am. Chem. Soc.* **2006**, *128*, 16028-16029.
- <sup>18</sup> (a) Muniz, K. *Angew. Chem., Int. Ed.* **2009**, *48*, 9412-9423. (b) Canty, A. J. *Dalton Trans.* **2009**, 10409-10417.
- <sup>19</sup>(a) Theimann, M.; Scheibler, E.; Wiegand, K. W. "Nitric Acid, Nitrous Acid, and Nitrogen Oxides." *Ullmann's Encyclopedia of Industrial Chemistry*, Wiley-VCH, 2005, Weinheim. (b) Laue, W.; Theimann, M.; Scheibler, E.; Wiegand, K. W. "Nitrates and Nitrites." *Ullmann's Encyclopedia of Industrial Chemistry*, Wiley-VCH, 2005, Weinheim.
- <sup>20</sup> Campora, J.; Palma, P.; del Rio, D.; Carmona, E. *Organometallics* **2003**, *22*, 3345-3347.
- <sup>21</sup> Reimann, R.; Singleton, E. *J. Organometallic Chem.* **1973**, *57*, C75-C77.
- <sup>22</sup> Shiri, M.; Zolfigol, M. A.; Kruger, H. G.; Tanbakouchian, Z. *Tetrahedron*, **2010**, 9077-9106.
- <sup>23</sup> Whitfield, S. R.; in *New Oxidation Reactions of Palladium: Synthetic and Mechanistic Investigations.* **2008**, University of Michigan, Thesis.

## Chapter 6: Conclusions and Outlook

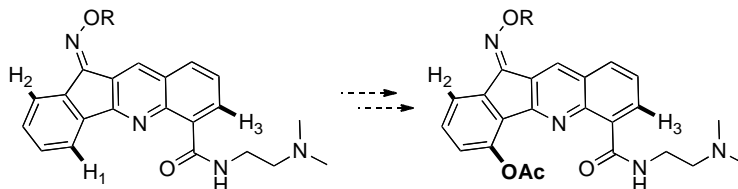
The work contained herein has covered mechanism and synthetic applications as two different aspects of C–H functionalization. The interplay between the synthetic and mechanistic work has allowed informed development of new transformations. These, in turn, require investigation about what is happening at the molecular level to obtain insight about the reactions. Such investigations can then provide new avenues for future transformations (Figure 6.1).

**Figure 6.1.** Interplay Between Mechanism and New Methodology



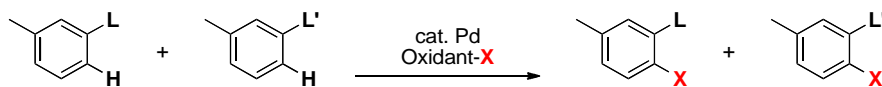
The mechanistic results from Chapter 2, for example, should facilitate rapid derivatization of complex molecules. The studies allow *prediction* of selectivity for molecules such as the Topoisomerase I/II Inhibitor shown in Figure 6.2. This molecule contains three potential directing groups: an amide, an oxime ether and a pyridine. Our competition studies have shown that, substrates with electron rich directing groups generally react preferentially, predicting that functionalization would occur predominately at H<sub>1</sub>.

**Figure 6.2.** Complex Molecule with Multiple Directing Groups and Functionalization Sites



Regarding the mechanistic studies from Chapter 3, the basicity of a ligand will determine selectivity for functionalizations with the same rate-limiting step. However, future work to probe whether or not this selectivity changes under a different rate-limiting step would allow better and more complete predictions. Conducting competition experiments for C–H arylation or chlorination (which involve rate-determining oxidation under some conditions) would provide this requisite insight (Table 6.1). Furthermore, the demonstration of these methods on a complex molecule to generate a library of congeners rapidly would highlight the utility of the selectivity principle described. The mechanistic insights gleaned from this and related work<sup>1</sup> is expected to continue to inform future applications in functionalization of complex molecules.

**Table 6.1.** Selectivity Preferences for Various C–H Functionalization Reactions

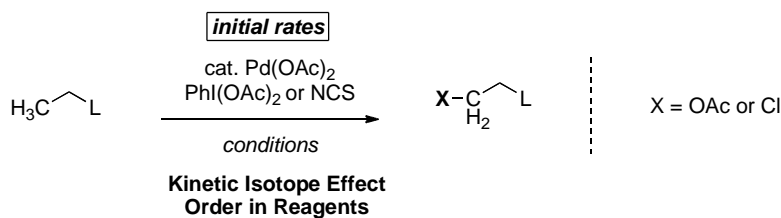


Functionalization	Rate-Limiting Step	Selectivity
Acetoxylation X = OAc	Cyclometallation	Basicity of the Ligand
Chlorination X = Cl	Cyclometallation	Basicity of the Ligand
Chlorination X = Cl	Oxidation	??
Arylation X = Ph	Oxidation	??

In Chapter 3, the mechanism of Pd-catalyzed directed C–H chlorination and acetoxylation of 2-*ortho*-tolylpyridine were compared. Most of the mechanistic work that has been investigated has centered on the mechanism for  $sp^2$  C–H functionalization. However, as introduced in Chapter 3, the differences in reactivity are most striking for those molecules with  $sp^3$  C–H bonds (Scheme 3.1). An investigation of the mechanism for  $sp^3$  C–H acetoxylation with  $\text{PhI}(\text{OAc})_2$  may provide understanding of the reasons that  $sp^3$  C–H chlorination proceeds in very low yields. A comparison of the rate-limiting steps of the cycles for aromatic *versus* aliphatic compounds could lend insight into the differences in undirected

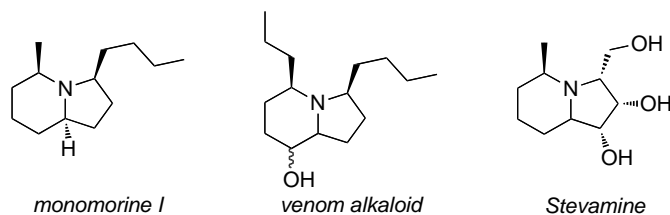
functionalization of those same classes of compounds (Figure 6.3). Preliminary data showed that  $sp^3$  C–H chlorination is indeed possible and conditions for optimization are currently under investigation by a current member of the Sanford Laboratory.

**Figure 6.3.** Proposed Mechanistic Studies for Aliphatic Acetoxylation



Switching from mechanism to synthetic applications, a new Pd-catalyzed reaction for the pyridine-directed aerobic olefination of unactivated  $sp^3$  C–H sites described in Chapter 4 has proved extremely interesting to the synthetic community.<sup>2</sup> This transformation provides a convenient route to 6,5-N-fused bicyclic cores that are present in a number of naturally occurring compounds (Figure 6.4).<sup>3</sup>

**Figure 6.4.** Naturally Occurring 6,5-N-fused Bicyclic Compounds

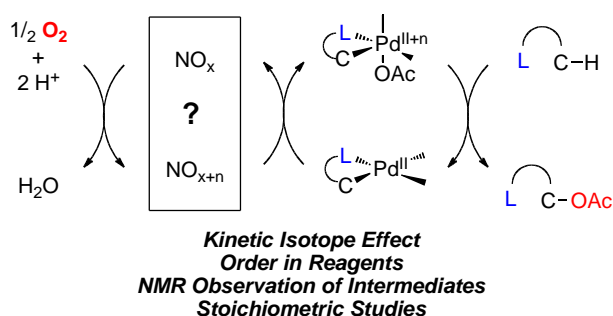


The possibility of synthesizing these compounds using the methodology described, would allow rapid substitution on the 6-membered ring and would be complementary to existing methods.<sup>4,5</sup> The olefination of substrates containing other directing groups did not lead to high yields or selectivity for the desired compounds. Investigation of the mechanism may allow new methods for better generalization of  $sp^3$  C–H olefination. In addition, because the separation of the

organic salts from the acidic solvent proved challenging, it would be advantageous for the methodology to be conducted in a non-acidic solvent while still providing adequate catalyst turnover. Future work to address these issues would further improve the utility of olefination.

Finally, in Chapter 5 we demonstrated the synthetic applicability of nitrate salts that have been underutilized thus far as an appropriate alternative oxidant for oxygenation methodology. The use of nitrate salts is exciting as it provides an affordable non-waste-generative method for oxygenation and preliminary halogenation. Future work investigating the mechanism of the cooperative catalysis between  $\text{NO}_3^-$  salts and acetic acid will be especially insightful since little information exists about these details. Using the information obtained will be critical for determining how general this method will be for future C-H functionalization transformations (Figure 6.5).

**Figure 6.5.** Proposed Investigation of the Mechanism of Nitrates as an Oxidant



These new methods and the insights provided from studying C-H activation methodology is changing the synthetic landscape for researchers in drug discovery and synthesis. These methodologies are increasingly finding applications in accessing drugs and agrochemicals more efficiently and also more affordably. With that in mind, there is much yet to be explored to continue to contribute to this effort.



## 6.1 References

---

<sup>1</sup> Dai, H. X.; Stepan, A. F.; Plummer, M. S.; Zhang, Y. H.; Yu, J. Q. *J. Am. Chem. Soc.* **2011**, *133*, 7222-7228.

<sup>2</sup> Knochel, P.; Steib, A. K. *Synfacts* **2011**, *7*, 765.

<sup>3</sup> (a) Jones, T. H.; Voegtle, H. L.; Miras, H. M.; Weatherford, R. G.; Spande, T. F.; Garraffo, M.; Daly, J. W.; Davidson, D. W.; Snelling, R. R. *J. Nat. Prod.* **2007**, *70*, 160-180. (b) Lin, G.-J.; Huang, P.-Q. *Org. Biomol. Chem.* **2009**, *7*, 4491-4495. (c) Michalik, A.; Hollinshead, J.; Jones, L.; Fleet, G. W. J.; Yu, C.; Hu, X.; van Well, R.; Horne, G.; Wilson, F. X.; Kato, A.; Jenkinson, S. F.; Nash, R. J. *Phytochemistry Lett.* **2010**, *3*, 136-138.

<sup>4</sup> (a) Liu, H.; Su, D.; Cheng, G.; Xu, J.; Wang, X.; Hu, Y. *Org. Biomol. Chem.* **2010**, *8*, 1899-1904. (b) Paderes, M. C.; Chemler, S. R. *Org. Lett.* **2009**, *11*, 1915-1918. (c) Iska, V. B. R.; Verdolino, V.; Wiest, O.; Helquist, P. *J. Org. Chem.* **2010**, *75*, 1325-1328.

<sup>5</sup> (a) Hu, G.-H.; Bartholomew, B.; Nash, R. J.; Wilson, F. X.; Fleet, G. W. J.; Nakagawa, S.; Kato, A.; Jia, Y.-M.; van Well, R.; Yu, C.-Y. *Org. Lett.* **2010**, *12*, 2562-2565. (b) Delso, I.; Tejero, T.; Goti, A.; Merino, P. *Tetrahedron*, **2010**, *66*, 1220-1227.